An analysis of the NET1 proteins: a group of novel plant actin-binding proteins

INGLE, ELIZABETH,KATE,SELBY

An analysis of the NET1 proteins

a group of novel plant actin-binding proteins

Elizabeth Kate Selby Ingle

School of Biological and Biomedical Sciences

Durham University

Submitted in accordance with the requirements for the degree of Doctor of Philosophy

September 2011

Abstract

The NET protein superfamily is a recently discovered family of novel, plant-specific actin binding proteins. The identification of this family represents a significant discovery as the plant cytoskeleton is not identical to the animal cytoskeleton and plant cells show plant specific processes and subcellular structures which rely on actin. There is a need for plant specific proteins which are capable of modelling actin within plant cells.

The NET family comprises thirteen proteins in *Arabidopsis thaliana*, which share the NET actin binding domain (found at the N-terminal end of each protein). Based on the C-terminal domains of the proteins, the family can be separated into four groups, each with a particular localisation. The localisations of these proteins are frequently within plant specific cell types, such as pollen tubes, guard cells or roots, or to plant specific cell structures such as plasmodesmata. It is thought that these proteins may be involved in modelling the actin cytoskeleton at junctions between actin and membranes (either cell membranes or membrane bound structures such as the endoplasmic reticulum).

The NET1 proteins are a group of four proteins, each consisting of an N-terminal actin binding domain and C-terminal coiled-coil domains. NET1a was the first protein to be discovered in a high-throughput screen of plant proteins for novel localisations carried out by Karl Oparka, where it was shown to bind to filaments. Work by Calcutt (Calcutt 2009) showed the filaments to be the actin cytoskeleton.

The aim of this thesis has been to complete the characterisation of all Group 1 NET proteins, building on the analysis of NET1a by Calcutt (Calcutt 2009) and to investigate the possible functions of the NET1 subfamily proteins. All four proteins have been shown to be capable of actin binding and to be expressed in, and locate to structures within, the roots of *A. thaliana*. NET1a has been linked to plasmodesmata, and the combined absence of NET1a and NET1b in the plant results in a cumulative, long root phenotype. Theories to explain this phenotype are suggested here, although the validation and testing of these will form the basis of future work.

Work described within this thesis has been submitted for publication:
Deeks MJ*, Calcutt J*, Ingle EKS*, Hawkins TJ*, Chapman S, Dixon M, Cartwright F, Smertenko AP, Oparka K, and Hussey PJ (2011) A novel superfamily of actin-binding proteins link actin to membranes in higher plants. *Current Biology* (Submitted for review). *These authors share co-first authorship.

Declaration

I confirm that this thesis and the original research described within it are my own work with the exception of the phylogenetic analysis of the NET proteins and alignment of the NET actin binding domains which was undertaken by Dr TJ Hawkins (Durham University), and the analysis of the evolution of the NET proteins which was undertaken by Dr MJ Deeks (Durham University). Fixation and sectioning of GUS stained roots was carried out by Dr Christine Richardson (Durham University). Work carried out by Dr J Calcutt has been used as a basis for certain experiments within this thesis (production of the NET1a-DSRed construct, NET1a-GUS plants and NET1a/NET1b double mutants in particular) and where this work, constructs or plant lines have been used credit has always been given. Credit has been given within the body of the thesis wherever reference has been made to the work of others.

No material contained within this thesis has been submitted for the award of a higher degree elsewhere.

Acknowledgements

Firstly I would like to thank Professor Patrick Hussey, who has supervised this project and provided much help and guidance during my four years. I would also like to thank Professor Karl Oparka, for carrying out the screen which first identified NET1a, without whom this project would not have taken place.

I have received help and support from every member of my lab and I would like to thank them all, but in particular Dr Andrei Smertenko for help with production of antibodies, Dr Mike Deeks for his assistance with the genetics aspect of this project, Dr Hsin-yu Chang for her help with the yeast two hybrid work and Dr Tim Hawkins for his help with Bioinformatics, imaging and much more. Tim has been a friend, a mentor and my proof reader throughout my project and I owe him many thanks! Martin and Orla also deserve a mention for shared optimism and laughter, and good music when needed! I wish Martin all the best as he continues the NET project. Thanks also go to Dr Jo Calcutt, who carried out the first work on the NET1 proteins, and who has consequently provided the foundations to this project.

My thesis committee, Dr Martin Cann, Dr Tony Fawcett and Dr Marc Knight, have always given me encouragement, help, ideas to solve problems, and the chance to talk about my project with enthusiasm – thank you.

My family has been the most amazing support during my whole project and thesis writing. Many, many thanks to Grandma, Mum, Dad and Jonathan. Without your help, encouragement and love this project would never have been completed! Extra thanks to Mum for proof-reading, editing and support and to Jon, who has kept me sane through many ups and downs with suggestions, hugs and tea.

Last but not least, I would like to thank Rosemary and Thyme, without whom Chapter Five would not have been possible. I hope that they enjoy their retirement!

List of Abbreviations

2,4-D	2,4-dichlorophenoxyacetic acid
3AT	3-amino-1,2,4-triazole
ABD	Actin binding domain
ADP	Adenosine diphosphate
ATP	Adenosine triphosphate
BLAST	Basic local alignment search tool
DMSO	Dimethyl sulphoxide
ER	Endoplasmic reticulum
FRAP	Fluorecence recovery after photobleaching
GFP	Green fluorescent protein
GUS	β-glucuronidase
ROI	Region of interest
SAIL	Syngenta arabidopsis insertion line
SEL	Size exclusion limit
TAIR	The Arabidopsis information resource
TRITC	Tetramethyl rhodamine isothiocyanate
X-gluc	5-bromo-4-chloro-3-indolyl-β-D-glucoronide
α-gal	5-bromo-4-chloro-3-indolyl-α-D-galactopyranoside

Index

Chapter Four: Investigation of the actin binding properties of the N-terminus of NET proteins NET1c, NET1d and NET2a, and an investigation of potential protein interactions with NET1a actin binding domain

Chapter Five: Analysis of the localisation and expression patterns of the NET1 group proteins

List of Figures

Chapter 1

Chapter 3

Chapter 4

Chapter 5

Chapter 6

Chapter One:

Introduction

1.1 Introduction

The NET1 proteins are a group of four plant specific, actin binding proteins found in *Arabidopsis thaliana*. The first protein of these four to be discovered was NET1a, the founding member of the NET protein superfamily. This protein had been analysed by Dr J Calcutt (Calcutt 2009) and was shown to be a novel actin binding protein. The NET1 protein sharing the greatest homology with NET1a, NET1b was also analysed and shown to be capable of actin binding. NET1a and NET1b are expressed in root tissue and the proteins have a punctate subcellular localisation to the cortex of the root cells. Mutation of these proteins had a putative phenotype of decreased root growth when both genes were absent but no discernible phenotype when only one protein was absent (Calcutt 2009).

The punctate pattern of expression observed in the subcellular localisation of NET1a had been linked to a possible colocalisation with the connections between adjacent plant cells known as plasmodesmata. This potential interaction had not been fully understood and the function of NET1a remained unknown. The remaining three proteins had not been analysed as fully as NET1a and NET1c and NET1d have not undergone any experimental analysis.

The aim of this project was to analyse the NET1 proteins, with particular emphasis on NET1c and NET1d. Actin binding was established in all members of the group of proteins as the potential for this had previously been assumed but not tested. Investigations were carried out to analyse the expression patterns and subcellular localisations of NET1c and NET1d and were completed for NET1b to allow comparison between these four highly similar proteins. The effect of mutation of all four NET1 proteins was also carried out to further understanding of the root growth phenotype, now known to cause an increase in root growth, and to aid understanding of the function of these proteins. While function is yet to be established, more information on the potential role of these proteins has been obtained.

This group of actin binding proteins represent a significant discovery in the process of understanding the plant actin cytoskeleton. The actin cytoskeleton is not equivalent in plants and animals, and while some proteins are found in common, others are utilised differently or absent in plant species. Plants also require plant specific uses of the

actin cytoskeleton, for example in regulation of plasmodesmata which have no animal equivalent. The use of homology with known animal cytoskeletal proteins will not allow a complete understanding of actin in plants. The discovery of novel, plant-specific proteins is essential for this. The actin cytoskeleton is therefore discussed in more detail below. Understanding the function of the NET1 proteins has the potential to enable understanding of areas of the plant cytoskeleton that have not yet been fully explored.

1.2 The discovery of NET1a

Analysis of the NET1 proteins began in 2003 with the discovery of NET1a by Karl Oparka during a screen of an *Arabidopsis thaliana* cDNA library with the aim of identifying the localisation of novel proteins in plant cells (Escobar *et al.* 2003). A cDNA library was transformed into a Tobacco Mosaic Virus vector, and each protein was labelled with green fluorescent protein (GFP) to allow visualisation of the localisation of the protein of interest. The virus vector allowed a high throughput screen of the library as the virus was used to infect the leaf tissue of *Nicotiana benthamiana* plant to create fluorescent lesions. These could then be imaged using confocal microscopy to identify localisation and the sequence of the cDNA could then be recovered from the infected leaf tissue.

The NET1a protein was identified when it was seen to bind to a net-like mesh of filaments for which the family of proteins are named. This network of filaments was thought to be related to the cytoskeleton of the plant cell. Analysis of the section of NET1a used during the library screen, using anti-cytoskeletal drugs and co-localisation with actin-markers, demonstrated that NET1a was associating with the actin cytoskeleton (Calcutt 2009). Co-sedimentation of NET1a with F-actin indicated that the interaction between the two proteins was a direct interaction since the presence of F-actin was able to cause precipitation of the NET1a protein (Calcutt 2009).

The NET1a protein does not share homology with any currently known actin binding proteins and no homologous proteins appear outside the plant kingdom although there are other previously unidentified proteins in plants which appear to be NET proteins. This lack of homology led to the conclusion that the NET1a protein was a novel, plant-specific actin binding protein. As the founding member of the NET protein family, NET1a was the first protein to be analysed experimentally. The results of this initial analysis will be discussed in the following section.

1.3 Initial analysis of NET1a

The discovery of a completely novel protein, with no homology of sequence or structure to known proteins, or as has been the case with some plant actin binding proteins, equivalence to known animal proteins, is very interesting as no parallels could be drawn from existing proteins as to potential function and only the actin binding property of the protein was known.

To begin the analysis of the NET proteins computational techniques such as bioinformatics were used and experimental data were obtained on analysis of the actin binding capabilities of the protein. The majority of this initial analysis was carried out by Calcutt (Calcutt 2009) and this forms the base of the NET1 protein analysis on which this thesis was developed. Figure 1.1 shows the structure of the NET1a protein.

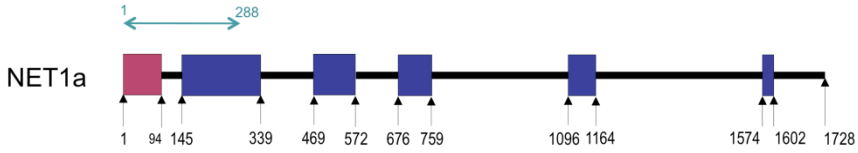

Figure 1.1: Structure of the NET1a protein, showing the N-terminal NET actin binding domain (red) and the C-terminal coiled-coil domains (blue).

After the discovery of its ability to bind to a filament network, the domain used in the original screen was analysed and found to be homologous to the KIP1 domain of PiKIP1, a kinase interacting protein in *Petunia inflata* (Skirpan *et al.* 2001). While this initially suggested a potential for interaction with a kinase, closer analysis of the domain demonstrated that the area of the gene homologous to the NET1a actin binding domain was not in fact the domain interacting with the kinase PRK1. This led to the reclassification of the KIP1 domain as the NET actin binding domain and the PiKIP1 protein as a NET protein (Calcutt 2009). Consequently potential interaction between NET1a and a kinase was not investigated further. Instead the focus of the research was on evaluating NET1a as an actin binding protein. Later work concluded that the region necessary for actin binding included the first 94 amino acids of the N-terminus of NET1a, rather than the 288 amino acids found within the initial construct used (Calcutt 2009).

The C-terminal region of the protein following the newly reclassified N-terminal NET actin binding domain consists of a series of long coiled-coil domains. The prediction of these domains and their significance is discussed further in Chapter 3, but they are a commonly occurring domain with a wide variety of roles within the cell (Rose and Meier 2004). They are capable of dimerisation or oligomerisation so are commonly found in protein-protein interactions and their presence may suggest a structural or organisational protein (Rose and Meier 2004) but their exact role cannot be predicted without further experimental evidence.

Transient expression of regions of NET1a from the middle and C-terminus of the protein, which were tagged with green fluorescent protein (GFP) in *Nicotiana benthamiana*, using an *Agrobacterium tumefaciens* mediated expression system was used to identify potential localisation of the C-terminal domains. The middle section of the protein located to the cytoplasm, the endoplasmic reticulum and nucleus while the C-terminal end was found to localise to the nucleus. The location of the middle section of NET1a was not conclusive, as free GFP showed a similar localisation but the nuclear localisation was interesting to note (Calcutt 2009).

While localisation of sections of the protein may provide some indication of function, the localisation of the whole protein when driven by the native promoter can be more indicative of protein behaviour *in vivo.* The NET1a gene, including the promoter region and a C-terminal GFP tag, was transformed into a stable *Arabidopsis thaliana* line. This allowed analysis of the location of the protein within the cell under a less perturbed system than the transient expression of a protein in *N. benthamiana* leaves. Under these conditions NET1a demonstrated subcellular localisation to the cortex of the root cells in a punctate pattern, with some additional fluorescence observed in a filamentous pattern. This localisation is dependent on the presence of an intact actin cytoskeleton as treatment with anti-actin drugs disrupts the localisation (Calcutt 2009).

More recent work has identified this punctate pattern covering the cell membranes as being similar to that seen with plasmodesmata. Work has also been undertaken staining root tissue with aniline blue which stains callose in the cell wall. This is a known marker of plasmodesmata and has been shown to colocalise with the areas of NET1a binding at the edges of the cell (F Cartwright, TJ Hawkins, Durham University, UK).

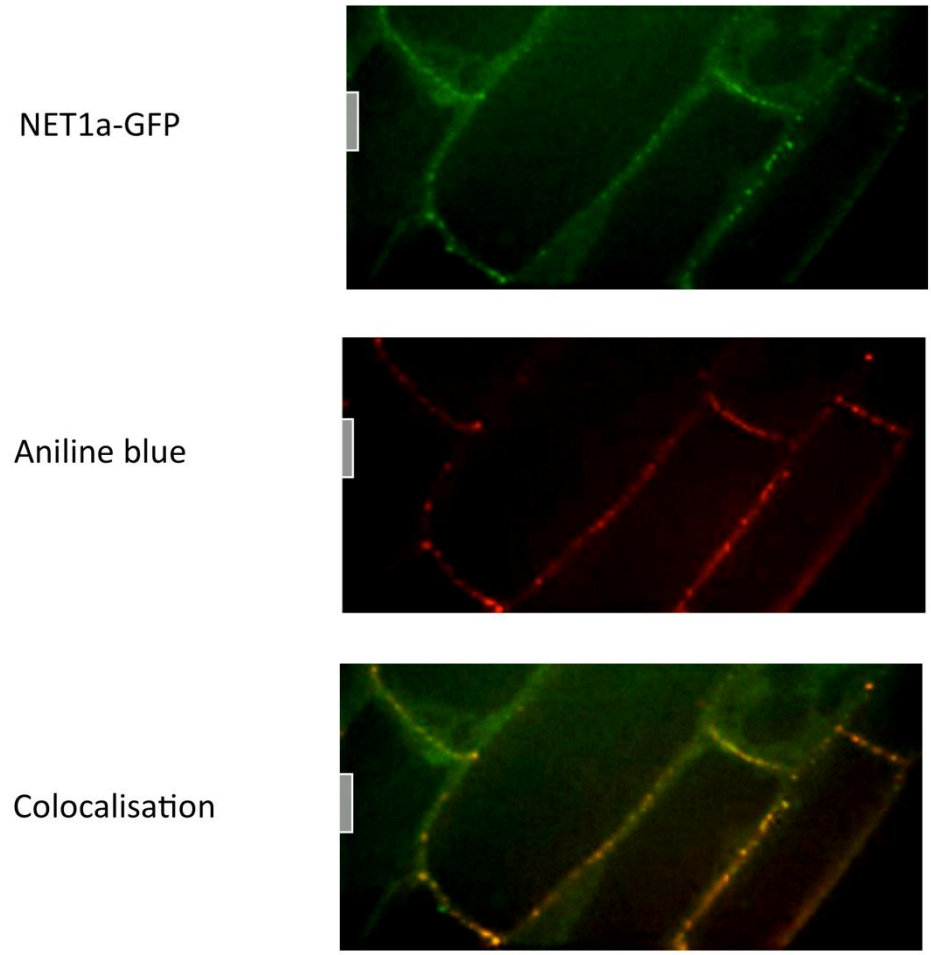

Figure 1.2: Punctate pattern of NET1a-GFP localisation at the cell cortex, compared to aniline blue staining of callose as a marker of plasmodesmata. Images created by TJ Hawkins (Durham University) and reproduced here with his permission.

The location of NET1a in root tissue is supported by evidence from GUS histochemical staining using the NET1a promoter to drive the GUS reporter gene. Transgenic *A. thaliana lines* containing this construct display blue staining in the root tissue, located primarily to vascular tissue and the meristematic tissue in the root tip (Calcutt 2009).

Figure 1.3: GUS histochemical staining driven by the NET1a promoter. Staining is present in the vasculature and in all cell files of the meristematic tissue and transition zone. Image created by J Calcutt (Calcutt 2009) and reproduced here with permission.

T-DNA insertion lines with inserts into NET1a, and therefore lacking a functional form of the NET1a protein, were examined for mutant phenotypes in root development but no visible phenotypes were observed. Formation of double mutants, by crossing the lines lacking the NET1a protein with lines lacking the most closely related NET1 protein, NET1b, produced more interesting data. Plants from these lines showed a decreased length of the primary root when grown on vertical plates (Calcutt 2009). This indicated that the NET1 proteins were necessary for root growth, but the phenotype had not been fully analysed and required further investigation. This is explored further in the work presented here.

In conjunction with the analysis of NET1a, the most closely related NET1 protein, NET1b was also used in experimental work. In many respects NET1b shows similar structural characteristics to NET1a as it consists of an N-terminal NET actin binding domain (ABD) followed by a series of long coiled coil regions with interspersed regions of low complexity. Use of transient expression of the N-terminus of the NET1b protein with a GFP C-terminal tag demonstrated a very similar pattern of net-like filaments and use of anti-actin drugs and co-localisation with an actin marker indicated that NET1b was also capable of association with the actin cytoskeleton.

The entire protein was not cloned for labelling with a C-terminal GFP tag in a stably transformed *A. thaliana* line, but antibodies raised against NET1b and NET1a were used to ascertain that the punctate pattern, observed with the NET1a-GFP construct under the NET1a native promoter, was consistently found with both proteins. In both cases this immunolabelling of the proteins occurred in root tissue (Calcutt 2009).

T-DNA insertion lines were also examined for possible phenotypes caused by removal of the NET1b protein. No such phenotypes were observed although the potential effect of the absence of both protein is described above in relation to NET1a (Calcutt 2009). Since no definitive mutant phenotype has been established this is an area for further research.

While this initial study of NET1a provided much information on the behaviour of NET1a within the cell it has not revealed an exact function for the protein or enabled an understanding of the effect of the absence of the NET1a protein. This required further experimental analysis of both NET1a and NET1b and also the analysis of the remaining proteins of the NET1 group, NET1c and NET1d. The work carried out with NET1a required replication with NET1c and NET1d to establish actin binding capability as a function shared universally in the NET1 proteins. Some work carried out with NET1a, such as the analysis of expression pattern through the use of the GUS reporter gene driven by the protein of interest was not carried out in NET1b. Completing this analysis for all four proteins formed the beginning of this project, to allow comparison of the proteins within the NET1 group and identify areas for further experimentation.

1.4 Potential plasmodesmal localisation of NET1a

The most interesting aspect of the initial analysis of NET1a, beyond the actin binding capabilities of the protein, was the punctate pattern of the protein found at the cell cortex in root tissue and the potential link between this pattern of expression and the location of plasmodesmata.

An unusual feature of plant cells is their ability to connect to adjacent cells via continuous cytoplasm through the spaces between the cell walls known as plasmodesmata. This connection between cells, known as the symplasm, is required in plant cells due to the cell wall that would otherwise reduce communication between cells. Figure 1.4 shows the current model for the structure of simple plasmodesmata (Mongrand *et al* 2010). Simple plasmodesmata consist of a pore through the cell wall between adjacent cells that is lined with cell membrane. The centre of the pore contains a narrow region of the endoplasmic reticulum known as the desmotubule surrounded by the cytoplasmic sleeve which is continuous with the cytoplasm in both cells (Ding *et al* 1992).

The role of plasmodesmata is transport between cells, but this is not a simple free-flow between adjacent cells. Transport through plasmodesmata is controlled by the diameter of the neck region of the pore (Aaziz *et al* 2001), which determines the size exclusion limit (SEL). Small molecules are capable of diffusion through the cytoplasm but larger molecules, such as the KN1 transcription factor (Lucas *et al* 1995) require a conformational change in the pore to allow transport through the symplast. The exact structure of the plasmodesmata which allows this control has not been completely identified although several control mechanisms have been discovered, including calcium signalling pathways (Holdaway-Clarke *et al* 2000). The location of plasmodesmata embedded in the cell wall renders the constituent proteins inaccessible for experimental analysis and a large proportion of the initial analysis of plasmodesmata has been based on transmission electon micrographs which provide structural information but not identification of individual proteins (Roberts and Oparka 2003). Globular proteins are found within the cytoplasmic sleeve in what appears to be a spiral pattern and it is thought that these assist in limiting the transport of molecules through cytoplasm by creating channels in the cytoplasmic sleeve through which transport occurs (Fisher 1999).

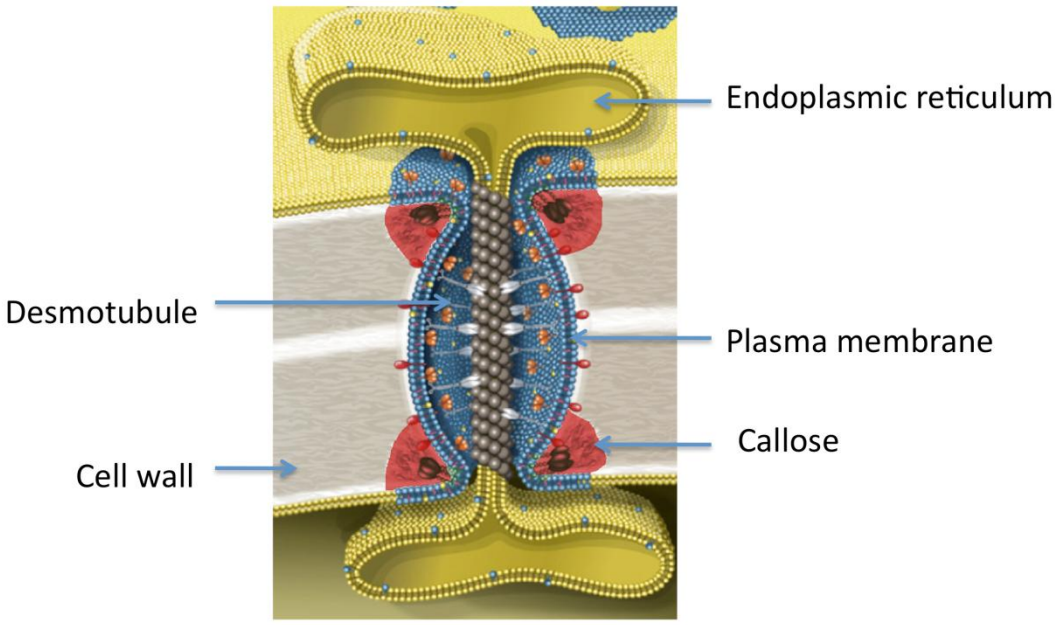

Figure 1.4: The predicted structure of a simple plasmodesma showing the cytoplasmic sleeve within a membrane bound channel and the desmotubule present in the centre of the structure. Globular proteins are also shown associating with the desmotubule and symplast. Adapted from Mongrand et al 2010

Two forms of plasmodesmata structure are found within plant cells: simple and branched. The structure of branched plasmodesmata is similar in basic structure to the simple plasmodesmata but contains links between multiple pores in the middle lamella of the cell wall that are also continuous with the cytoplasm.

Simple plasmodesmata are the first to form (Oparka *et al* 1999), but branched plasmodesmata are found more frequently in more developed tissues and are thought to be a more evolved form of plasmodesmata (Lucas *et al* 1993). Some simple plasmodesmata will develop as primary plasmodesmata, which are formed in the cell plate during cell division by a process of incomplete cytokinesis (Lucas *et al* 2009). As a result of this early development of the structure daughter cells are connected from the point of their formation.

Secondary plasmodesmata are those that are created after this stage and may be formed either to connect adjacent cell files or to increase the potential for transport between cells (Ehlers and Kollmann 2001). The level of connection between cells via this transport route varies depending on age of cell and tissue type and is controlled by the number and SEL of the plasmodesmata (Mezitt and Lucas 1996). For example

where loading or unloading of photoassimilates to and from the phloem occurs, a greater number of plasmodesmata are required with an increased SEL (Baluška *et al* 2001). Within meristematic tissue where NET1a is found primary plasmodesmata would be expected to localise to transverse walls where the majority of NET1a fluorescence is observed so the NET1a protein may be associated with this subset of plasmodesmata where a high flux of small molecules is transported and subject to rapid regulation (Rutschow *et al* 2011).

When considering the potential for connections between NET1a and plasmodesmata, the most important feature of plasmodesmatal structure is the presence of actin, linking the known function of NET1a to its putative localisation. Myosin-like proteins have been located to plasmodesmata (Radford and White 1998) and are presumed to bind to actin but the exact role of the actin filaments has not been established. Actin filaments are known to target proteins for transport to the pore (Chen and Kim 2006) but some models of plasmodesmata also contain a central actin filament passing through the pore (Overall and Blackman 1996). Actin at plasmodesmata forms an array around the neck region of the pore and has also been identified as one of the forms of control of SEL. A loss of actin has been demonstrated to widen the neck of the pore and increase the SEL of the plasmodesmata and a stabilisation of actin has been shown to decrease the occurrence of symplastic transport (Ding *et al* 1996) so an intact actin cytoskeleton with dynamic properties is clearly required for control of transport through plasmodesmata. This makes plasmodesmata an interesting localisation for a novel actin binding protein like NET1a.

1.5 The NET superfamily

The NET1 proteins are not the only NET protein to be found within the *A. thaliana* genome. NET1a is one of a superfamily of fifteen proteins which share the NET actin binding domain and these have the potential to be a very interesting family of novel plant-specific proteins (Calcutt 2009). These fifteen proteins were identified after the discovery of NET1a through the use of Bioinformatics (Calcutt 2009). The proteins do not all share homology beyond the presence of the actin binding domain, so the functions of the various proteins may be very different. The NET actin binding domain may be a generally utilised domain for enabling interaction with the network of actin filaments in the cell while the C-terminal domains designate specific function but this remains to be investigated.

At present all fifteen proteins in the NET family are unknown proteins based on predicted genes after the sequencing of the *A. thaliana* genome. Initially EMB1674, a protein identified during a screen for embryo lethal insertion mutants (McElver *et al* 2001) was thought to be part of the NET family but this was later discovered not to be the case. The classification of EMB1674 as a NET protein was due to a miss-prediction of putative genes in the genome and masks the presence of an unknown gene now thought to code for NET2a (MJ Deeks, Durham University, UK). This lack of known proteins leaves a wide area of potentially interesting research of the NET proteins in *A. thaliana.*

When the analysis of the NET1 proteins began, no other proteins belonging to the NET family, beyond NET1a and NET1b had been subjected to experimental analysis. This project will briefly consider the actin binding capacity of the founding member of the Group 2 proteins, NET2a. This represents an initial analysis of the association between actin filaments and NET proteins outside the NET1 group as proof of concept for the potential for the NET actin binding domain to be universally capable of interaction with actin filaments.

1.6 Bioinformatic analysis of the NET protein superfamily

The 94 amino acid sequence of NET1a identified as the actin binding domain of the protein has been used as the search term for a blastP search using NCBI BLAST (Basic Local Alignment Search Tool, Altschol *et al.* 1997) to find proteins demonstrating homology with this domain. Fifteen proteins in the *A. thaliana* genome were identified as containing this domain and are now thought to form an actin binding superfamily of NET proteins. Figure 1.5 shows an alignment of the amino acid sequence of the fifteen actin binding domains (including the PiKIP1 protein where the KIP1 domain which is now known to be the NET actin binding domain) was first identified. A very high level of conservation is apparent, particularly in the case of the rare triple tryptophan sequence at the N-terminal end of the domain. There are two proteins At3g17680 and At1g48405 which show far less conservation of the actin binding domain and no capacity for actin binding has yet been found (Hussey group, unpublished work). These two proteins are thought to be outliers and are usually not considered to be true NET proteins.

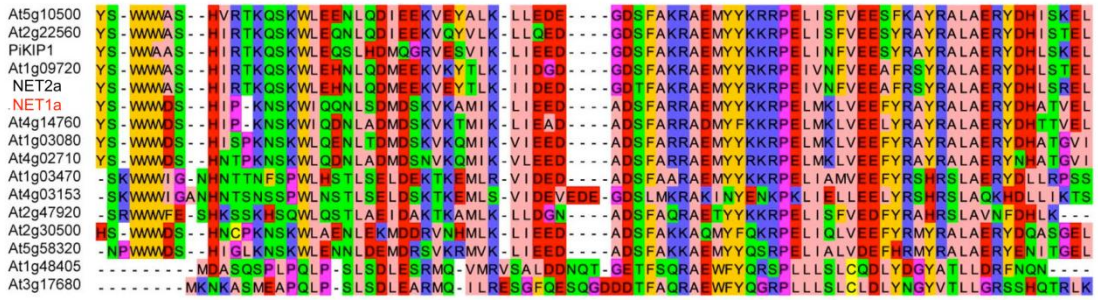

Figure 1.5: An alignment of the amino acid sequence of the NET actin binding domain in the fifteen NET proteins found in the A. thaliana genome. Produced by TJ Hawkins and reproduced here with his permission.

While the NET actin binding domain is well conserved between thirteen of the proteins in *A. thaliana*, the C-terminal domains of the proteins are varied and, for this reason, it has been possible to further subdivide the proteins into groups within the family based on whole protein homology beyond the shared actin binding domain, through the use of phylogenetic analysis. Figure 1.6 shows the thirteen *A. thaliana* proteins in the four groups into which they can be ordered. The first of these contains the founding member of the family, NET1a and is therefore the Group 1 of the NET proteins on which this project is focussed.

The creation of a phylogenetic tree provides an indication of the evolutionary relationships between proteins by assessing the homology between proteins and the likelihood of these changes in homology occurring.

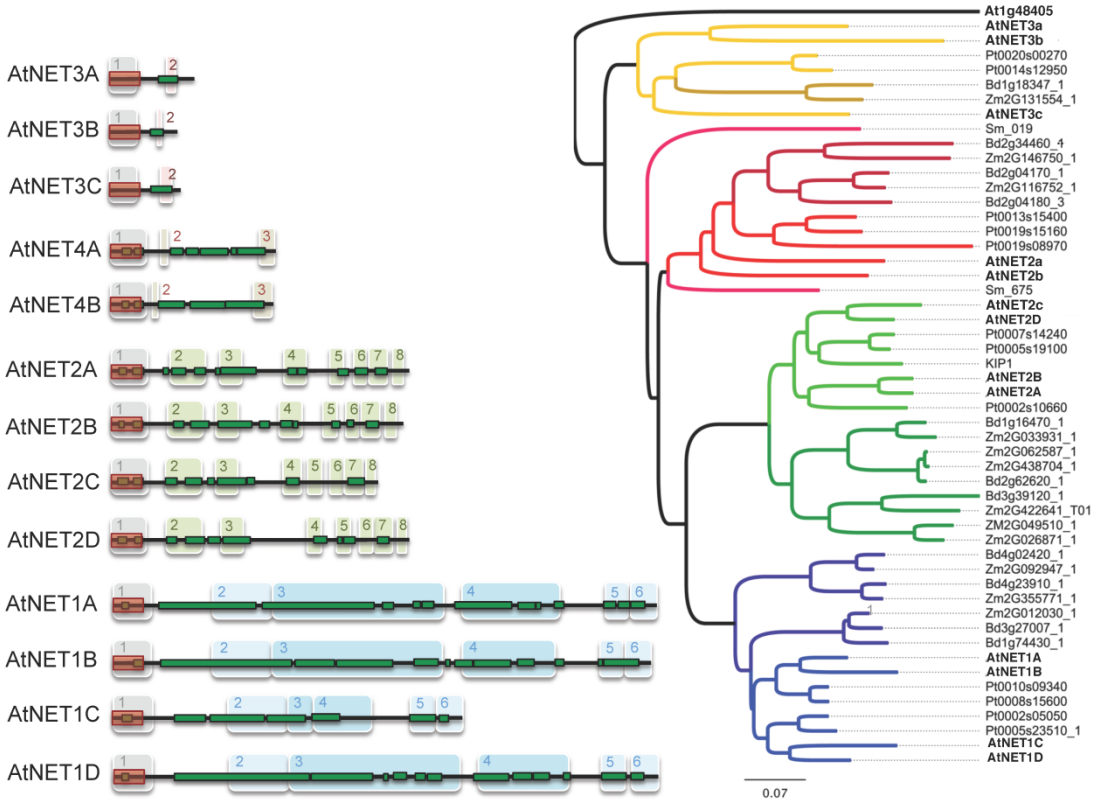

Figure 1.6: Phylogenetic analysis of the NET actin binding superfamily in A. thaliana and the wider plant kingdom. On the left four groups of A. thaliana NET proteins are shown, representing ordering of the thirteen proteins according to phylogenetic analysis and homology of C-terminal domains. NET1a is present in Group1. Actin binding domains are shown in red and coiled coil domains in green. On the right is shown a phylogenetic tree created from NET proteins in a variety of species. The same four groups are observed. Image created by MJ Deeks and used here with his permission.

As discussed above, Group 1 contains the original NET1a protein and the family of four proteins that contain an N-terminal actin binding domain and a relatively long region of coiled-coil domains. These are some of the largest of the NET proteins with the greatest regions of coiled coils. Group 2 contains the NET actin binding domain and a PRK interacting domain. This group contains PiKIP1, the *Petunia inflata* gene in which the KIP1 domain, now known to be the NET actin binding domain, was first discovered. These proteins also contain homology to the region of the *P. inflata* gene shown, through the use of yeast two hybrid, to be phosphorylated by the receptor-like kinase PRK1 (Skirpan *et al.* 2001). Groups 3 and 4 are predicted to contain a further five previously unidentified proteins. The Group 3 proteins represent the smallest of

the *A. thaliana* NET proteins. Both groups contain the characteristic N-terminal actin binding domain and a series of coiled coil domains. A fifth potential group, not shown here, contains the two proteins with the most divergent form of the NET actin binding domain.

The categorisation of proteins into related groupings is useful because it can indicate proteins that may share similar functions or expression patterns. When seeking proteins on which to focus an experimental analysis, it can suggest proteins which may be similar and which more divergent so that work may be planned more effectively. In this case, the high level of homology between the four NET1 proteins appears to indicate a potential for highly similar functions or methods of function between the proteins. Currently unpublished work carried out by the Hussey lab into the actin binding capacity of the four groups began with the selection of one protein from each of the NET groups to provide an indication of how widespread was the ability to associate with the actin cytoskeleton. In this project, actin binding capacity has been demonstrated in the NET1 proteins and in NET2a.

1.7 Evolution of the NET proteins

Another aspect to the analysis and understanding of the NET proteins has been to consider the evolution of the NET proteins and how the occurrence of these proteins relates to plant evolution. The ordering of the NET groups according to phylogenetic analysis shown in Figure 1.6 includes only the proteins found in *A. thaliana* but this is not the only plant genome to contain NET proteins. Work carried out by Dr MJ Deeks (Durham University, UK), identified other instances of proteins containing the NET actin binding domain occurring in a variety of species, ranging from crop species such as maize to club mosses such as *Selaginella moellendorffii*. The proteins were discovered through BLAST searches using the NET1a actin binding domain as a search term. Once found, phylogenetic analysis enabled these genes to be categorised according to the previously discovered four groups of NET proteins. No further groups were discovered. This not only demonstrated the presence of NET proteins in a wide variety of plant genomes but also provides an insight into the possible evolution of the NET proteins and the evolutionary preservation of the four groups. Not all plant genomes have been sequenced, so the data is not comprehensive but it does provide an indication of the spread of the NET genes throughout the plant kingdom.

To assess the evolution of the NET genes, the presence of NET genes is analysed in sample species from the stages of plant evolutionary complexity (shown in Figure 1.7). This analysis was undertaken by Dr MJ Deeks (Durham University, UK). Proteins characteristic of the Group 4 appear in *Selaginella moellendorffii* which is a club moss. This is the first stage of plant evolution where the NET proteins appear, as they have not been found in mosses or worts. This is a significant point in the evolution of plants as it marks the change from simple seedless, nonvascular plants such as mosses and worts to plants with a developed vasculature, enabling much larger plants to develop due to increased facility for transport of water and nutrients (Raven 1992). This development of vasculature is a period of significant change in plant evolution, with corresponding changes in the challenges faced by the plant. The concurrent evolution of the NET4 proteins points towards a link between these proteins and the processes and structures necessary for growth of a vascularised and much larger plant. Consequently the NET4 proteins are less likely to be involved basic actin dynamics and regulation. Their role may be in creation of higher order actin arrangements or in processes that utilise the actin cytoskeleton.

It is unclear at precisely which stage of plant development the Group 3 proteins appear due to the incomplete nature of sequenced genomes of plants belonging to the Ferns. These genomic sequences do not contain any NET proteins, but they may be found after the completion of the sequencing. The NET3 proteins are not present in *S. moellendorffii* but are present at the point of the evolution of the gymnosperms.

Groups 1 and 2 also appear first within gymnosperms but they appear as a 'hybrid' form of the group 1 and 2 proteins with characteristics of both groups. Regions of homology characteristic of each group are shared in this hybrid, which is only present in the gymnosperms. When the genomes of Angiosperm plants are considered, the two proteins have separated into the two groups as found in *A. thaliana*. This is particularly interesting as the Group 2 proteins are found exclusively in pollen and this divergence of the group corresponds to the divergence of reproductive actin (Kandasamy *et al* 2002). This is a significant change in the use of plant actin and the appearance of a new form of NET protein at this stage is interesting to consider.

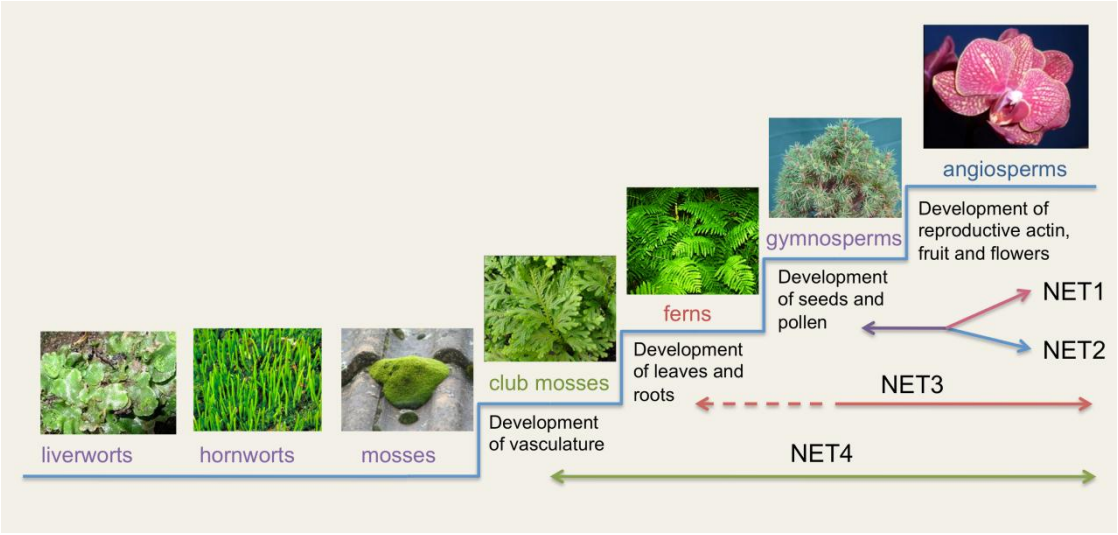

Figure 1.7: Occurrence of NET proteins in plants relative to the evolution of plants from the first land plants to angiosperms.

In conclusion, the NET proteins appear to be connected with significant changes in plant physiology and development. The proteins have a specific role and have evolved accordingly. To understand the significance of the discovery of a novel group of proteins capable of association with actin filaments, and in particular a group which appears to be specific to plants, it is also necessary to consider what is currently known about the plant actin cytoskeleton and the proteins associated with it and to place these novel proteins in context.

1.8 The actin cytoskeleton

The plant cytoskeleton consists of two filament networks: actin and microtubules. Unlike animal cells they do not contain a third cytoskeletal network in the form of intermediate filaments. Actin and microtubules form the basis of the cytoskeleton but many other proteins are associated with these networks (Hussey 2004).

The actin cytoskeleton is highly dynamic, and this dynamic nature is due to the ability of the helical polymer filaments to polymerise and depolymerise between the two forms of actin (Pollard and Borisy 2003). F-actin is the polymerised filamentous form and G-actin exists as a monomer (Steinmetz *et al* 1997). Filaments are built from the monomeric units through the process of nucleation and elongation. In the process of nucleation thermodynamically unstable dimers and trimers of actin monomers form and can act as a seed for the formation of the polymer. Addition of further G-actin monomers causes elongation of the filament (Pollard *et al* 2000).

F-actin filaments consist of two protofilaments forming a right-handed double helix. The two ends of the filament are not identical, owing to the asymmetric structure of the actin monomer. The barbed end of the filament is capable of a higher rate of polymerisation than the pointed end so growth frequently occurs at this end of the filament (Pollard 1986). Depolymerisation primarily occurs at the pointed end. The rate of polymerisation can be controlled by the concentration of monomer available and under steady state conditions the rates of polymerisation and depolymerisation are equal (Pollard *et al* 2000). Dynamic growth and shrinkage of filaments occurs when one of these processes occurs at a higher rate than the other. Control of the dynamics of actin filament formation is highly important in maintaining the necessary forms of the actin cytoskeleton within the cell (Blanchoin *et al* 2010). Figure 1.8 illustrates the dynamics of the actin cytoskeleton and the proteins involved in the regulation of those dynamics.

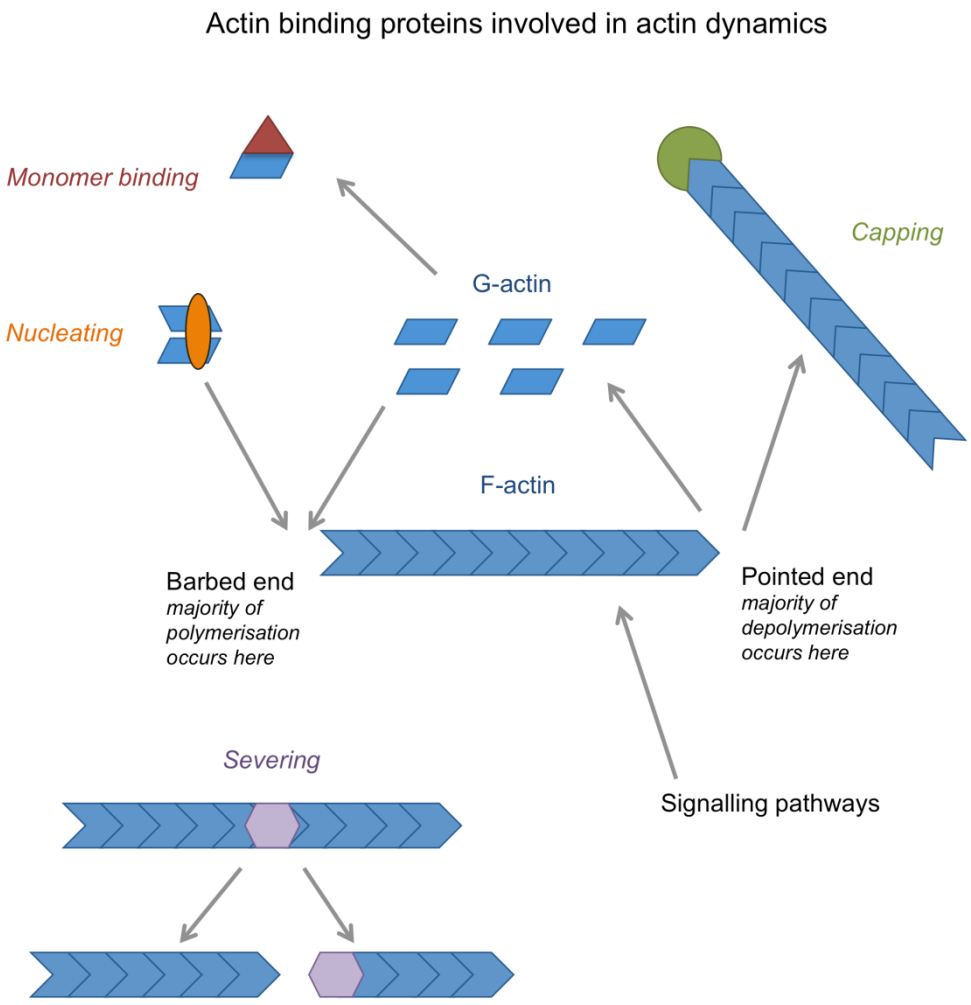

Figure 1.8: Diagram to illustrate the proteins involved in the regulation of actin dynamics in eukaryotic cells.

A feature of F-actin which assists in control of depolymerisation is the binding of ATP and ADP to actin monomers. G-actin monomers undergoing addition to the filament are bound to ATP and the ATP bound to F-actin gradually undergoes hydrolysis to ADP. This decreases the stability of the association between monomers and therefore increases the likelihood of depolymerisation occurring (de la Cruz *et al* 2000). Control of this process allows corresponding control over filament dynamics. Recent work has demonstrated that complete depolymerisation of the filament is not necessary for remodelling of the actin cytoskeleton. Filaments may be severed and then reassembled from filament fragments, presumably speeding up the process of remodelling of the network (Smertenko *et al* 2010).

The highly dynamic nature of actin and an array of actin binding proteins allow modelling of the actin cytoskeleton into a wide range of structures and to connect the cytoskeleton to a wide range of processes such as cell division (Yu *et al* 2006), cell expansion (Hussey *et al* 2006) and the response of the cell to its external environment. In this control and arrangement of the cytoskeleton variations between plant and animal cells are apparent due to differing demands on the network. Plant cells, for example, have no need of actin filaments in the process of cell motility but do require actin in the movement of chloroplasts in response to light levels (Lehmann *et al* 2010).

The structure of actin within a plant cell shows a variety of conformations of actin filaments in different subcellular localisations. The cortex of the cell contains a dense network of actin filaments; in the net-like pattern that appears so characteristic of the transient expression of the NET domain in *Nicotiana benthamiana* leaves and which gave rise to the name of these proteins. Actin is also found surrounding the nuclear envelope and in long filaments running through cytoplasmic strands between vacuoles (de Ruijter and Emons 1999; Nick 1999). Actin is also utilised during the process of cell division where actin filaments are required for formation of the preprophase band and the phragmoplast and are also associated with mitotic spindles (Yu *et al* 2006).

The actin cytoskeleton has been linked to a wide range of cellular processes encompassing cell division and growth, transport (including movement of organelles) and communication with the environment outside the cell in the form of cell-to-cell communication and signal transduction. In cell growth, actin filaments are found to define regions of elongation (Ketelaar *et al* 2001) and a fine meshwork of actin is required for expansion of areas of the cell such as the lobes of epidermal cells (Fu *et al* 2002). The actin cytoskeleton is also utilised for transport of vesicles to areas of cell wall growth in processes such as elongation (Miller *et al* 1999). In root cells longitudinal bundles of actin fiaments are also located in these regions during cell elongation and are thought to be stress-bearing structures (Baluška *et al* 2001).

An example of utilisation of the actin cytoskeleton in the movement of organelles is the movement of chloroplasts. These organelles are surrounded by a basket of actin filaments and are transported along actin fibres in response to light levels (Kandasamy and Meagher 1999). The protein CHUP1 forms a link between the chloroplast membrane and the filament (Lehmann *et al* 2010). The response of

chloroplasts to high light levels, moving to the anticlinal cell wall to avoid photodamage and returning to the periclinal section of the cell when light levels decrease in order to maximise photosynthetic processes, is also an example of the involvement of actin in a signalling process. In this case the actin cytoskeleton is the target of the signalling process, as the level of blue light detected by phototropin photoreceptors begins the transduction of the signal via several intermediate proteins to the actin cytoskeleton (Kong and Wada 2011). Actin can also be involved in signalling as a transducer rather than the target (Drøbak et al 2004).

A further example of actin response to external stresses is in the response of the actin cytoskeleton to pathogens. One example of this response is during infection by plant viruses. Some plant viruses, such as the Tobacco mosaic virus, utilise the actin cytoskeleton for movement of the virus through plasmodesmata to spread the infection between cells. This process requires an intact actin cytoskeleton and can be halted if the cytoskeleton is disrupted using anti-actin drugs (Kawakami *et al.* 2004). In the case of the Cucumber mosaic virus, the viral movement protein which enables the spread of the virus by increasing the size exclusion limit of the plasmodesmata appears to do so by severing actin filaments (Su *et al.* 2010).

Another example of the actin cytoskeleton responding to pathogens is during the infection of flax by the Flax rust fungus which causes reorganisation of the actin filaments to focus on the site of penetration of the fungus into the cell. The same reorganisation of actin is observed in adjacent cells and in infected cells hypersensitive cell death occurs. This process is actin linked as treatment with Cytochalasin D can prevent cell death occurring (Kobayahsi *et al* 1994). This is an interesting example of signalling to the actin cytoskeleton as filaments undergo a complete remodelling rather than specific sites of change or utilisation of the filaments for transport seen with some other actin responses downstream of signalling pathways.

During signalling cascades, the actin cytoskeleton is responding to the external environment of the cell indicated by various sensors and receptors which make up the point of perception of an external stimulus. The actin cytoskeleton has also been implicated in the ability of cells to communicate with adjacent cells via structures known as plasmodesmata. These cell wall channels allowing transport between cells through connected cytoplasm and endoplasmic reticulum are known to be associated with actin filaments (White *et al* 1994). These are thought to track components for

transport to the plasmodesmata or even to regulate transport through the cytoplasmic sleeve (Chen and Kim 2006, Ding *et al* 1996).

The examples of utilisation and control of the actin cytoskeleton described here are of vital importance to the growth, development and maintenance of plant cells. None of these processes would be possible without the presence of a wide array of actin binding proteins, including the NET protein family, to regulate, remodel and use the actin cytoskeleton.

1.9 Actin binding proteins

Actin binding proteins encompass a large and diverse group of proteins with a multitude of functions and the diversity of the actin cytoskeleton is reflected by the diversity of the proteins that associate with it. Just as the plant actin cytoskeleton differs from the animal actin cytoskeleton there are marked differences in the actin binding proteins found in plants and animals. A far greater number of proteins have been found in animals and fungi and homologous proteins are not always found in plants (Hussey *et al* 2002). One study attempted to find homologues of 70 animal and fungal proteins in the *A. thaliana* genome but only 36 of these produced results (Meagher and Fechheimer 2003). This shows the scale of the variation between plant and animal actin binding proteins but while these proteins show a great range of forms and functions, they can be loosely grouped according to their relationship with the actin cytoskeleton.

When actin binding proteins are grouped according to their function the most fundamental of these are the proteins which regulate the dynamics of the actin filaments. Figure 1.8 illustrates the function of proteins within this group. As discussed above, actin filament dynamics are controlled by the polymerisation and depolymerisation of actin. The proteins within this group include those which sequester G-actin monomers to regulate polymerisation, those which promote nucleation of filaments, and those which sever filaments, effectively promoting their depolymerisation (Hussey *et al* 2006). Filament polymerisation and depolymerisation can also be promoted or prevented, for example by capping proteins that bind to filaments and stabilise them to prevent depolymerisation (Schmidt and Hall 1998). Examples from this group include ADF/cofilin which severs filaments to create an increase in the number of filament ends capable of polymerisation and promotes depolymerisation at the pointed end of the filament to provide an increase in available monomer for elongation at the barbed end. This role in dynamics is utilised in processes such as the elongation of root hairs (Hussey *et al* 2002). Formin is another example of an actin regulatory protein. This promotes the creation of filaments by stabilising the dimers and trimers of actin necessary for nucleation of filaments and allowing initiation of polymerisation (Deeks *et al* 2002). Formin can also bind to the pointed end of the filament to inhibit depolymerisation and increase filament growth (Hussey *et al* 2006).

The second group of proteins are those which organise actin filaments into higher order structures. Figure 1.9 illustrates the structures formed by this organisation of actin filaments. This organisation involves the linking of adjacent actin filaments into tight bundles, cross-linking filaments into looser, mesh-like conformations or anchoring filaments to a surface (Hussey *et al* 2006). Fimbrin, containing two actin binding domains through which a connection can be made between adjacent filaments, is one such protein which bundles actin to form cables for cytoplasmic streaming (Wasteneys and Galway 2003).

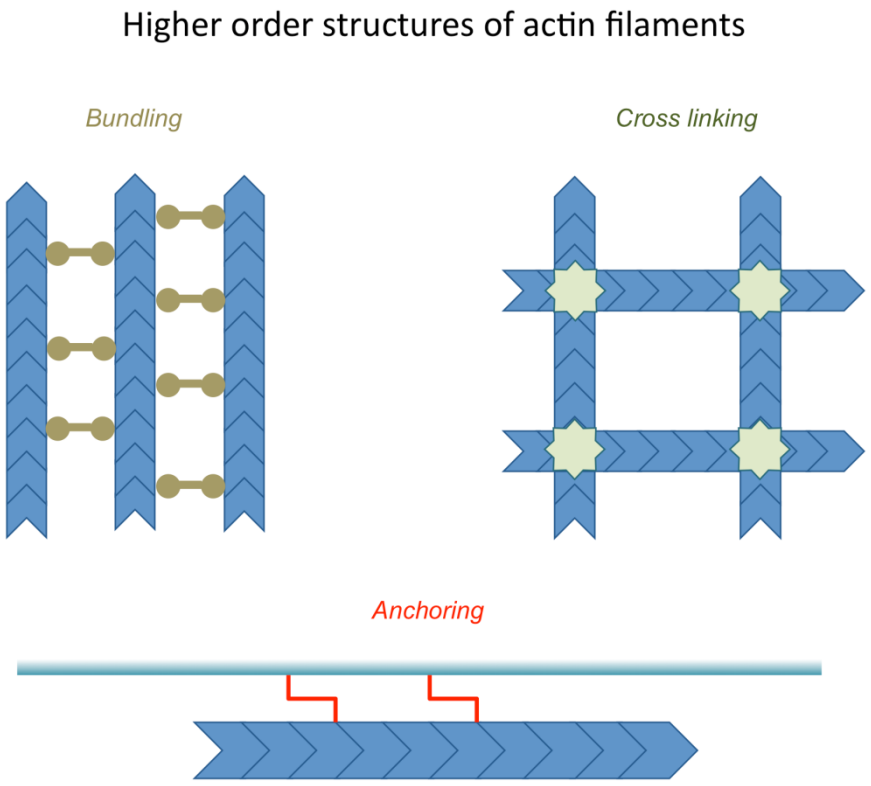

Figure 1.9: Diagram to illustrate the structures that can be formed by the organisation of actin filaments by actin binding proteins. The higher order structures shown here are bundles of actin filaments, a meshwork of actin filaments and the anchoring of actin to a structure or surface, such as a cell membrane.

The final group of actin binding proteins contains those that utilise the actin cytoskeleton as a means of transport. These are the myosins, proteins which use ATP hydrolysis to provide energy for transport along actin filaments (Schliwa and Woehlke, 2003). Myosins associate with a 'cargo' consisting of an organelle or vesicle through a coiled coil tail domain, one of three domains found in myosin proteins. The other domains are the neck domain, which can bind calmodulin or

calmodulin-like proteins and the motor domain, which associates with the filament and causes the movement by translocation along the actin. Seventeen myosin-like proteins have so far been identified in *A. thaliana* (Reddy and Day 2001).

While some aspects of the actin cytoskeleton and actin binding proteins are shared between plant and animals, others are divergent to a greater or lesser extent. Some actin binding proteins in plants show homology to animal proteins but are either utilised or regulated in a different manner. An example of this would be ADF, the filament severing protein discussed above (Cooper and Schafer 2000), which in animals is regulated by phosphorylation by the LMI and TESK1/TESK2 kinases (Arber *et al* 1998; Toshima *et al* 2001). In plants however the action of ADF is regulated by plant and protozoa specific Calmodulin Domain-like Protein Kinases (Allwood *et al* 2001) or, in the case of the LiADF1 protein, by AIP1 which is an actin-interacting protein rather than a kinase (Allwood *et al* 2002).

Even this variation in the utilisation of proteins cannot account for all the questions still unanswered about the actin cytoskeleton in plants and the proteins which bind to it. To achieve a complete understanding of plant actin, novel plant-specific proteins must be identified through the use of techniques such as affinity chromatography to discover novel proteins associated with F-actin (Yu *et al* 2000). The discovery of a group of novel actin binding proteins such as the NET1 proteins may allow some of the gaps in our knowledge of plant actin binding spaces to be filled.

1.10 Aims for the analysis of the NET1 proteins

Chapter Four

The initial aim of the investigation of the NET1 proteins was to establish whether the N-terminus of the proteins NET1c and NET1d, containing the NET-ABD, were capable of association with actin filaments. This had not been experimentally proven although it was predicted that the NET ABD would be universally capable of binding to actin. Chapter four describes the analysis undertaken using fluorescence labelling techniques used to assess the actin binding properties of NET1c and NET1d. Analysis of the NET2a ABD was also undertaken.

In a continuation of the analysis of the NET1a protein a yeast two hybrid library screen was carried out in order to discover proteins which could potentially interact directly with NET1a as discovery of protein-protein interactions involving the protein of interest would have had the potential to enable the discovery of a process or structure to which NET1a is linked. Some potential interactors were identified but have yet to be taken further as the accuracy of the yeast two hybrid screen was unclear.

Chapters Three and Five

To identify the expression pattern of the NET1 proteins a combination of Bioinformatics and transgenic lines containing the GUS reporter gene under the control of the NET1 promoter regions have been used. GUS histochemical staining had only been previously used in NET1a so NET1b was included in this analysis. Subcellular localisation has also been investigated through the use of antibodies raised against regions of NET1c and NET1d and the pattern of subcellular localisation compared with that observed with NET1a and NET1b. NET1c and NET1d show a similarly paired pattern to NET1a and NET1b which is notable as these two proteins form a second pair of closely related proteins within the NET1 group (the first being NET1a and NET1b). (Calcutt 2009)

Chapter Six

Use of T-DNA insertion lines which create knock out (KO) mutants had already been used to assess potential mutant phenotypes caused by the lack of a functional form of NET1a and NET1b has already been carried out (Calcutt 2009). This chapter contains an analysis of the NET1c and NET1d mutants. So far no phenotype has been observed when only one NET1 protein is missing. This may be due to some level of redundancy between the proteins, perhaps caused by the high levels of homology between the proteins. It is possible that when the levels of one NET1 gene are decreased the other genes may be able to compensate to a level that prevents a

physical phenotype from being observed although subcellular defects may be occurring. This compensatory effect does appear to be occurring between NET1a and NET1b as a double mutant line which contains T-DNA insertions into both genes shows a slight root phenotype of a shortened primary root (Calcutt 2009).

The original analysis of the NET1a/NET1b double mutant was carried out using a small sample size and the plants under comparison were from different generations of seed which had therefore been set under differing environmental conditions. Since seed quality can effect growth of the plant, assays on the change to the primary root in the double mutant have now been carried out on a much larger scale. The phenotype has also been tested in a variety of environmental conditions. The effect of the loss of three NET1 genes in a triple mutant line was also investigated.

The analysis of proteins from a family about which so little is known has the potential to produce very exciting results. While the analysis of the proteins within this thesis has not yet provided a comprehensive answer as to the function of the proteins, considering the unique structure of actin within plant cells compared to animals or yeast and the areas of research into the actin cytoskeleton that are still to be discovered, there is wide scope for the function of the novel NET1 proteins.

Chapter Two:
Materials and methods

2.1 Materials

2.1.1 Bacterial strains

Two *Escherichia coli* strains have been used: DH5α for cloning and BL21DE3 Rosetta2 TM (referred to as Rosetta 2) for protein expression. Two *Agrobacterium tumefaciens* lines have also been used: GV3101 for transient expression for construct in *Nicotiana benthamiana* and C58C3 for stable transformation of *Arabidopsis thaliana*. GV3101 is a strain from the C58 background, which has resistance to rifampicin. pMP90 is the chromosomal marker gene, pTiC58DT-DNA the Ti plasmid and the plasmid marker gene confers resistance to gentamycin (Koncz & Schell 1986). C58C3 is an industrial strain of the C58 background whose specific genotype is unknown. The strain is resistant to nalidixic acid and streptomycin.

DH5α Genotype:	supE44, σlacU169, (Φ80 LacZσM15), hsdR17, recA1, endA1, gyrA96, thi-1, relA1
Rosetta 2 Genotype:	F-, ampT, $hsdS_B(r^B\text{-}m^B\text{-})$, gal, dcm(DE3), pRARE2($Cam^R$)

Key to *E. coli* genotype*:*

hsdR17	Abolishes restriction but not methylation of certain sequences
recA1	Abolishes homologous recombination
endA1	Endonuclease 1 activity absent, thought to improve quality of minipreps
gyrA96	Mutation in DNA gyrase. Resistance to nalidixic acid
thi-1	Requires thiamine for growth on minimal media
relA1	'Relaxed' mutation - permits RNA synthesis in absence of protein synthesis
F-	Strain does not contain the F episome
ampT	Causes lack of outer membrane protease to improve recovery of recombinant proteins
hsdS	Abolishes restriction and methylation at certain sites
Gal	Strain unable to utilise galactose
dcm	No methylation of cytosines in sequence CCWGG
DE3	Contains lambda prophage in which the gene for T7 RNA polymerase is under control of the lacUV5 promoter
pRARE2	Cam^R plasmid carrying the tRNA genes for seven codons rarely used in *E. coli*
Cam^R	Confers chloramphenicol resistance

2.1.2 Yeast strains

Two strains of *Saccharomyces cerevisiae* were used: AH109 (*MAT**a**, trp1–901*, *leu2–3*, *112*,*ura3–52*, *his3–200*, *gal4*, *gal80, LYS2*::*gal1*$_{UAS}$ *-GAL1*$_{TATA}$*-HIS3*,*GAL2*$_{UAS}$ *-GAL2*$_{TATA}$,*ura3*::*MEL1*$_{TATA}$ *–lacZ*) for bait vectors and Y187 (MATα, ura3-52, his3-200, ade2-101, trp1-901, leu2-3, 112, gal4Δ, met-, gal80Δ, URA3::GAL1UAS-GAL1TATA-lacz) for the cDNA library prey.

2.1.3 Plant material

Nicotiana benthamiana plants were used for transient expression of GFP fusion proteins and all subsequent experiments using this expression. *Arabidopsis thaliana* plants of the Col-0 ecotype were used for stable transformation and as a source of plant protein for Western blotting and, as a cell culture, for RNA extraction, cDNA synthesis and cloning. Seeds were obtained from Lehle Seeds.

T-DNA insert mutants of *A. thaliana* (Columbia background) were obtained from the Salk Institute Genomic Analysis Laboratory. Seed from these lines was obtained from ABRC.

2.1.4 Table of plasmids

Plasmid	Antibiotic resistance	Gene section	Use of plasmid	Obtained from
pDONR207	25 µg/ml gentamycin	Multiple	Donor vector in LR cloning	Invitrogen
pBI101G	50 µg/ml kanamycin	Promoter	Uses insert to drive GUS reporter gene	Dr M Kieffer, University of Leeds
pMDC83	50 µg/ml kanamycin	N-terminus	Labels insert with C-terminal GFP and expresses under 35S promoter	ABRC (from University of Zurich)
pGAT4	100 µg/ml ampicillin	Antigen fragments	Labels insert with HIS tag for protein purification	Dr T. Ketelaar, Durham University
pGBKT7	50 µg/ml kanamycin	Yeast two hybrid	Bait vector for yeast two hybrid library screen	Clontech

2.1.5 Table of primers

2.2.5.1 Cloning primers

Name	Sequence (5' to 3')	Annealing temperature ^{o}C	Use
NET1cABDFw	GGG GAC AAG TTT GTA CAA AAA AGC AGG CTT CAT GGA GAT TGC AGC AAA GAG TAA CTC G	65	Amplification of ABD of NET1c
NET1cABDRv	GGG GAC CAC TTT GTA CAA GAA AGC TGG GTC CTT GTC AGT TTC GGC CTT GGC	65	
NET1dABDFw	GGG GAC AAG TTT GTA CAA AAA AGC AGG CTT CAT GAC TGC TGT TGT GAA TGG TAA CTC	65	Amplification of ABD of NET1d
NET1dABDRv	GGG GAC CAC TTT GTA CAA GAA AGC TGG GTC CTT GTC AGT TTC GGA ACT AAC AAG GC	65	
NET2aABDFw	GGG GAC AAG TTT GTA CAA AAA AGC AGG CTT CAT GTT GCA GAG AGC AGC GAG CAA TG	63.5	Amplification of ABD of NET2a
NET2aABDRv	GGG GAC CAC TTT GTA CAA GAA AGC TGG GTC TGC GCT TTG AAG CTC TCT AGA TAA	63.5	

NET1aABDFw	GGG GAC AAG TTT GTA CAA AAA AGC AGG CTT CAC CAT GGC TAC TGT CTT GCA CTC AG		Amplification of Construct 4 from NET1a for yeast two hybrid
NET1aABDRv	GGG GAC CAC TTT GTA CAA GAA AGC TGG GTC CTT CTC AGA ATG CAA TCT ACT ATG C		
Yeast2 Fw	GGG GAC AAG TTT GTA CAA AAA AGC AGG CTT CAT GAT TGC TGA GCG AGC TAA CTT GC	62	Amplification of Construct 2 from NET1a for yeast two hybrid
Yeast2 Rv	GGG GAC CAC TTT GTA CAA GAA AGC TGG GTC TCA GAC ACG TTG TTC AAG GCG ATA GC	62	

AntiC Fw	GGG GAC AAG TTT GTA CAA AAA AGC AGG CTT CAT GTC TTT GGA GGA TTA TGT TTT CAC AC	63.6	Amplification of antigen fragment from NET1c
AntiC Rv	GGG GAC CAC TTT GTA CAA GAA AGC TGG GTC TCA TAC CAT CTC GGT TTC GTG ACT C	63.6	

AntiD Fw	GGG GAC AAG TTT GTA CAA AAA AGC AGG CTT CAT GCT TCA CGA ATT CGA GAA TGG ACC	65.3	Amplification of antigen fragment from NET1d
AntiD Rv	GGG GAC CAC TTT GTA CAA GAA AGC TGG GTC TCA CCC ATA TGA TGA GCA ATC AGA AAC	65.3	

GUSbFw	GGG GAC AAG TTT GTA CAA AAA AGC AGG CTT CTA TCT CAC CGA TCC TCC CGT T	60	Amplification of NET1b promoter for control of GUS reporter gene
GUSbRv	GGG GAC CAC TTT GTA CAA GAA AGC TGG GTC AGC TGC TGC AAG AAG CTC AAC	60	
GUSdFw	GGG GAC AAG TTT GTA CAA AAA GCA GGC TTC TTA ATG GGC CTA TCT GCA CGA AG	55	Amplification of NET1d promoter for control of GUS reporter gene
GUSdRV	GGG GAC CAC TTT GTA CAA GAA AGC TGG GTC TTT TCC CGG CAA AAT CAC ACA A	55	

2.2.5.2 Genotyping primers

Name	Sequence (5' to 3')	Annealing temperature ^{o}C	Use
S_151290Fw	ATT TCC GGT AAG CCT CAC AG	55	Genotyping of salk_151290 line, NET1d mutant
S_151290Rv	CTC TCA AAG CCA AGT ACA CC (used with Lba for insert PCR)	55	
S_069202Fw	GTG TAA TGT GTA TGT ATG TGA TGC G	55	Genotyping of salk_069202 line, NET1c mutant
S_069202Rv	GAC AAA TGA AAT CAC CCT AAT TTT G (used with Lba for insert PCR)	55	
S_139608Fw	GGC AGA TAT GGA TAG TAA TGT GAA GCA G	63	Genotyping of salk_139608 line, NET1c mutant
S_139608Rv	TCA TTG ATA AGC CTT GCA TCT TCC TC (used with Lba for insert PCR)	63	

S_032243Fw	GGT GTA CTT GGC TTT GAG AGA GAC TTG (used with Lba for insert PCR)	55	Genotyping of salk_032243, salk_033948 and salk_032339 lines, NET1d mutants
S_032243Rv	GAT AGG TGG ATA ACT GTC AGG CGT TTG T	55	
NETdGABIFw	GAT GAA AAC CAG CAC TCT GCC ATA G (used with Gabi RB for insert PCR)	60	Genotyping of NET1d GABI_KAT line
NETdGABIRv	TCG TTT TGT CCT TTG TTC GCA TCT	60	
NET1cSAILFw	AAT CCT CCA CTC ATC ATA ACC TAA GC	60	Genotyping of NET1c SAIL line
NET1cSAILRv	TCA AAG CAC CAC CAT GTG ACT CAT C (used with LBb for insert PCR)	60	
LBa1	TGG TTC ACG TAG TGG GCC ATC G	Determined by second primer in pair	Used for insert PCR during genotyping
Gabi RB	ATG GTT CAC GTA GTG GGC CAT C	60	Used for insert PCR during genotyping

NET1aQFw	CAA AGA CCA CAG AGA TAA ACC	56	qPCR to analyse expression of NET1a
NET1aQRv	GAG CTT CGT CTT CTC AGC TTC	56	
NET1bQFw	GTC AGC TTA TGA TCC TGT GAT AG	56	qPCR to analyse expression of NET1b
NET1bQRv	GCT TCG TGT TAT TTG CCT TGA TAG	56	
NET1cQFw	GCA TCG AGA GAT GCG GAT ATT G	56	qPCR to analyse expression of NET1c
NET1cQRv	CCA TTA TTG CTT CTG CGA TAG	56	
NET1dQFw	GAA GAT GCG AAC AAA GGA C	56	qPCR to analyse expression of

NET1dQRv	TGG TTA TTG CCT CCT CAA TAG	56	NET1d
Actin Fw	GGA TCG GTG GTT CCA TTC TTG	56	qPCR to analyse expression of actin
Actin Rv	AGA GTT TGT CAC ACA CAA GTG CA	56	

LBa1 and LBb1 primers designed by Salk Institute Genomic Analysis Laboratory. Primers used for Yeast Two Hybrid Construct 4 were designed by J. Calcutt (Calcutt 2009).

2.2 Methods

2.2.1 Cloning of NET1 proteins *(Chapters 4 and 5)*

2.2.1.1 RNA Isolation from plant tissue

The Qiagen RNeasy Plant Mini Kit was used for RNA isolation.
10 ml of plant cell culture was allowed to settle and the liquid medium removed, or frozen plant tissue was used. The tissue was placed in a pre-cooled mortar which had been previously baked at 180 ^{o}C overnight. The tissue was ground to a fine paste in liquid nitrogen and transferred to an Eppendorf tube without being allowed to thaw.

No more than 0.1 g was added to a second frozen Eppendorf tube and vortexed with 450 µl of RLT buffer (Qiagen). This was then added to a QIAshredder column and centrifuged at 13000 g for 2 minutes.

The supernatant of the flowthrough was added to an Eppendorf tube with 0.5 volume of EtOH and mixed by pipetting. This mix was added to an RNeasy column which was centrifuged at 8000 *g* for 15 s.

The flow through was discarded ant 700 µl of Buffer RW1 was added to the column. This was centrifuged at 8000 g for 15 s and the column placed in a new collection tube.

500 µl of Buffer RPE (Qiagen) was added and centrifuged at 8000 *g* for 15 s. A further 500 µl were added and centrifuged at the same speed for 2 minutes. The column was spun again for 1 min at 8000 *g* to dry the column.

The column was placed in an Eppendorf tube and 50 µl of RNase free water was added directly to the membrane. The tube was centrifuged at 8000 *g* for 1 min and the eluted RNA stored on ice until flash freezing in liquid N_2 for storage. This elution step was repeated to provide two elutions of RNA from each tissue sample.

2.2.1.2 Preparation of cDNA for amplification of gene fragments

RNA was purified from *Arabidopsis thaliana* cell suspension using the Qiagen RNeasy plant mini kit. It was then DNase treated using 20 µl of RNA, 10 µl of 10x DNase buffer, 1.37 µl or RNasin, 7.2 µl of RNase-free DNase and the volume was made up to 100 µl with DEPC treated water. This was incubated for 20 mins at 37 ^{o}C. After DNase treatment the Quiagen RNeasy mini protocol for RNA cleanup was used, eluting into a final volume of 50 µl.

For cDNA synthesis from this extracted RNA, the following was mixed in a PCR tube: 1 µl of gene specific primer (from a 100 µM stock), 5 µl of RNA and 4 µl of H_2O. Using a G-storm PCR machine, the mix was heated to 70 ^{o}C for 10 mins and then transferred to ice for 5 mins. The following were then added: 4 µl of first strand buffer, 1 µl of DTT, 1 µl of RNasin and 1 µl of dNTPS (from a 10 mM stock). This was heated to 50 ^{o}C for two minutes before the addition of 1 µl of Superscript III and being returned to 50 ^{o}C for 50 mins. The temperature was then increased to 70 ^{o}C for 15 mins. All reagents were obtained from Invitrogen except the dNTPs which were obtained from Bioline and the gene-specific primers and Superscript III enzyme which were from Sigma-Genosys.

2.2.1.3 Amplification of gene fragments using the polymerase chain reaction (PCR)

Unless previously mentioned, all reagents are from Promega. Reaction mix assembled on ice, adding the polymerase last.

Reagent	Volume/ µl
cDNA	1.0
dNTPS	1.0
5x HF buffer	10.0
Forward primer	1.5
Reverse primer	1.5
Phusion DNA Polymerase	0.5
H_2O	34.5

PCR programme used on a G-Storm PCR machine:

Temperature/^{o}C	Time/ s	Repetitions
98	30	1
98	10	35
65*	30	35
72	60	35
72	600	1
4	hold	1

* The 65 ^{o}C step is variable depending on the primer pair used. See Table of Primers.

2.2.1.4 Preparation of chemically competent *E. coli* cells

One hundred ml of SOB medium was inoculated with three colonies of DH5α and incubated at room temperature with shaking until an OD_{600} of 0.6 was achieved. The culture was placed on ice for 10 minutes then centrifuged at 2500 *g* for 5 minutes at 4 ^{o}C. The supernatant was poured away and the pellet resuspended in 32 ml of ice-cold TB buffer. This was incubated on ice for 10 minutes and then centrifuged at 2500 *g* for 5 minutes. The pellet was again resuspended in 8 ml of TB buffer with 0.61 ml DMSO and incubated on ice for 10 minutes before flash freezing in liquid N_2 in 400 µl aliquots. Cells were stored at -80 ^{o}C

SOC liquid media- 1litre

- 20g Triptone
- 5g yeast extract
- 0.5 g NaCl
- 2.5 mM KCl
- Adjust to pH 7.0 then sterilise by autoclave
- After sterilisation add filter sterilised 10 mM $MgCl_2$ and 20 mM glucose

TB buffer - 200 ml

- 10 mM PIPES, pH 6.7
- 15 mM $CaCl_2.2H_2O$
- 250 mM KCl
- Adjust to pH 6.7 with KOH
- After adjustment of pH, add 55 mM $MnCl_2.4H_2O$ and sterilise by filtration.

2.2.1.5 Transformation of chemically competent *E. coli* cells

Competent *E. coli* cells were thawed on ice and 1 - 20 µl of plasmid DNA added to each aliquot of 200 µl of cells. The cells were incubated on ice for 30 mins and then heat shocked at 42 ^{o}C for 30s. The cells were returned to ice for 10 mins. After incubation, 800 µl of SOB media was added and the cells were incubated at 37 ^{o}C for 1 hr with shaking. The cells were then plated on antibiotic selection, LB agar plates.

LB (Luria-Bertani) agar media – 1litre

- 10 g NaCl
- 10 g peptone
- 5 g yeast extract
- 20 g agar (solid media only)
- pH 7.0

2.2.1.6 Gateway cloning (used for cloning of promoter region, N-terminal fragments of NET1d and c and the cloning of gene fragments for use as antigens)

Gateway cloning (Invitrogen) relies on the ability of the Clonase (Invitrogen) enzymes to replace one section of a plasmid with another when a specific sequence of bases is recognised. For successful gateway cloning, Gateway sequences are added to both forward and reverse primers, and are used to amplify the gene of interest with the extra Gateway sequence on each end. The BP Clonase enzyme is then used to remove the toxic cassette from the donor vector, pDONR207 and replace it with the gene of interest. The toxic cassette ensures that cells taking up plasmid DNA without the gene of interest do not survive, and antibiotic selection ensures that only cells containing the pDONR207 plasmid grow on the selection plates after transformation.

Once the gene of interest is inserted into the pDONR207 vector, the LR Clonase enzyme can be used to move the gene to a destination vector (such as pMDC83 which adds a C-terminal GFP tag) for further use. Use of Gateway cloning technology increases speed and simplicity of cloning and has been used in all cases.

After amplification of the gene of interest using PCR, the BP reaction is set up to insert the gene into the donor vector. For the BP reaction the following were added to

6 µl of PCR reaction: 1 µl of pDONR207, 1 µl of TE buffer (10 mM Tris, 1mM EDTA, pH 7.5) and 2 µl of BP Clonase II (Invitrogen).
This was incubated at 25 ^{o}C for 1 hour before addition of 1 µl of Proteinase K (Invitrogen) and incubation at 37 ^{o}C for 10 minutes.

One – eight µl of BP reaction were added to 50 µl of chemically competent DH5α cells and placed on ice for 25 minutes. The cells were then heat shocked at 42 ^{o}C for 40s before being returned to ice for 2 minutes. Three hundred µl of LB media was added and the cells were incubated at 37 ^{o}C for 45 minutes. The cells were plated out on 25 ml LB plates with 25 µg/ml gentamycin.

After an overnight incubation at 37 ^{o}C the resulting colonies were used for plasmid purification using the Promega mini-prep kit. The plasmid was sequenced by the Durham University DNA sequencing service to confirm that the correct gene fragment was present.

Two µl of the purified plasmid was added to 1 µl of destination vector, 5 µl of TE buffer and 2 µl of LR Clonase II (Invitrogen) and incubated for 1 hour at 25 ^{o}C followed by addition of 1 µl of Protienase K and incubation at 37 ^{o}C for 10 mins. Chemically competent DH5α cells were transformed as above, but using 1 µl of LR reaction and plating out onto LB agar containing the antibiotic appropriate to the destination vector. The plasmids were purified and checked as before. The specific gene sections, plasmids and antibiotics are listed in the Materials section.

10 x Tris EDTA (TE) buffer

- 100 mM Tris-Cl
- 10 mM EDTA
- pH 7.4

2.2.1.7 Miniprep plasmid purification from *E. coli* after transformation

Plasmid DNA was purified using the Promega Wizard SV Miniprep DNA Purification System. Five ml of overnight culture were grown for approx 16 hours in LB liquid media with any antibiotic needed for selection of the bacteria grown (see antibiotic resistance of plasmids). The cultures were spun down at 5000 g for 5 minutes and resuspended in 250 µl of Resuspension solution by vortexing. Two hundred and

fifty µl of Lysis solution was added, followed by 350 µl of Neutralisation solution. The solutions were transferred to an Eppendorf tube and centrifuged at 4000 *g* for 10 minutes.
The supernatant was place in a spin column and centrifuged at top speed for 1 minute. The flow through was removed and 750 µl of Wash solution was added and spun as before. This was repeated with 250 µl of Wash solution. The flow through was removed and the columns centrifuged for two minutes at maximum speed to dry the column. Fifty µl of nuclease free water was added to the column membrane and centrifuged at the same speed for 1 min. Eluted DNA was stored at -20 ^{o}C.

2.2.1.8 Restriction digest of plasmid DNA and agarose gel electrophoresis

Restriction digests were used during cloning to establish whether individual cloning steps had been successful prior to sequencing using DBS Genomics. Gel electrophoresis was used to analyse the DNA fragments produced by the digest, but the same technique was used for analysis of the results of genotyping.

For a restriction digest the following reagents were added to an Eppendorf tube:

- DNA - 4 µl
- 5 x Buffer - 2 µl
- H_2O - 13 µl
- Enzyme 1 - 0.5 µl
- Enzyme 2 - 0.5 µl

Enzymes varied depending on plasmid and insert, with the aim to cut the plasmid within the vector backbone and within the inserted gene fragment. Buffer varied depending on the enzyme used. Enzymes and buffers were from both Promega and Fermentas.

The digest mix was incubated at 37 ^{o}C for two hours and 15 µl was run on a 1% (w/v) Agarose Low EEO (Melford) gel containing 1 µM ethidium bromide, at a 100 V for 20 - 30 mins. Gels were made with, and run in, 1 x TAE buffer (40 mM Tris acetate and 1 mM EDTA). Samples were loaded with 5 µl of Loading Buffer and one lane was loaded with 5 µl of Hyperladder I (Bioline).

2.2.2 Plant growth conditions *(Chapters 4, 5 and 6)*

2.2.2.1 Seed sterilisation protocol for sowing seeds on solid media plates

Seeds were placed in an Eppendorf tube with 600 µl of 6% (v/v) sodium hyperchlorite solution for 10 minutes at room temperature. The bleach was then removed and replaced with 600 µl of dH_2O. This wash step was repeated five times. Seeds were then removed onto filter paper to dry and either placed on the solid media plates using tweezers of shaken over the plate once completely dried. The plates were then sealed with micropore tape and placed either at +4 ^oC to ensure synchronised germination, or under normal growth conditions for *A. thaliana.*

½ MS media – 1litre

- 2.2 g Murashige & Skoog Basal Medium 5524 (Sigma Aldrich)
- 8 g/l Plant agar (Duchefa Biochemie)
- pH 5.7, use KOH to adjust

2.2.2.2 Growth conditions for *A. thaliana* and *N. benthamiana*

N. benthamiana seeds were sown directly onto a mixture of 3 parts compost (J Arthur Bowers) and 1 part sand. Several seeds were sown per pot, and the soil was watered with Intercept insecticide (Bayer) at a concentration of 0.2 g/l dissolved in water. Pots were placed in a greenhouse with 16 hours light and 8 hours darkness a day. The day temperature was 20 ^oC and the night temperature dropped to 18 ^oC. The pots were covered with cling film until seedlings were 1 – 2 cm high to create a humid environment. The film was then removed and the seedlings thinned to one or two per pot. These were then grown under the same conditions and kept well watered until use, preferably when plants are young and have approximately 6 – 10 leaves.

A. thaliana seeds can be sown directly on to soil or transferred from plates from 6 – 15 days post germination. In either case, a mix of 3 parts compost (J Arthur Bowers) and 1 part sand or individual peat plugs (Jiffy) were used. The compost mix was watered with Intercept insecticide (Bayer, 0.2 g/l) but the peat plugs are already sterilised. If using seeds, they were scattered onto the surface of the soil and covered

with compost until 1 cm high seedlings had grown. They were then thinned or transferred to fresh soil and covered using a propagator lid until the beginning of bolting.

If using plants previously germinated on soil, they were transferred to the soil using tweezers and covered with a propagator lid until the beginning of bolting.

The *A. thaliana* seeds were grown using a cycle of 16 hours light and 8 hours dark. The daytime temperature is 20 ^{o}C and the night temperature is dropped by 2 ^{o}C to 18 ^{o}C.

2.2.3 Transient expression on NET1 proteins and imaging of plant tissue *(Chapter 4)*

2.2.3.1 Preparation of competent *A. tumefaciens*

Colonies of A. tumefaciens were added to 50 ml LB media and grown until OD_{600} = 0.5 - 1. The cultures were then incubated on ice for 30 minutes before centrifugation at 3000 *g* for 6 minutes at 4 ^{o}C. The supernatant was removed and the cells resuspended in 2 ml of 20 mM $CaCl_2$. One hundred µl aliquots were flash frozen in liquid N_2 and stored at -80 ^{o}C until use.

2.2.3.2 Transformation of *Agrobacterium tumefaciens* and infiltration of *N. benthamiana* leaves

One µl of the construct was added to 50 µl of chemically competent *A. tumefaciens* and frozen in liquid nitrogen. The cells were thawed by incubating at 37 ^{o}C for 5 minutes. 300 µl of YEB media was added and the cells were incubated at 30 ^{o}C for 4 hours. The cells were then plated out on 20 ml YEB agar plates with 25 µg/ml gentamycin, 25 µg/ml rifampicin and the antibiotic specific to the destination vector (usually 50 µg/ml kanamycin).

For infiltration of plant leaves the method is based on that described by Brandizzi *et al.* 2002. Four ml overnight cultures of the transformed bacteria and bacteria containing the P19 construct (used to suppress silencing of the gene) were set up and allowed to grow to an OD_{600} of 0.5 – 1.0. The liquid cultures were YEB with the same antibiotic concentrations as the YEB agar plates. These were then centrifuged at 4000 *g* for 5 minutes and resuspended in 2 ml of infiltration solution (10 mM MES pH 6.5, 10 mM $MgCl_2$, 200 µ M acetosyringone (2-(N-Morpholino)-ethanesulfonic acid)). This was repeated twice and the cells were then left at room temperature to incubate for four hours.

The construct and P19 solutions were mixed in a 1:1 ratio prior to infiltration. When two constructs were infiltrated simultaneously into the leaf the *Agrobacterium* solutions were mixed in a 1:1:2 ratio of construct 1: construct 2: P19. The solutions were injected into leaves using a needleless syringe after three small cuts had been made on the leaf with a scalpel blade. The plants were kept under their previous growth conditions for two to three days before sections of leaf were taken for imaging.

YEB media – 1litre

- 5 g beef extract
- 1 g yeast extract
- 5 g peptone
- 5 g sucrose
- 0.5 g $MgSO_4.7H_2O$
- 20 g Agar (plates only)
- pH 7.2

2.2.3.3 Imaging

Leaf samples were mounted in dH_2O and cells of the lower epidermis were viewed using a Zeiss LSM 510 confocal laser scanning microscope. The lens was a x40 oil lens. The GFP samples were excited with a 30 mW argon laser at 488 nm. In all cases, GFP is used to refer to Enhanced GFP, or EGFP. The emission fluorescence was detected between 505 – 530 nm. DSRed samples were imaged using 10 mW helium neon laser at 543 nm to excite the samples and the fluorescence was detected at approximately 560 nm.

Imaging was also undertaken on a Leica SP5 confocal microscope, also using x40 or x63 oil lenses. Sample mounting was as above, GFP was imaged using 488 nm laser line and fluorescence detected at 500 – 530 nm. DSRed was imaged using a 543 nm laser light and fluorescence was detected at 555 – 620 nm. Roots stained with calcofluor were imaged using the 405 nm laser, with fluorescence emitted between 409 – 487 nm.

Imaging of whole plant tissue for GUS staining and Lugol staining used an Olympus Research Stereo SZH10 light microscope (capable of magnification between x0.7 and x10) with a Photometrics Coolsnap cf video camera and Openlab 3.1.1 software.

2.2.3.4 Co-localisation of two constructs

The GFP and DSRed constructs were infiltrated into the leaves simultaneously according to the infiltration protocol above and the leaf was imaged three to four days post infiltration as the DSRed is expressed at a lower level than the GFP and requires a greater time for expression to be detectable.

Leaf sections of 1 cm x 1 cm were cut from the leaf and mounted in dH_2O. The leaf sections were imaged with the Zeiss 510 confocal microscope, using 488 nm light to excite the GFP (fluorescence detected between 505 and 530 nm) and 543 nm light to excite the DSRed (fluorescence detected at approximately 460 nm).

2.2.3.5 Drug studies

For all drug studies, leaves of *N. benthamiana* were infiltrated with *A. tumefaciens* solution to induce transient expression of the NET1x-ABP-GFP construct. Two to three days post infiltration small sections of leaf (approximately 1 cm x 1 cm) were cut and incubated with either the anti-actin drug or the control solution or DMSO as described below. After treatment, the leaf sections were imaged on the Zeiss 510 microscope, using 488 nm light to excite fluorescence in the green fluorescent protein.

Latrunculin B (Calbiochem): sections of leaf were incubated with 50 µM Latrunculin B (50 µl of 1 mM Latrunculin B in 950 µl PBS (100 mM Na_2HPO_4, 100 mM NaH_2PO_4)) for 30 mins. For a control leaf sections were incubated with 50 µl of DMSO and 950 µl PBS as the drug stocks is in DMSO.

Cytochalasin D (Sigma-Aldrich): sections of leaf were incubated with 100 µM Cytochalasin D (10 µl of 10 mM of Cytochalasin D in 990 µl PBS) for 30 mins. For a control leaf sections were incubated with 10 µl of DMSO and 990 µl PBS.

2.2.3.6 Fluorescence recovery after photobleaching

Leaves of *N. benthamiana* were infiltrated with the NET1c-ABD GFP or NET1d-ABD GFP construct using the infiltration protocol. Three days post infiltration 1 cm x 1 cm sections of leaf were cut and mounted in dH_2O. The leaf samples were imaged on a Leica SP5 confocal microscope, using 488 nm light to excite fluorescence.
The Leica FRAP Wizard was used to undertake the experiment. The experiment was set up to take one initial image of the cell, and then to focus on the selected region with the 488 nm laser at full power to photobleach the region of interest for three frames, each frame taking approximately 0.7 s. After bleaching, the wider cell around the region of interest was again imaged for a further 20 – 30 frames to assess recovery of fluorescence.

2.2.4 Yeast two hybrid *(Chapter 4)*

2.2.4.1 Yeast transformation

A 10 ml YPDA overnight culture of either AH109 or Y187 strains of yeast was set up and used to inoculate a 100 ml YPDA culture which was grown until it reached an OD_{600} of 0.4 – 0.6. This culture was pelleted at 1000 *g* for 5 minutes and resuspended in 50 ml of H_2O. It was spun down as above and resuspended in 1 ml Li/TE, then spun again and resuspended in 500 µl of Li/TE.

Eighty µl of salmon sperm DNA was incubated at 100 ^oC for 20 minutes and added to 10 µl of the plasmid. One hundred µl of yeast cells with 10 µl DMSO, 600 µl PEG/Li/TE were added to the plasmid and salmon sperm DNA and gently mixed. The cells were incubated as 30 ^oC for 30 minutes and 42 ^oC for 15 minutes. They were then spun down at 1000 *g* for 1 min and resuspended in 250 µl of H_2O. One hundred µl of the yeast were plated onto a 25 ml SD plate with the appropriate drop out solution and incubated at 30 ^oC for three days.

2.2.4.2 Autoactivation test

The four constructs and the formin control were transformed into the AH109 yeast strain. Three colonies of each construct and the control were suspended in 30 µl of ddH_2O and 5 µl of each colony was placed on each of four plates (-W, -W-A, -W-H and -W+X-α-gal). The drops were allowed to dry and the plates were incubated for between 1 and 3 days at 30 ^oC.

2.2.4.3 Mating test

The three constructs that did not show autoactivation were transformed into the Y187 yeast strain and 10 ml SD overnight cultures of each construct and the oligodT library were set up and used to inoculate 100 ml SD overnight cultures. These were allowed to grow to an OD_{600} of approximately 1 and the numbers of cells were counted. The ratio of library : bait was set at 1:4 and for construct 4 3×10^8 cells of the library were used and with constructs 3 and 1, 1.5×10^8 cells were used. The relevant volumes of cells were mixed and spun for 5 minutes at 1000 *g* before being resuspended in 1 ml of YPDA. 200 µl of cells were plated out on each of 5 25 ml YPDA plates and incubated overnight at 30 ^oC. The cells were then washed from the plates using ½ YPDA and spun for 5 minutes at 1000 *g* before being resuspended in 10 ml of ½ YPDA. The cells were diluted 1:100, 1:1000, 1:10,000 using H_2O and 100 µl of each

dilution was plated on a -W, -L and -W-L plate. After three days at 30 ^{o}C the numbers of cells were counted and the mating efficiency calculated.

2.2.4.4 Library screen

A 10 ml (-W) SD culture of the construct was grown overnight and used to inoculate a 100 ml (-W) SD overnight culture. This was grown to an OD_{600} of approximately 1 and the cells were counted. One ml of random primer library and 625 µl of oligodT library were mixed to give 3 x 10^8 cells and mixed with the relevant volume of yeast cells containing the construct. The mixed cells were spun down at 1000 *g* for 5 mins and resuspended in 1 ml of YPDA. Two hundred µl of the cells were plated onto each of two 25 ml YPDA plates and incubated overnight at 30 ^{o}C. The following day the cells were washed from the plates using ½ YPDA, spun down as above and resuspended in 10 ml ½ YPDA. One hundred µl were used for sequential dilutions as above in the mating test to check for mating efficiency and the remainder of the cells were plated out onto 200 mm -W-L-H SD plates containing 5 mM 3AT to inhibit histidene synthesis and 50 µg/ml kanamycin. Two hundred µl of yeast cells were used per plate and the plates were incubated at 30 ^{o}C for two weeks. Colonies that appeared were transferred to 3 dropout and 4 dropout plates to confirm the ability to grow on drop out medium.

2.2.4.5 Plasmid rescue

Each colony was rescued from the plate and grown in 10 ml 3 or 4 dropout SD for 48 hours at 30 ^{o}C. The cultures were spun down at 5000 *g* for 2 minutes and resuspended in 50 µl yeast lysis buffer. The cells were vortexed to mix and incubated at 37 ^{o}C for 1 hr. Two hundred µl of P1 resuspension buffer (Qiagen) was added and vortexed, followed by 250 µl of P2 buffer (Qiagen) which was mixed and incubated at room temperature for 4 minutes. Three hundred and fifty µl of P3 neutralisation buffer was added (Qiagen) and the Promega miniprep procedure was followed from the point following addition of neutralisation solution and eluting into a final volume of 25 µl H_2O. The rescued plasmids were sequenced using the Durham University DNA sequencing service.

2.2.4.6 Yeast one-on-one mating test to confirm interaction

Construct 4 and the empty bait vector (pGBKT7) were transformed into Y187 and the potential interactors were transformed into the AH109 yeast strain.

One colony of yeast containing the bait vector was resuspended in 30 µl of H_2O and 3 µl of this was placed on a YPDA media plate and allowed to dry. One of the prey vectors was then resuspended in 30 µl of H_2O and 3 µl was placed on top of the drop containing the bait vector and allowed to dry. The plates were sealed and left at room temperature for 24 hours.

The mated yeast were selectd for diploid yeast by streaking a small quantity of yeast from the YPDA plate onto a -W-L drop out plates. The plates were sealed and stored at 30 ^{o}C.

After four days, one colony of diploid yeast from the -W-L plates was resuspended in 30 µl of H_2O and 3 µl was placed onto one of each of -W-L, -W-L-H and -W-L-H-A plates. Each potential prey vector was mated with both construct four and the empty bait vector. Plates were sealed and the presence of absence of colonies was observed after one day.

10 x Tris EDTA (TE) buffer

- 100 mM Tris-Cl
- 10 mM EDTA
- pH 7.4

10 x LiAC

- 10 mM Tris-HCl, pH 8.0
- 1 mM EDTA
- M Lithium acetate

Li/TE – 3 ml

- 0.3 ml 10x LiAc
- 0.3 ml 10 x TE buffer
- 2.4 ml H_2O

PEG/Li/TE – 3 ml

- 0.3 ml 10 x LiAC
- 0.3 ml 10 x TE buffer
- 2.4 ml 50% (v/v) PEG

Dropout mix (amino acids from sigma)

- 3 g L-isoleucine
- 15 g L-valine
- 2 g L-arginine HCl
- 3 g L-lysine
- 2 g L-methionine
- 5 g L-phenylalanine
- 20 g L-threonine
- 3 g L-tyrosine
- 2 g L-uracil

10 x dropout solution – 400 ml

- 2.2 g dropout mix
- The following were added depending on the dropout required:
- 80 mg L-adenine hemisulphate
- 80 mg L-histidine HCl monohydrate
- 400 mg L-leuine
- 80 mg L-tryptophan

YPDA growth media – 1litre

- 20 g peptone
- 10 g yeast extract
- 20 g agar (solid media only)
- pH 6.5, sterilised by autoclaving
- After sterilisation, addition of 50 ml 40% (v/v) glucose and 15 ml 0.2% (w/v) adenine hemisulfate
- ½ YPDA requires half of all quantities in the same volume

SD minimal growth media – 1litre

- 6.2 g Difco yeast nitrogen base without amino acids (BD)
- 20 g agar (solid media only)
- pH adjusted to 5.8 and then sterilisation by autoclave
- After sterilisation, addition of 50 ml 40% (w/v) glucose solution and 100 ml 10 x dropout solution

2.2.5 Creation of *A. thaliana* lines, genotyping of plants and staining of plant tissue from transgenic lines *(Chapters 5 and 6)*

2.2.5.1 Crossing of *A. thaliana* plants

Flowers of the plant to be pollinated, which showed the stigma at the correct stage of development, were prepared the day before crossing was carried out. The sepals, petals and anthers were removed using fine forceps under a dissecting microscope. They were then marked with tape and left overnight so that any damaged flowers would die before crossing took place.

The pollen from the donor plant was then collected by removing the whole flower with fine forceps so that the anthers were exposed and pollen was applied to the pre-prepared parent plant. Flowers that had been cross-pollinated were marked with tape and seed collected from the resultant silique.

2.2.5.2 Edwards prep for genotyping Arabidopsis

This method of genomic DNA extraction was based on the method described in Edwards *et al.* 1991. One leaf, approximately 1.5 cm in length, was collected in an Eppendorf tube from each plant to avoid cross-contamination between plants. These were immediately frozen in liquid nitrogen.

The sample was then ground using an Eppendorf grinder within the tube until it formed a fine powder. Four hundred µl of extraction buffer was added to the tube and vortexed for five seconds.

All samples were centrifuged at 16000 *g* for 4 minutes and 300 µl of the supernatant was transferred to a new tube where 300 µl of isopropanol was added. This was left to incubate at room temperature for two minutes to allow genomic DNA to precipitate before centrifugation at 16000 *g* for 5 minutes.

The supernatant was removed and 200 µl of 70% (v/v) EtOH was added to wash the pellet before centrifugation at 16000 *g* for 5 minutes.

The EtOH was removed and the pellet allowed to dry completely at room temperature before the addition of 30 µl of H_2O.

Extraction buffer:

- 200 mM TrisHCl pH 7.5
- 250 mM NaCl
- 25 mM EDTA
- 0.5 % (w/v) SDS

2.2.5.3 Genotyping of *A. thaliana*

Genomic DNA was extracted from the leaves of the plants using the Edward's Prep method. This DNA was then used as the template for a genotyping PCR. In this case, RedTaq polymerase (Bioline) was used. The following reagents were added to a PCR tube on ice.

Reagent	Volume /µl
DNA	1
dNTPs	1
10 x NH_4 buffer	5
$MgCl_2$	2
Forward primer	1.25
Reverse primer	1.25
H_2O	35
RedTaq polymerase	1
Total volume	50

The tubes were placed in a G-storm gradient PCR machine and run using the following program.

Temp /^oC	Time /mins	Repetitions
94	2	1
94	1	35
65*	1	35
72	1.5	35
72	10	1
4	hold	1

** Temperature varies depending on the annealing temperature of the primers (see Table of Primers)*

Five µl of the products of the PCR were run on a 1 % (w/v) agarose gel with 5 µl of Loading Buffer (Bioline). For gel electrophoresis protocol see 'Restriction digest of plasmid DNA and agarose gel electrophoresis'.

2.2.5.4 qPCR to analyse levels of expression of the NET1 genes

Total RNA was extracted from seedlings 2 - 3 days post-germination, using the RNA extraction protocol. This RNA was used as a template for cDNA production, using oligo dT primers to give a sample of all mRNAs within the seedlings.

SYBRgreen mix (Sigma-Aldrich) was used to provide the DNA polymerase and the SYBRgreen fluorescent dye, and the mix includes both buffer and dNTPs with the enzyme for greater consistency. The following template and primer mixes were made for each cDNA template and each primer combination. Using master mixes for each cDNA and each primer improves consistency of mixes which is key for successful results.

Template mix - for 1 reaction

- 2 x Sybr green mix - 7.5 µl
- H_2O - 7 µl
- cDNA - 0.5 µl
- Total volume - 15 µl

Primer mix – for 1 reaction

- Primer 1 (10pmol/µl) - 0.5 µl
- Primer 2 (10 plmol/µl) - 0.5 µl
- H_2O - 4 µl
- Total volume - 5 µl

For each cDNA of interest, there must be two primer pairs - the primers to the gene of interest and primers to a control gene, in this case actin. For each primer pair, there must be three cDNA templates - the wild type control, the mutant of interest and the water only negative control. In some cases there is no mutant, only the wild type plant when the technique is used to analyse expression rather than lack of transcription in a mutant plant.

A Rotorgene 3000 Real Time PCR Machine was used, which can take a maximum of 36 tubes. To set up the reaction, 5 µl of primer mix was added to each tube. Fifteen µl of template mix was then added to the primer mix and mixed by gentle pipetting to avoid introducing air bubbles to the mix. All preparation is carried out on ice.

The tubes were placed in the machine and the following program used:

Temp /^{o}C	Time /s	No. Cycles
95	120	1
95	20	60
56	20	60
72	40	60

After this, melt curve analysis was used, ramping the temperature from 55 ^{o}C to 99 ^{o}C at intervals of 1 ^{o}C, pausing for 30 s on the first step and for 5 s for each subsequent step.

2.2.5.5 Stable transformation of *A. thaliana*

The method of transformation by floral dipping is taken from the method used by Clough and Bent 1998. The construct to be transformed into the *A. thaliana* plant was transformed into *A. tumefaciens* strain C58C3. Colonies from this transformation were grown in liquid YEB media with 25 mg/l nalidixic acid, 100 mg/l streptomycin and the selection antibiotic for the gene of interest. The cultures were grown for 48 hours and then centrifuged at 2000 *g* for 20 minutes. The pellet was resuspended in 1 litre of 5 % (w/v) sucrose solution. 0.005% (v/v) Silwett L-77 (Lehle Seeds) was added to the solution.

Wild type Columbia var. *A. thaliana* were grown in individual pots until bolting. Any siliques that had formed were removed prior to dipping.

Plants were inverted and dipped into the *A. tumefaciens* solution for 15 - 30 seconds, and then placed on a tray inside an autoclave bag. The bag was sealed and the plants left in the dark for 24 hours. Plants were then removed from the bag to the greenhouse growth conditions (16 hours light at 20 ^{o}C and 8 hours dark at 18 ^{o}C) and allowed to set seed. Aracons (BetaTech) were used to prevent seed loss and seed was collected once the plant had dried.

2.2.5.6 Selection of transformants after stable transformation of *A. thaliana*

In this project, the selection of transformants was for those containing the pBI101G plasmid for the GUS reporter gene driven by the promoter of the gene of interest. This plasmid confers resistance to kanamycin.

Fifty µg/ml kanamycin for selection of plants containing the pBI101G plasmid, and 300 µg/ml of augmentin (to prevent growth of any *A. tumefaciens* remaining on the seeds) were added to 20 - 30 ½ MS media in 25 ml horizontal plates. Seeds for selection were then sterilised and scattered thinly over the surface of the plates. The plates were sealed with micropore tape and placed under 16 hour, 20 ^{o}C day and 8 hour, 18 ^{o}C night growth conditions.

After germination, plants lacking the pBI101G plasmid begin to die before progressing past the two cotyledons stage of development. Seeds which do contain the plasmid are resistant to the selection and go on to develop true leaves. These can be rescued from the plate either to soil or to another plate to develop further before eventual transfer to soil.

2.2.5.7 GUS histochemical staining

After stable transformation and selection of transformants, the T1 plants were allowed to set seed. Seed was collected from these plants, sterilised according to the Seed Sterilisation Protocol and grown on vertical plates until six days post germination. Seedlings were then removed from the plate and immersed in GUS buffer. The seedlings in buffer were placed at 37 ^{o}C until visible blue colouration of the tissue was observed. Staining was apparent between one and twelve hours after the beginning of incubation.

Once staining had occurred, an ethanol series was used to clear the tissue without causing damage to root observed when seedlings were placed immediately in 95% (v/v) EtOH. The seedlings were incubated for 1 hour each in 10%, 30%, 50%, 70% and 95% (v/v) EtOH before imaging using an Olympus Research Stereo SZH10 light microscope, using a magnification between x0.7 and x10 and Openlab 3.1.1 software.

GUS buffer

- 61 mM Na_2HPO_4
- 39 mM Na_2HPO_4
- 10 mM EDTA
- 0.1% (v/v) Triton X-100
- Buffer was made and stored at 4 ^oC until use, when the following were added
- 5 mM potassium ferricyanide
- 0.5 mM potassium ferrocyanide
- 1 mM X-Glc (5-bromo-4-chloro-3-indolyl-β-D-glucuronide) (stock in DMF)

2.2.5.8 Fixation of roots after GUS histochemical staining

This fixation protocol is based on Karnovsky, MJ. 1965. After staining in GUS buffer as above, but prior to placing seedling in the ethanol series, the seedlings were immersed in Karnovsky's fixative on ice for three hours. The fixative solution was then replaced before incubation overnight at 4 ^oC. The seedlings were then rinsed in 0.1 M phosphate buffer for 30 mins. This rinse was repeated three times and the seedlings were then placed in the same ethanol series as conventional GUS staining – 1 hour each in 10%, 30%, 50%, 70% and 95% (v/v) EtOH. The seedlings were then placed in 95% (v/v) EtOH overnight.

Samples were embedded using the Historesin Embedding kit (Leica). Infiltration solution was prepared using 50 ml Basic Resin liquid with 1 packed of Activator and the samples were incubated at 4 ^oC in 3:1 v/v EtOH:Infiltration solution for 6 hours, 1:1 v/v EtOH:Infiltration solution overnight, 1:3 v/v EtOH:Infiltration solution for 6 hours and finally Infiltration solution overnight. The seedlings were embedded using Embedding medium (15 ml Infiltration solution and 1 ml Hardener) and left to harden overnight. Samples were sectioned in 50 µm sections using a Reichert Ultracut ultramicrotome and floated onto water before drying and mounting on slides.

Karnovsky's fixative

- 2% (w/v) paraformaldehyde dissolved in 60 ^oC H_2O with 0.1M KOH added dropwise until pH > 8
- HCl used to return pH to 7.0
- 2.5% (w/v) gluteraldehyde
- 0.1 M phosphate buffer (pH 7.4)

2.2.5.9 Lugol staining

Seedlings of *A. thaliana* were grown on vertical plates of ½ MS media under the usual plant growth conditions until 3 or 9 days post germination. The whole plant was then immersed in Lugol Stain for 4 minutes until the ends of the roots appeared dark. The seedlings were removed and rinsed in dH_2O. The plants were then mounted on slides and one drop of Hoyer's solution applied. The coverslip was added and the plants allowed to clear for 30 mins before imaging.

Hoyer's Solution:

- 30 ml H_2O
- 2.5 g gum arabique
- 100 g chloral hydrate
- 5 ml glycerol

2.2.6 Production of antibodies for immunostaining *(Chapter 5)*

2.2.6.1 Protein expression in *E. coli*

The gene to be expressed was cloned into the pGAT4 vector and transformed into chemically competent Rosetta2 cells. Five colonies from this transformation were added to 100 ml of LB media with 50 µg/ml kanamycin and 10 µg/ml chloramphenacol. The culture was shaken overnight at 37 ^{o}C.

One ml of this overnight culture was added to 1 l of LB media with the same antibiotics and shaken at 37 ^{o}C until an OD_{600} between 0.4 and 0.8 was reached. At this point 1 ml of 1 M IPTG was added and the culture was incubated at 37 ^{o}C for three hours with shaking. The culture was then centrifuged at 6000 *g* for 10 minutes and resuspended in 10 ml Lysis buffer. The cells were then flash frozen in liquid N_2.

2.2.6.2 Protein purification

The frozen cells produced during protein expression were transferred to a 37 ^{o}C water bath until just thawed and were then centrifuged at 90,000 *g* for 15 minutes at 4 ^{o}C. The supernatant was filtered and stored on ice.

Two ml of nickel-nitrilotriacetic acid (Ni-NTA) resin slurry (Qiagen) was spun down at 500 g for 5 minutes and resuspended in Lysis buffer before repeat centrifugation and removal of the buffer to give a 1 ml bed volume of beads in a 50 ml tube. The supernatant was added to the beads and incubated on ice for 20 minutes with shaking. The mix was then spun down at 450 *g* for 5 minutes.

The beads were resuspended in 10 ml Wash solution and centrifuged as before. This was repeated four times. One ml of Elution buffer was then added to the beads and incubated on ice for 5 minutes. This was centrifuged as before and the eluted fraction stored on ice. The elution stage was repeated three times. Concentration of protein was measured using a Nanodrop Spectrophotometer.

Lysis buffer

- 100 mM NaH2PO4
- 10mM Tris-Cl
- 8M Urea
- pH 8.0, adjust using NaOH

Wash Buffer

- 100 mM NaH2PO4
- 10mM Tris-Cl
- 8M Urea
- pH 6.3, adjust using HCL

Elution Buffer

- 100 mM NaH2PO4
- 10 mM Tris-Cl
- 8M Urea
- pH 4.5, adjust using HCl

2.2.6.3 Dialysis of protein into phosphate buffer

The purified protein was eluted into a buffer containing urea before storage and this was removed before use by dialysis. The protein was allowed to thaw slowly on ice and then placed in a short length of dialysis tubing, sealed at each end and with any air excluded from the tube. This was placed immediately into 2 litres of pre-chilled 1 x PBS buffer. The buffer was incubated at 4 ^{o}C with gentle stirring and changed at least five times within 1.5 hours. After dialysis the protein was used immediately.

10x PBS

- 0.14 M NaCl
- 2.68 mM KCl
- 1.25 mM Na_2HPO_4
- 1.98 mM KH_2PO_4
- pH 7.0

2.2.6.4 Production of polyclonal antibodies in rat and rabbit

Antibodies to NET1c were raised in rabbits and antibodies to NET1d were raised in rats. Freshly dialysed protein was used in a 1:1 mix with Freund's Incomplete Adjuvant (Sigma-Aldrich) for each inoculation. Prior to the first inoculation, a test bleed was carried out and used to check for reactions to *A. thaliana* proteins.

Three rats were injected four times with 100 µg protein in 100 µl buffer (making a total volume of 200 µl, spread between two injection sites). Inoculations were carried out

at an interval of two weeks for the first three injections, followed by a test bleed a week after the last injection. The final boost was carried out four weeks after the third inoculation and a cardiac bleed was used to collect the blood nine days after the fourth and final inoculation.

Two rabbits were injected four times with 500 µg protein in 250 µl buffer (as with rats, the total volume of protein in buffer and adjuvant was spread over two injection sites) at intervals of three weeks. Test bleeds were carried out a week to nine days after the second and third bleeds and 10 – 14 ml of blood was taken nine days after the final inoculation.

Serum was collected from the test bleeds and final bleeds and used in Western blotting to test for presence of an immune response and for immunofluorescence imaging.

All injections, test bleeds and final collection of serum were carried out in house.

2.2.6.5 Total protein purification from plant tissue for Western blotting

Four or five seedlings were ground in liquid N_2 in a pestle and mortar and mixed with 3 ml 15% (v/v) TCA. This mix was transferred to an Eppendorf and centrifuged at 16000 *g* for 3 mins. The supernatant was removed and the protein pellet resuspended in 80% (v/v) acetone with 50 mM Trick-HCl at pH 8. The tissue was again centrifuged at 16000 *g* for 5 mins and the wash step was repeated twice. After the last wash, the pellet was resuspended with 100 mM Tris-HCl pH 6.8 before centrifugation. The pellet was resuspended in 2 x SDS PAGE loading buffer and boiled for 3 mins, centrifuged again and loaded onto an SDS PAGE gel.

2.2.6.6 SDS PAGE gel electrophoresis

Concentration of acrylamide is dependent on the resolution of protein fragments required. Acrylamide was added in the form of Protogel (National Diagnostics) to form first resolving gel and then stacking gel. Gels were run using an Atto AE-6400 tank with 1 x Electrode buffer. Amples were mixed with 2 x Sample loading buffer and boiled at 100 ^{o}C for 3 mins before use. PageRule Protein Ladder (Fermentas) was used as a size marker. If the gel was used for resolving protein fragments rather

than Western Blotting, the gel was stained using Coomasi Blue gel stain for 30 mins with gentle shaking, and then destained overnight in Destain.

Resolving gel

- Appropriate volume Protogel (National Diagnostics)
- 0.1% (w/v) SDS
- 375 mM Tris
- 0.1% (v/v) APS (ammonium persulphate solution, Sigma-Aldrich)
- 1.4 µl/ml TEMED (NNN'N'-Tetramethylethylenediamine, BDH)

Stacking gel

- Appropriate volume Protogel
- 0.1% (w/v) SDS
- 125 mM Tris
- 0.1% (v/v) APS
- 4 µl/ml TEMED

10 x Electrode buffer

- 25 mM Tris
- 190 mM Glycine
- 0.1% (v/v) Glycerol

Sample loading buffer

- 250 mM Tris, pH 6.8
- 4% (w/v) SDS
- 20% (v/v) glycerol
- 100 mM β-mercaptoethanol

Coomassie Blue gel stain

- 35% (v/v) EtOH
- 7% (v/v) acetic acid
- 0.25% (w/v) Coomassie Blue R-250 (BDH)

Destain

- 35% (v/v) EtOH
- 7% (v/v) acetic acid

2.2.6.7 Western blotting

SDS-polyacrylamide gels were used to separate proteins from total protein purification of *A. thaliana* seedlings, according to the protocol above. The gels were then washed in 1x Transfer buffer for 10 mins. The proteins were then transferred from the SDS-PAGE gel to nitrocellulose membrane (Whatman) at 20 V overnight in 1x Transfer buffer. The membrane was then washed in dH_2O and stained with approximately 0.01% (w/v) amino black for 2 mins until protein staining was observed. The membranes were washed in distilled water and allowed to dry at room temperature between sheets of filter paper.

Once dry the membrane was cut into thin strips and these were incubated in 2 x TBST buffer with 5% (w/v) fat free milk powder (Tesco). After fifteen minutes the strips of membrane were placed on parafilm in a humid environment and the primary antibody was added to the membrane in TBST buffer with milk powder (the primary antibody was diluted 1:250, 1:500 or 1:100 in buffer). The antibody was incubated for 1 hour and then the membrane was washed three times in TBST buffer, each wash taking 10 mins.

The secondary antibody was diluted 1:3000 in TBST milk buffer and incubated with the membrane in the same way as the primary antibody for 1 hour. The membranes were again washed three times in TBST. To visualise the presence of antibody binding the membrane was incubated with ECL Western Blotting Detection Reagent (Amersham Biosciences) for 1 – 5 mins. This provides a substrate for the horseradish peroxidise conjugated to the secondary antibody and luminescence was detected using a Fujifilm Intelligent Dark Box II.

Transfer buffer

- 48 mM Tris
- 38 mM Glycine
- 0.04% (w/v) SDS
- 20% (v/v) methanol

Amido black solution

- 45% (v/v) methanol
- 2% (v/v) acetic acid

- 0.1% (w/v) amido black (Sigma-Aldrich)

TBST buffer

- 10 mM Tris
- 150 mM NaCl
- 0.1% (v/v) Tween 20
- pH 7.4
- For TBST milk buffer, 5% (w/v) dried skimmed milk powder (Tesco)

2.2.6.8 Immunolabelling of *A. thaliana* roots

This method was based on that used by Friml *et al.* 2003. Seedlings were grown on vertical plates until six days post germination and then fixed in Fixative solution for 1 hour. The seedlings were then washed five times in MTSB with 0.1% (v/v) Triton-X100 and then incubated with MTSB with 20 mg/ml driselase, 2 mM PMSF and 10 µg/ml leupeptine for 15 minutes. The seedlings were washed five times in MTSB with 0.1% Triton-X100. The seedlings were then incubated with MTSB with 10% (v/v) DMSO and 3% (v/v) Nonidet P40 (BDH) for 1 hour. This was followed with 30 minutes incubation in 1X PBS with 2% (w/v) Bovine Serum Albumen (Sigma-Aldrich) and 3 mM NsN_3. Primary antibodies were applied in a 1:300 dilution in the same PBS, BSA and Sodium azide buffer. The antibody was left on the samples for 1 hour at room temperature and 4 ^{o}C overnight.

Seedlings were then washed six times in 1 x PBS. Secondary antibodies were then applied at a dilution of 1:100 as for the primary antibodies and incubated for the same length of time. Anti-rat-TRITC (tetramethylrhodamineisothiocyanate) (Jackson ImmunoResearch) was used for detection of NET1d and anti-rabbit-ALEXA-546 (Invitrogen) was used for detection of NET1c. The following day the seedlings were washed four times in 1 x PBS and then mounted in one drop of Vectashield (Vector Laboratories). The final PBS wash also contained 300 nM DAPI stain (4',6-diamidino-2-phenylindole) for nuclear staining. In both cases, samples were images using a Leica SP5 confocal microscope, using a 543 nm laser to excite fluorescence. TRITC emits fluorescence at 576 nm and ALEXA-546 at 573 nm. DAPI staining was imaged using the 405 nm laser, with fluorescence emitted at 461 nm.

Fixative solution

- 3.7% (w/v) paraformaldehyde
- 50 mM PIPES, pH 6.8
- 5 mM EGTA
- 2 mM $MgSO_4$

MTSB (microtubule stabilising buffer)

- 50 mM PIPES
- 5 mM EGTA
- 5 mM $MgSO_4$
- pH 7

1x PBS

- 3.2 mM Na_2HPO_4
- 10.5 mMNaH_2PO_4
- 137 mM NaCl

2.2.7 Analysis of mutant lines *(Chapter 6)*

2.2.7.1 Analysis of single, double and triple mutant

Seventy to one hundred seeds from each line to be analysed were sterilised according to the sterilisation protocol. Seeds were placed on ½ MS media in vertical plates, containing approximately 50 ml of media per plate. Seeds were placed approximately 1.5 cm from the top of the plate in a row of approximately 15 – 18 seeds per plate.
Plates were wrapped in aluminium foil and placed at +4 ^{o}C for three days to ensure that germination was synchronous.

At days 3, 6, 9 and 12 post germination the plates containing the lines to be analysed were scanned and measured as described in the root measurement protocol.

2.2.7.2 Assay to assess effect of sucrose concentration on root length

Three different variations of ½ MS media were made for this assay: ½ MS as the control, ½ MS10 which contains 1% (w/v) sucrose and Pleiade media which contains 4.5% (w/v) sucrose.

Vertical plates containing 50 ml of media were made for each media. Seventy to one hundred seeds of each line (mutant and azygote) were used per type of media.

The seeds were sterilised and transferred to the media as for the analysis of the single, double and triple mutants. The method of measurement of roots was also the same.

½ MS media – 1litre

- 2.2 g Murashige & Skoog Basal Medium 5524 (Sigma Aldrich)
- 8 g/l Plant agar (Duchefa Biochemie)
- pH 5.7, use KOH to adjust

½ MS10 media – 1litre

- 2.2 g Murashige & Skoog Basal Medium 5524 (Sigma Aldrich)
- 8 g Plant agar (Duchefa Biochemie)
- 10 g Sucrose
- pH 5.7, use KOH to adjust

MS Pleiade

- 4.4 g Murashige & Skoog Basal Medium 5524 (Sigma Aldrich)
- 8 g Plant agar (Duchefa Biochemie)
- 45 g Sucrose
- pH 5.7, use KOH to adjust

2.2.7.3 Measuring of roots for analysis

The vertical plates on which the plants were grown were scanned using an Epson Perfection 4490 Photo scanner, at a resolution of 300 dpi. A ruler was also placed on the scanner bed to provide a known distance with which to calibrate the measurements. ImageJ (Abràmoff *et al*. 2004) was used to trace the primary root using the 'segmented line' tool and measured using the 'measure' tool. This was repeated for each individual plant at days 3, 6, 9 and 12 post germination.

2.2.7.4 Fixation and staining of *A. thaliana* roots for cell measurement

Azygote and mutant lines for the NET1a/NET1b-A cross were grown on vertical plates until nine days post germination, with 30 – 40 plants per line. The seedlings were then transferred to a petri dish and submerged in 20 ml of fixative solution for 1 hour at room temperature. The fixative was then removed and replaced with 1 x PBS. The seedlings were stored at +4 ^{o}C.

The seedlings were removed from the storage solution of 1 x PBS and rinsed in dH_2O. They were then placed in a second petri dish with 20 ml of 55 µM calcofluor (based on Falconer & Seagull 1985). This was incubated at room temperature for 15 minutes. The seedlings were then washed in dH_2O and mounted in the same. The seedlings were then imaged on a Leica SP5 confocal microscope, using the 405 nm laser to excite fluorescence which was detected at 409 – 487 nm. The Tile Scan feature was used to obtain images of the entire root from root tip to the development of secondary roots.

Fixative solution – 40 ml

- 1.48 g paraformaldehyde, added to a small quantity of water and dissolved by the addition NaOH to decrease pH, the pH is then returned to neutral using HCl
- 0.4 ml 1M PIPES
- 2 ml 0.1 M EDTA
- 0.4 ml 0.2M $MgSO_4$
- H_2O to a total volume of 40 ml

10x PBS

- 0.14 M NaCl
- 2.68 mM KCl
- 1.25 mM Na_2HPO_4
- 1.98 mM KH_2PO_4
- pH 7.0

Chapter Three:

Analysis of the NET1 protein family in *A. thaliana* using Bioinformatics

3.1 Introduction

When the NET1a protein fragment was first identified by Karl Oparka during the high-throughput screen for novel protein localisations, only the first 288 amino acids of the N-terminus were present. This domain was discovered to contain a novel and potentially plant specific actin binding domain. An important tool in identifying the gene responsible for the NET1a protein and in finding related proteins was the use of bioinformatics. This computational analysis of the proteins and the use of large databanks of genomic, protein and structural information allows the identification of previously unknown genes and predictions of their potential structures and functions based on structural homology with known proteins. It is also possible to use a novel protein, or a domain of a novel protein to identify other proteins that may be worth further investigation.

In this case, work by J Calcutt, MJ Deeks and TJ Hawkins (Calcutt, J. 2009) has enabled the identification of the NET1a protein and subsequently led to the identification of a superfamily of NET proteins in the *A. thaliana* genome as well as in other plant species (*see Chapter One)*. Bioinformatics has also allowed prediction of the structure of the NET1 genes and proteins and has suggested patterns of protein expression that can lead towards particular experimental approaches to understanding the function of these genes.

3.2 Preliminary identification and analysis of the NET1a and NET1b proteins

In progressing from the C-terminal section of NET1a initially discovered, Bioinformatics has played an important role. One important tool in identifying and analysing NET1a has been the TAIR database (The Arabidopsis Information Resource, Huala *et al.* 2001). This database contains the data from the sequencing of the *A. thaliana* genome. The chromosome sequences have been compiled and separated into predicted genes. These are labelled according to location on the chromosome, in the following format: At, the chromosome number, g, a number based on location within the chromosome. This database is searchable using gene name or a sequence of amino acids or nucleotides. The use of a blastN search of the TAIR database using the nucleotide sequence of the NET1a-GFP construct used in the initial screen identified the NET1a protein as gene At3g22790, and therefore located on Chromosome 3. The data contained in the database shows that the gene has two introns and three exons and encodes a protein of 195 kDa (Calcutt 2009).

The protein fragment used during the initial screen that identified NET1a consists of a domain that was identified as the KIP1 domain. This domain was found in the *Petunia inflata* protein PiKIP and is a supposed to interact with a kinase, PRK1. In fact, the domain that is identified as the KIP1 domain is part of the kinase interacting protein but is distinct from the area of the protein involved in kinase binding. The area used for yeast two hybrid analysis of the kinase interaction is downstream from the 'KIP1' domain (Skirpan *et al.* 2001). This domain has now been identified as the NET actin binding domain (ABD). It is thought that this domain is therefore unlikely to have a function linked to kinase interaction, which had at first been thought a possibility.

The NET1a protein contains this N-terminal actin binding domain but also contains a series of C-terminal coiled coil domains. According to the ARABI-COIL database, which is thought to produce the least number of false positives for coiled coil prediction (Rose *et al.* 2004), there are five of these domains. The domains are based on a twisting together of several α-helical domains to form a supercoil (hence, the coiled coil domain). The supercoil results in placement of hydrophobic residues within the α-helices at the centre of the structure, with hydrophilic residues located on the outer faces of the structure (Burkhard *et al.* 2001). This leads to a great stability of the structure. The repeating pattern of hydrophobic and hydrophilic residues (often seven amino acid repeats for a left-handed coil and eleven for a right-handed one)

allows prediction of the structures. The coiled coil domains found within NET1a are long coiled coil domains, suggesting that they may have a structural role in maintaining spatial arrangement within the cell, although it is possible for these domains to be involved in regulatory as well as organisational roles within the cell (Rose and Meier 2004).

a)

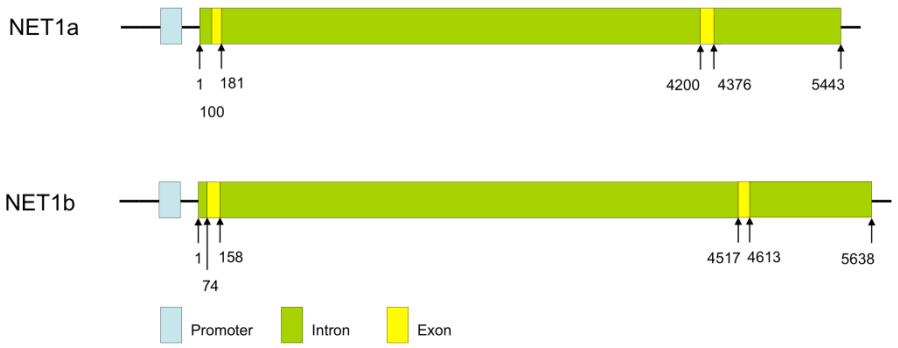

b)

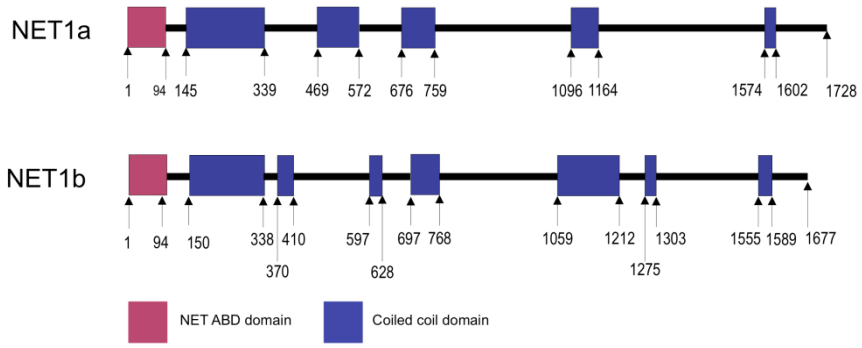

Figure 3.1: a) The gene structure of At3g22790 (coding for NET1a) and At4g14760 (coding for NET1b) with predicted structure of introns and exons. b) Predicted protein structure of NET1a and NET1b with actin binding domain in red and coiled coil domains shown in blue.

In the initial analysis of the NET1 proteins, work focussed on the two most homologous proteins within the family, NET1a and NET1b. These make up the first of two pairs of more closely related proteins within the family. NET1b consequently shares many of the characteristics of NET1a. The predicted gene, At4g14760, contains the same pattern of two introns and two exons. The NET1b protein also contains the N-terminal actin binding domain common to all NET proteins and a series of seven long coiled coil domains. Figure 3.1 shows a representation of the NET1a and NET1b genes with the location of the introns and exons, and the NET1a

and NET1b proteins to demonstrate the location of the NET-ABD and coiled coil domains.

3.3 Analysis of the NET1c and NET1d proteins

The focus of this thesis is the NET1 group NET proteins within *A. thaliana.* In particular, analysis has focused on the proteins NET1c and NET1d, which were not analysed through experimental means by J. Calcutt (Calcutt 2009). Consequently the structure and expression of these two proteins has been more closely examined.

NCBI BLAST (Basic Local Alignment Search Tool, Altschol *et al.* 1997) was used to search for the homologues of NET1a and NET1b (using the full length nucleotide sequence of the NET1a protein to search for homology) and two related proteins were found, NET1c (gene At1g03080) and NET1d (gene At4g02710), which complete the NET1 group. TAIR (Huala *et al.* 2001) provided further information on the structure of these two genes. Both have two introns and contain the KIP1 domain that makes them part of the kinase interacting family proteins. They also contain myosin tail-like domains, a common feature for proteins containing coiled coils.

The first of these, NET1c, encoded by 3336 nucleotides not including the two introns, is a protein 1112 amino acids in length and approximately 128 kDa in weight, the smallest of the four proteins (NET1a and NET1b having a predicted molecular weight of 195 and 193 kDa respectively). The second of these two proteins is NET1d, which is encoded by 5235 base pairs, producing a protein 1745 amino acids in length and with a predicted molecular weight of 200 kDa, the largest of the NET1 proteins and also the largest of all the NET proteins found in *A. thaliana*. The TAIR database also predicts an isoelectric point of 5.83 for NET1c and of 4.72 for NET1d. The information from the TAIR database provides useful information as to the size and sequence of the gene, but provides less information on secondary or tertiary structure and any possible function or location of the protein. To achieve an understanding of the protein, further analysis must be undertaken.

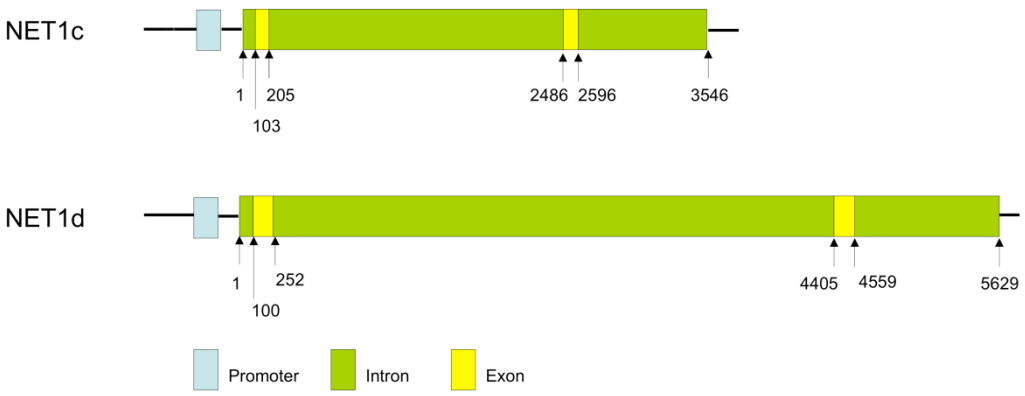

Figure 3.2: Diagram showing the location of the introns and exons in the genes At4g02710 and At1g03080, coding for NET1c and NET1d respectively.

The NET1 proteins are known to contain the NET actin binding domain at the N-terminus of each protein. The ARABI-COIL database (Rose *et al.* 2004) was also used to examine the proteins as the C-teminal section NET1a and NET1b, following the actin binding domain, contains a series of coiled-coil domains separated by areas of low complexity (Calcutt 2009). The database uses the MultiCoil programme to predict the presence of coiled coil domains and is thought to reduce the number of false positives (Rose *et al.* 2004). The presence of several coiled coil domains in the NET1a and NET1b proteins appears to be replicated in the two proteins considered here. NET1d is predicted to contain five coiled-coil domains and NET1c to contain four. The exact location of these coiled-coils is shown in Figure 3.3.

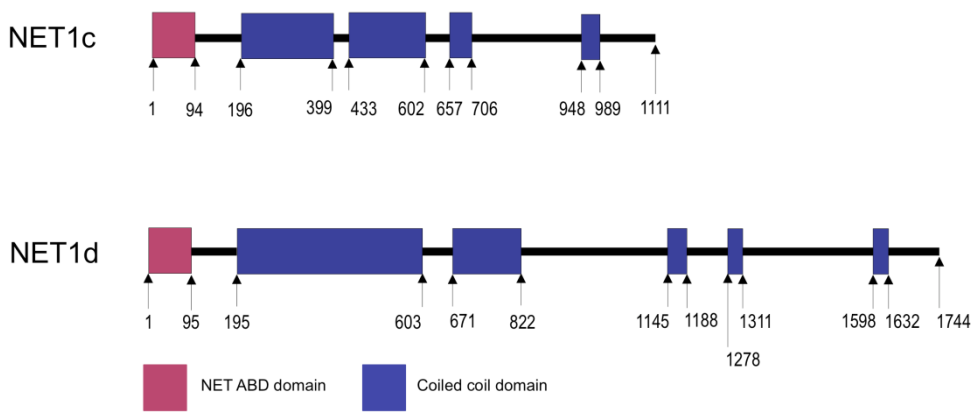

Figure 3.3: The location of the predicted coiled coil domains found within NET1c and NET1d

In order to target proteins to the correct sub-cellular localisation some proteins contain localisation sequences, such as the HDEL sequence that causes retention of proteins to the endoplasmic reticulum in yeast and animal cells, although it may not be sufficient in plant cells (Gomord *et al.* 1997).

The WoLF pSORT programme (Horton *et al.* 2006) was also used to confirm the numbers of coiled-coil domains and search for localisation sequences and potential trans-membrane domains, which might indicate the location of the protein to cellular structure or membranes. Neither protein contains a trans-membrane domain, but both show potential nuclear localisation sequences, something that will have to be considered as a potential clue to function, although none of the proteins previously analysed have demonstrated a nuclear localisation in experimental analysis of subcellular localisation, despite containing a similar potential for nuclear localisation (Calcutt, 2009).

3.4 Analysis of potential expression patterns of the NET1 proteins

The localisation of expression of a gene of interest can have important implications for the function of that gene, due to tissue specific processes within that localisation. It can also assist in discovering phenotypes associated with under or over expression of the gene. To analyse the expression of the NET1 genes, Genevestigator (Zimmerman *et al.* 2004) was used. This database contains an accumulation of Affymetrix data from a variety of different data chip sources to allow investigation of the levels of expression in different tissues and stages of development.

Genevestigator revealed that both proteins have differing patterns of expression depending on developmental stage and location within the plant. Quantitative comparison of expression levels is not possible as the results are expressed as a percentage of expression of that particular gene rather than as a total level which can be compared between genes. It does however allow a qualitative comparison of expression patterns and can identify tissues where a particularly large proportion of the protein is expressed.

In general NET1d is always expressed at a more varied level throughout development than NET1c. NET1d has a few marked peaks at young rosette stage and in flowers and siliques. NET1c shows a similar general pattern but at a much more consistent level and with a slight rise in expression during bolting which the other gene does not show. NET1d shows a broader pattern expression in the tissues of the plant, while NET1c is expressed in fewer tissues, suggesting a low or negligible level of expression of the gene throughout the plant, but at a noticeably higher level in the xylem. NET1d does not show a specific tissue where expression is noticeably at a higher level although it is also present in the xylem. Some expression of NET1d and NET1c is observed in root tissue, although this is more widespread in NET1d. NET1c expression occurs mainly in the elongation zone and root hair development zone. Figure 3.4 shows the comparison of these two expression patterns.

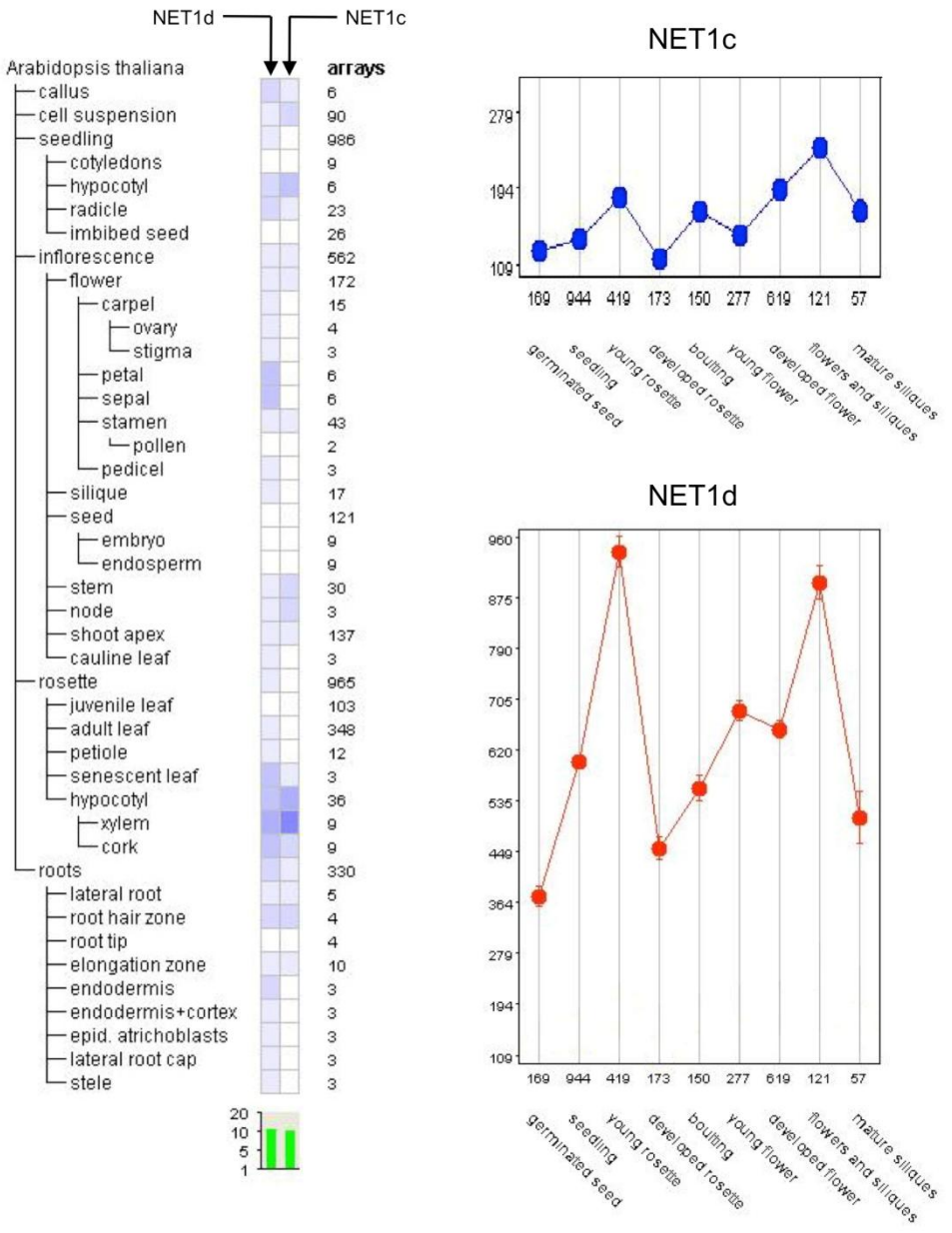

Figure 3.4: Expression patterns of NET1c and NET1d based on data obtained from the Genevestigator database. Expression levels are compared in plant tissues and stages of plant development.

The Arabidopsis Electronic Fluorescent Pictograph (eFP) Browser was also used as a secondary source of analysis of microarray data (Winter *et al.* 2007). This provides Affymetrix data from the ATH1 GeneChip (Craigon *et al.* 2004) and provides both absolute information on the level of expression of one gene of interest within the tissues and the ability to qualitatively compare patterns of expression between genes of interest. For analysis of NET1c and NET1d, levels of expression in root tissue,

above ground tissue, developmental stages and under various biotic and abiotic stresses were examined.

NET1c again appears to show a very low level of expression in the majority of plant tissues. Higher levels of expression are observed within the developing embryo, particularly within the embryo, endosperm and seed coat (at the pre-globular and globular stages, levels of expression decrease in the seed coat at the heart shaped stage). NET1c is also expressed within the hypocotyl to a lesser extent within the xylem tissue. Gene expression does not alter greatly in response to biotic and abiotic stresses although some increase in levels of NET1c occurs after cold treatment.

In contrast, NET1d shows a generally wider pattern of expression. NET1d is found in the embryo, as with NET1c, but is found mainly in the seed coat. High levels of expression are found within the xylem tissue, sepals, petals, stamens, stigma and ovary. A slight increase in expression levels are observed after stress (this is observed in many cases and may indicate a general stress response) but this is particularly noticeable after treatment with mannitol and sodium chloride so it is possible that NET1d may be involved in tolerance to osmotic stress.

Both NET1c and NET1d show some level of expression in root tissue, as do NET1a and NET1b (Calcutt, 2009) so in view of this experimental analysis of the pattern of expression of the NET1a and NET1b proteins and the potential root phenotype occurring in mutants lacking functional copies of NET1a and NET1b (Calcutt, 2009) the expression of the NET1 genes within root tissue has been compared in the three NET1 genes for which Affymetrix data is available. No data is available for NET1a due to an erroneous combination of NET1a data with that of another gene within the database (Calcutt, 2009). The result of this comparison of expression levels in roots is shown in Figure 3.5.

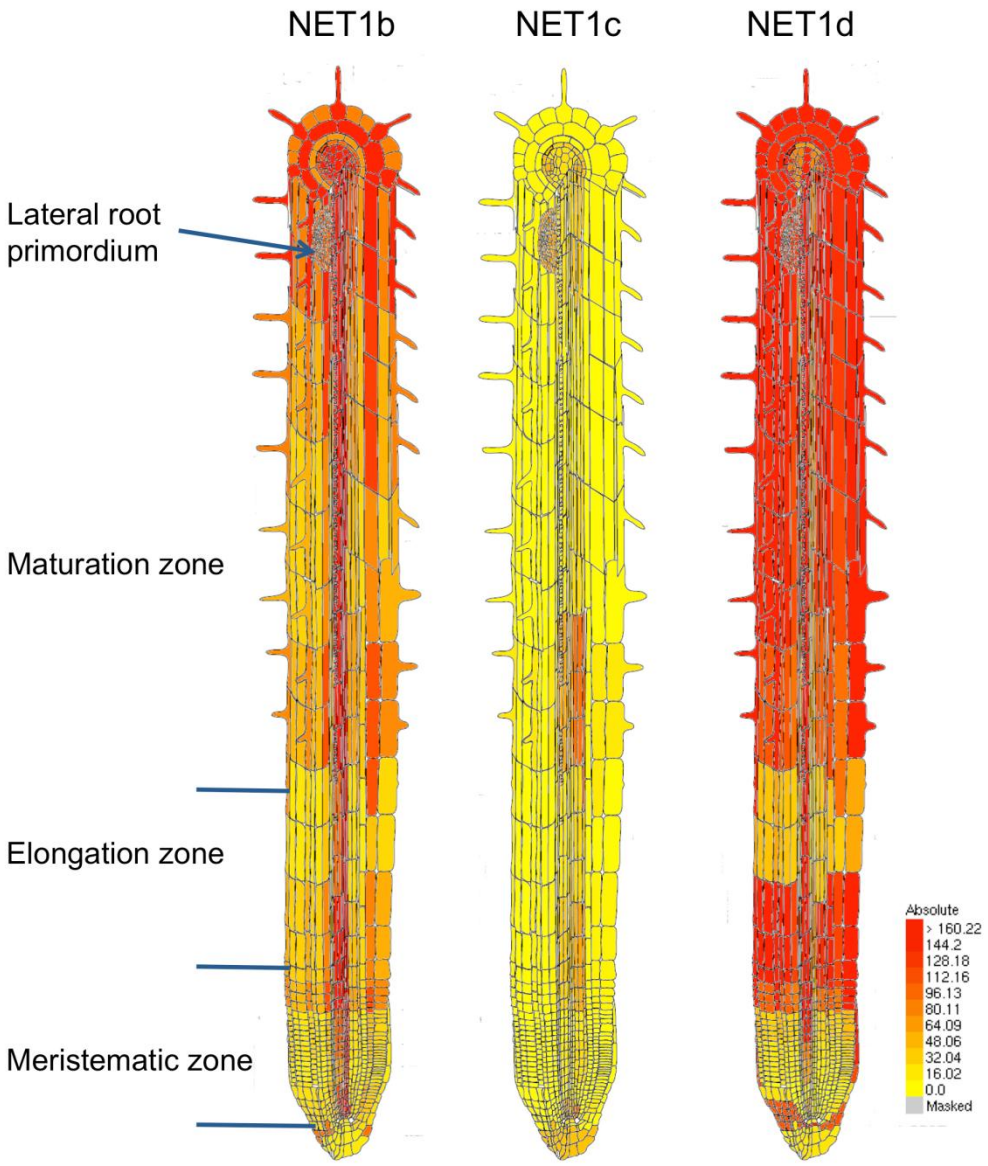

Figure 3.5: A comparison of pattern of expression of NET1b, NET1c and NET1d within root tissue. Images obtained from the eFP Browser (Winter et al 2007). Expression levels are absolute and the signal threashold was set to 160.23 for all three genes.

According to the data, NET1b is expressed within the endodermis, xylem and procambium while NET1d appears within the epidermis and root cortex as well as the endodermis and it also appears within the phloem pole pericycle. The pattern or expression of NET1d throughout the length of the root is also interesting as the level of expression of the gene decreases within the lower meristematic tissue and again within part of the elongation zone. This is noteworthy, as NET1a expression appears

to spread through all tissues, beyond the usual vascular localisation in this area so the patterns of expression appear complimentary (Calcutt 2009).

The data for NET1c expression is less clear, owing to the comparatively even levels of expression of the gene typical in all tissues. The gene does however appear to be expressed at a slightly higher level within the endodermis, pericycle and vasculature. The interaction of these three proteins and their overlapping and possibly complimentary expression patterns would be interesting to investigate in further detail.

3.5 Conclusion

The previous analysis of the NET genes using a computational, bioinformatics approach has revealed a superfamily of thirteen proteins within the *A. thaliana* genome and further proteins present within other plant species such as *S. moellendorffii* and *P. inflata*. The founding member of this family is the protein NET1a, which contains an N-terminal actin binding domain previously thought to be a kinase interacting domain and now re-labelled as the NET actin binding domain.

NET1a is a 195 kDa protein also containing a series of coiled-coil domains. Phylogenetic analysis places NET1a within a group of four *A. thaliana* proteins. The NET1 group consists of NET1a, NET1b, NET1c (At1g03080) and NET1d (At4g02710). The proteins range in size between 128 kDa and 200 kDa (NET1c and NET1d respectively) and all consist of an N-terminal NET actin binding domain and a series of coiled coil domains. These stable domains, frequently capable of protein-protein interactions, are suggestive of structural or organisational roles that may be useful to consider in relation to experimental data.

Affymetrix data from a variety of sources demonstrates great variation in the pattern of expression for each gene. In particular an overlapping expression pattern is observed in root tissue, where NET1a and NET1b thought to be expressed, based on experimental evidence using the GUS reporter gene to analyse activation of the NET1a and NET1b promoters (Calcutt 2009). This potential for expression of all four proteins in root tissue has been investigated further in terms of potential root phenotypes, although expression in other tissues has also been investigated.

Chapter Four:

Investigation of the actin binding properties of the N-terminus of NET proteins NET1c, NET1d and NET2a, and an investigation of potential protein interactions with NET1a actin binding domain

4.1 Introduction

The NET protein project began with the discovery that an N-terminal section of the protein now known as NET1a was capable of binding to a filament network during a high-throughput screen of an *A. thaliana* cDNA library to identify localisations of novel plant proteins carried out by Professor Karl Oparka's laboratory (Escobar *et al*. 2003). A viral expression system was utilised whereby fragments of *A. thaliana* proteins were tagged with a C-terminal green fluorescent protein (GFP) label. Tobacco mosaic virus was then used to infect *Nicotiana tabacum* leaves with the tagged library to produce fluorescent lesions which could be analysed through confocal microscopy to view the localisation of the protein. NET1a was localised to a filamentous network within the cell.

The NET1a fragment was shown to bind to the actin cytoskeleton by colocalisation with actin markers and disruption of the filament network by anti-cytoskeletal drugs and therefore to contain an actin binding domain. Bioinformatics was used to identify other proteins also containing this domain which resulted in work carried out to discover the extent to which the N-terminal actin binding domain of the NET proteins is capable of binding to the filament network of the actin cytoskeleton, as described in this chapter.

4.2 Previous work on the N-terminus of NET1a and NET1b

The first investigation into the NET proteins was carried out using a 288 amino acid N-terminal section of NET1a, tagged with C-terminal green fluorescent protein (GFP). This construct was initially used by Karl Oparka (Escobar *et al.* 2003) with a viral infection system, but was later used by J. Calcutt (Calcutt 2009) with an *Agrobacterium tumefaciens* expression system. The bacteria, which naturally infect higher plants and integrate their DNA into the plant genome using T-DNA to cause tumour growth in the plant, have been modified so that they are no longer capable of tumour induction. The T-DNA can be genetically engineered to contain the gene of interest (with a tag if necessary) and, once injected into a plant leaf, cause transient expression of the gene contained in the T-DNA plasmid. This transient expression allows the localisation of the gene to be studied in the leaf of *Nicotiana benthamiana*.

The 288 amino acid section of NET1a was found to bind to a filament network, which was shown by J. Calcutt (Calcutt 2009) to be the actin cytoskeleton using treatment with anti-cytoskeletal drugs and co-localisation with an actin marker. A homologous section of the NET1b protein was also analysed by this method and showed the same localisation to F-actin filaments with respect to the appearance of a filament network and the effect of anti-actin drugs. It was also shown to co-localise with NET1a.

4.3 Initial investigation of NET1c and NET1d actin binding

The NET1a and NET1b proteins form a pair of highly homologous proteins within the NET1 group. The remaining proteins (NET1c and NET1d) make a second pair of closely related proteins, even considering the high level of homology within the group (see Phylogenetic Analysis, Chapter 3).

Given the slight differences between the two pairs, and the lack of conclusive proof that the NET domain was universally capable of binding F-actin, the first investigation into the function of NET1c and NET1d was to establish whether they would show the same localisation.

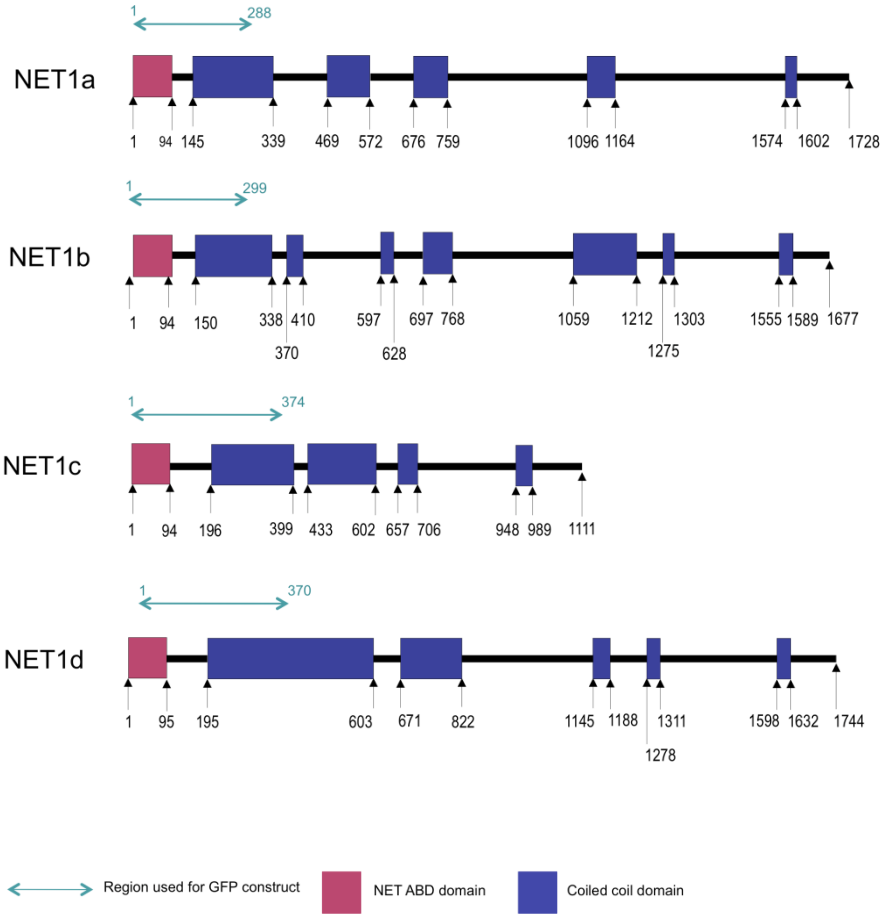

Figure 4.1: A comparison of the four NET1 group proteins and their domains. The region of the protein used for analysis of the actin binding domain is shown.

To establish the localisation of the actin binding domain the N-terminal 370 amino acid residues of NET1c and the N-terminal 374 amino acid residues of NET1d were cloned into the pMDC83 Gateway expression vector for expression of the protein with a C-terminal GFP tag. These constructs were designed to be directly equivalent to the 288 amino acid sequence used for analysis of the N-terminus of NET1a. These

constructs were used in the same transient expression of protein in *N. benthamiana* leaves using *A. tumefaciens* and were analysed by confocal laser scanning microscopy using a Zeiss 510 confocal microscope.

The two constructs were then used in a variety of experiments to confirm that the NET domain was capable of actin binding throughout the NET1 family. These experiments show a localisation to F-actin rather than a localisation to the other filament network found within plant cells, the microtubules, or to a filament network based upon self-dimerisation, which was thought possible due to the presence of many coiled-coil domains in the NET1 proteins.

4.4 Imaging of N-terminal domain tagged with GFP to study possible actin binding.

Figure 4.2 shows the initial images of NET1c and NET1d actin binding domains in the pavement cells of the leaf epidermis, three days after injection of the *A. tumefaciens* bacteria, which causes the transient expression. Images shown here and for all other transient expression experiments are a representative example of those observed during repeated experiments using multiple plants to ascertain true localisation. The network is visually similar to the network seen with the NET1a actin binding domain. The protein fragment binds to both thick bundled fibres and fine filaments, forming a mesh-like net that gives the protein family its name.

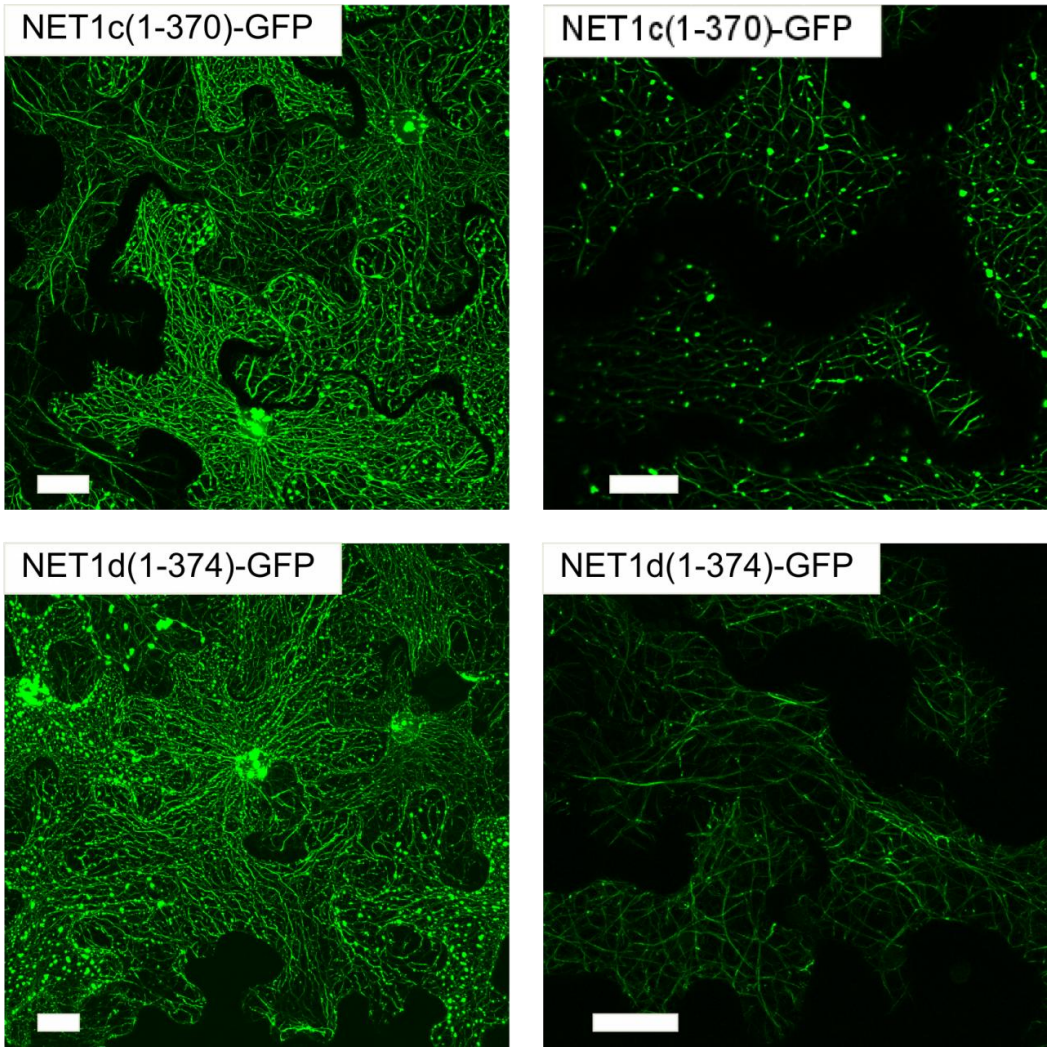

Figure 4.2: Initial confocal microscopy images of NET1c (top) and NET1d (bottom) actin binding domains labelled with C-terminal GFP and transiently expressed in N. benthamiana. Images were taken three days post-infiltration. Cells are shown with both high (right) and low (left) levels of expression. Both constructs are seen to decorate a filament network. Scale bar equivalent to 20 μm.

Cells are shown with both high and low levels of expression, giving an example of the range of behaviour of the protein. When expression levels are high, the filaments seem to become more bundled and there is often more protein present around the nucleus. Both high and low expressing cells show a stabilisation of the filament network. The filaments rarely move and are not dynamic. If any movement is seen, it is usually in one of the finer filaments and movement is frequently confined to one small portion of the filament, for example the end of the filament may be seen to 'wriggle' while the rest of the filament remains stationary. This suggests that the protein may be capable of stabilisation of actin filaments. If this is the case, this may indicate a possible role in tethering filaments to a certain location or of bundling or cross linking filaments.

Furthermore, Figure 4.2 shows the presence of aggregates of protein. These are occasionally separate from the filaments but often line up along it and are also found where some filaments are crossing over. This characteristic and the thicker filaments observed in cells with higher levels of expression indicate that bundling has occurred, which suggests a possible function for the protein in cross-linking or organisation of filaments, and also demonstrates a potential for the protein to be able to bind to itself to produce these aggregates. A pattern of filaments and punctuate patterns is typical for many NET proteins across groups 2, 3 and 4 (unpublished work by Professor Hussey group (Durham University). Although some images show either NET1c or d with a greater number of protein aggregates, this is coincidental and the presence of the aggregates is usually equally common for both proteins. Aggregates also appear surrounding the nucleus in cells with high levels of expression but these occur where thick bundles of filaments surround the nucleus and are not present within the nucleus itself.

The pattern of expression of NET1a, as demonstrated by J. Calcutt (Calcutt 2009), is a punctuate pattern at the edges of root cells. This pattern and the characteristics of filament binding described above indicate that a likely role for the protein is in binding to actin and tethering it to that location. The similarity of the effect of other NET1 proteins on actin filaments suggests that they may have similar functions, although it must be noted that the localisation of NET1a to the root cell cortex may also be dependent on the C-terminal domain of the protein which was not present during the transient expression of the NET1c and d actin binding domains. Variation in C-

terminal domains within the NET1 group may also cause variations in localisation, which are as yet unstudied.

4.5 Treatment of the transient expression system with anti-actin drugs

4.5.1 Introduction

The similarity of the pattern of localisation within the transient *N. benthamiana* system and the homology of the N-terminal domains of the NET1 proteins strongly suggests actin binding as the source of the filament network localisation. While the network was proven to be actin for NET1a and b, proof was needed for the remaining proteins in the family.

To do this leaves infiltrated with *A. tumefaciens* solution were left for three days post injection to allow the construct containing the N-terminus of the proteins with C-terminal GFP to begin to be expressed and for the protein to accumulate within the cell. Sections were then cut from the leaf and incubated for approximately 30 minutes with either an anti-actin drug or a control solution. Both Cytochalasin D and Latrunculin B were used to establish that any effect on the filament network was seen under a variety of modes of disruption of the actin cytoskeleton. Latrunculin B acts by binding to monomers of G-actin and preventing polymerisation into F-actin, while Cytochalasin D appears to interact directly with F-actin and cause breakdown of the filaments, initially into small fragments of actin filament and then into G-actin. Since both drugs were dissolved in dimethyl sulphoxide (DMSO), the control leaf sections were incubated in a solution of DMSO at the same concentration as that found in the anti-cytoskeletal drug solutions. DMSO can begin to adversely affect the leaf samples during the course of the incubation, most frequently at the cut edges of the leaf sample. The cells are put under stress and may start to undergo cell death, which could result in unusual formations of the cytoskeleton. For this reason the drug treated samples are carefully compared to control samples that have experienced the same concentration of, and incubation time in, DMSO. Imaging was carried out in the middle of the leaf section to avoid the cells most damaged by the DMSO treatment. Data shown here is a representative sample from multiple repetitions of the drug treatment experiment, with each experiment comprising several leaf samples from different plants and several leaves from each plant.

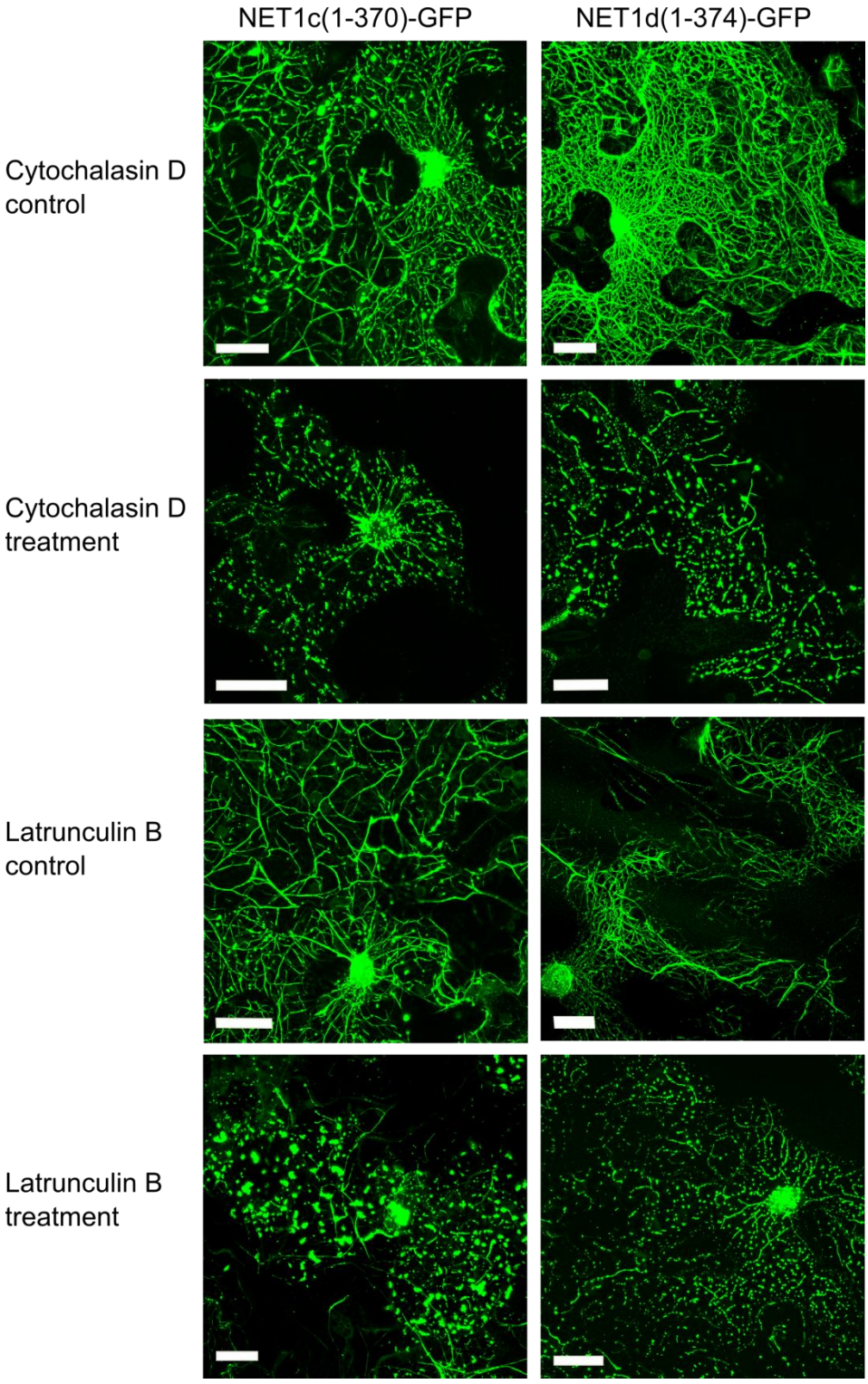

Figure 4.3: NET1c (left) and NET1d (right) ABD-GFP construct expressed in N. benthamiana and imaged using 488 nm wavelength light on a Zeiss confocal microscope. Treatment with 100 µM Cytochalasin D and control (top) and treatment with 50 µM Latrunculin B and corresponding control (bottom) imaged after 30 minutes of incubation with the drug treatment. In all cases, treatment with an anti-actin drug results in destruction of the filament network seen with NET1c and NET1d actin binding domains while leaf cells of the controls remain unaffected. Scale bar equivalent to 20 µm

4.5.2 Experimental data

Figure 4.3 shows the results of the drug treatments. In the case of Cytochalasin D the control leaf sections look almost normal, although perhaps the filaments are a little more bundled. When treated with 100 µM of the anti-cytoskeletal drug, the filament network is seen to have become highly disordered. Most of the protein seen has formed into large aggregates with some short sections of filament still remaining. This is typical for Cytochalasin D treatment as the actin filaments are first broken down into short sections and then into G-actin. It appears that once the filaments have been disorganised, the NET proteins gather together into aggregates. This may be a natural tendency of the protein, and may also suggest that they are gathering around any short sections of filament that remain. What is clear is that disruption to the actin cytoskeleton causes disruption of the filaments – this confirms the actin binding capability of the proteins as has been expected.

In the Latrunculin B images in Figure 4.3, the control samples appear normal, but the drug treated samples show much disorganisation. While Cytochalasin D treated cells show short filaments, these samples show very few remaining long filaments with most of the protein forming large aggregates. These aggregates tend to be larger than those seen with Lantrunulin B. This disrupted localisation follows the expected pattern for actin treated with 50 µM Latrunculin B. The drug does not affect F-actin filaments but instead prevents the polymerisation of new filaments by binding G-actin monomers and preventing them from undergoing polymerisation. This explains the few remaining filaments shown and also the large aggregates. This disruption of NET1 filaments on the disruption of actin filaments clearly indicates that the filaments bound by the NET1 proteins form the actin cytoskeleton. The aggregation of the remaining protein around the remaining actin filaments, rather than the appearance of cytoplasmic GFP, supports the hypothesis that the NET1c and d actin binding domains associate with filamentous F-actin rather than monomeric G-actin.

The treatment with anti-actin drugs caused a complete loss of the filament network after a certain time point so it is possible to conclude that all filaments associated with the NET1 proteins are actin filaments. In light of this, anti-microtubule drugs were not used although they were used by J. Calcutt (Calcutt 2009) on NET1a with no demonstrable effect. Absence of cytoplasmic fluorescence suggests that the actin binding domain associates with F-actin rather than G-actin although the association has not been proven to be direct. J. Calcutt demonstrated direct association between NET1a-ABD and F-actin so direct association is likely but requires further proof.

4.6 Co-localisation of NET1a N-terminus with N-termini of NET1c and d

4.6.1 Introduction

To demonstrate further evidence of actin binding in the N-terminus of NET1a, J. Calcutt (Calcutt 2009) used a red fluorescent protein (DSRed) construct, identical to the NET1a N-terminus-GFP construct but with the red fluorescent protein replacing the green, in an *A. tumefaciens* expression system and co-infiltrated *N. benthamiana* leaves with FABD2, a protein known to localise to F-actin, tagged with GFP. This resulted in a leaf with the actin cytoskeleton labelled with green fluorescence and the NET1a filaments labelled with red fluorescent protein. The filaments observed appeared to have a highly similar structure to those seen with the green fluorescent protein, suggesting that the fluorescent protein used does not alter the localisation. This enabled the study of cellular localisation where NET1a N-terminus co-localised with the actin cytoskeleton and further proved the hypothesised actin binding.

To provide further proof of actin binding in the NET1c and d proteins, the experiment has been repeated using the same N-terminal protein fragments tagged with GFP and the NET1a-DSRed construct used in the experiment mentioned above. Since NET1a has already been shown to co-localise closely with an actin marker the experiment provides evidence of actin binding in NET1c and d but has the advantage of also showing any variation between the patterns of binding to the actin cytoskeleton within the NET1 group.

4.6.2 Experimental data

Figure 4.4 shows the results of the co-localisation experiments. The images showing the individual channels of red and green fluorescence have been shown in black and white for greater clarity and ease of comparison. The image with both channels overlaid shows green where only NET1 c or d is present, red where only NET1a is expressed and yellow where these two patterns of localisation coincide.

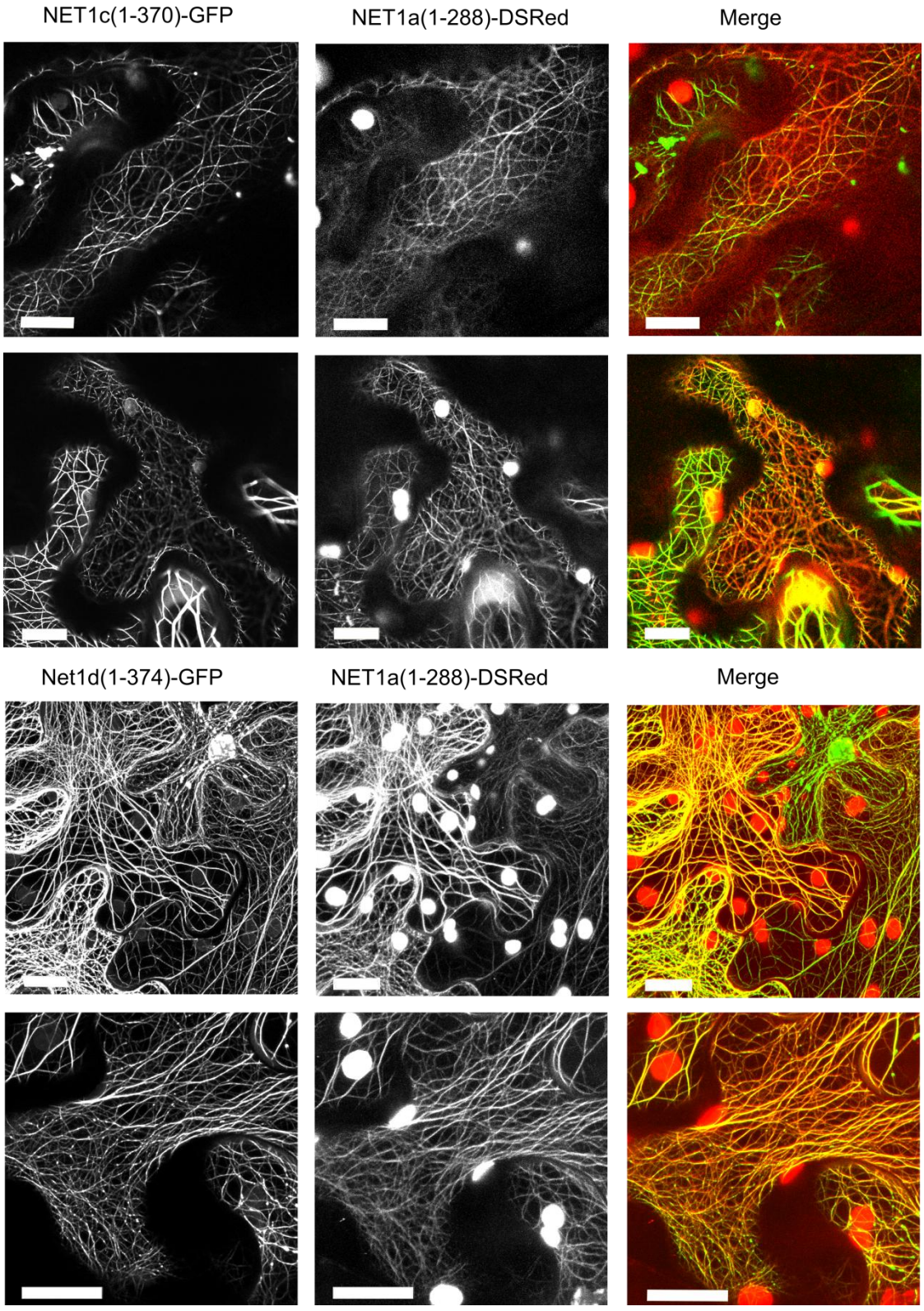

Figure 4.4: Colocalisation of NET1c ABD-GFP with NET1a ABD-DSRed and co-localisation of NET1d ABD-GFP and NET1a ABD-DSRed to show overlapping filament network localisation. Images containing DSRed also show red fluorescence from chloroplasts due to the wavelength of light and imaging method used. Scale bar equivalent to 20 μm

As these images show, the co-localisation between the NET protein actin binding domains is very close. There are areas of the cell where either the red or green fluorescence is the only visible signal but this tends to correspond to entire areas of high or low expression rather than a difference in pattern of expression. This also acts as an internal control, ensuring that the co-localisation seen is not an artefact caused by bleed through from one channel on the microscope to the other.

Also visible on the images of the red fluorescence are chloroplasts, auto-fluorescing under the laser used for imaging the DSRed. Figure 4.5 shows an image taken with identical microscope settings to those used during the co-localisation experiment. The auto-fluorescence can be seen from the circular chloroplasts, but no filaments are seen. This demonstrates that the circular structures are indeed chloroplasts and that they are not affected by the presence of the NET1a-DSRed protein. It also acts as secondary proof that the filaments seen with red fluorescence are not causing a false signal on the channel imaging the fluorescence from the GFP.

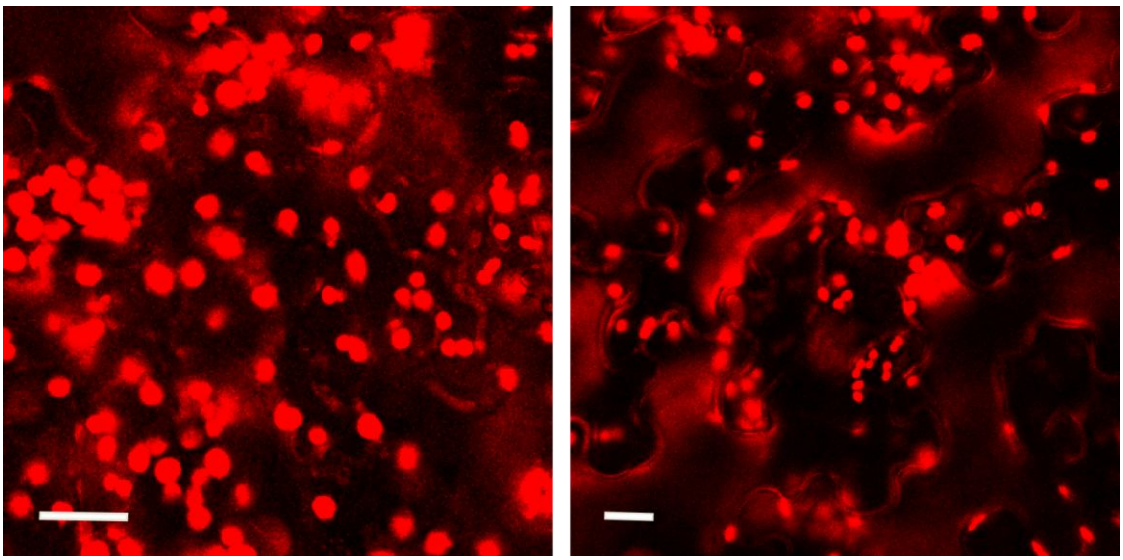

Figure 4.5: Control images of leaves not containing fluorescent proteins imaged using the same laser settings as the co-localisation experiments to show fluorescence of chloroplasts under the conditions used for imaging of DSRed. This establishes these structures as an artefact of imaging conditions rather than an effect of the NET1 proteins. Scale bar equivalent to 20 μm.

This experiment using co-localisation of the actin binding domains of the NET1 proteins shows that the pattern of actin binding within the NET1 group is very similar. Since the NET1a N-terminus was shown to co-localise with the entire population of actin filaments, it can be concluded that the remainder of the NET1 group do the same. There is no specific population of actin filaments being bound by the NET actin binding domain. They are likely to be capable of binding to any F-actin filament.

4.7 Dynamics of association with the actin cytoskeleton

4.7.1 Introduction

When investigating the properties of a domain interacting with another protein, it is interesting to consider the dynamics of the interaction. Interactions may be very fleeting and transitory or there may be great stability once the domain has bound and the proteins may continue to interact for a long period of time.

One technique used to study the stability of the interaction when a fluorescently labelled protein is known as Fluorescence Recovery After Photo bleaching (FRAP) (Axelrod 1976). In this experiment, a small area of the fluorescent protein that is bound to the protein or in the localisation of interest (in this case, the fluorescent NET1 protein ABD is bound to actin filaments) is exposed to a high intensity of the exciting laser light at the wavelength that causes fluorescence. This high level of concentrated exposure causes the fluorescent protein to lose the ability to fluoresce; at this point the protein has been photo bleached. If the interaction between the proteins is dynamic, the bleached area will begin to recover fluorescence as proteins that have been bleached dissociate and proteins that are still capable of fluorescing begin to replace them. The speed at which this occurs gives an indication of the dynamics of the interaction. Some proteins are sufficiently dynamic that recovery begins almost before imaging of the area has resumed and in other circumstances proteins have been shown to interact in such a stable manner that the bleached area never recovers fluorescence.

4.7.2 Experimental data

Both NET1c and NET1d ABD-GFP were used for this analysis to provide data for variation between the NET1 actin binding domains. Imaging was carried out three days after infiltration of the ABD-GFP construct into *N. benthamiana* leaves. A small region of interest (ROI) was chosen within the cell, containing labelled multiple labelled filaments (to provide an average of filament fluorescence and recovery in each sample area) and located in an area with a surrounding population of fluorescent protein. The size of the ROI was not set, but altered to cover approximately 15 – 20 filaments. The measurement of fluorescence is averaged over the area and recovery is measured in the same are so consistency of size is less important than averaging the response of several filaments. The cell was imaged with low laser power (5-10%) for one frame to provide an initial level of fluorescence and the ROI was subjected to imaging using the laser at 100% power for three frames.

After this time, the cell was imaged in its entirety and the level of fluorescence in the ROI was measured.

a)

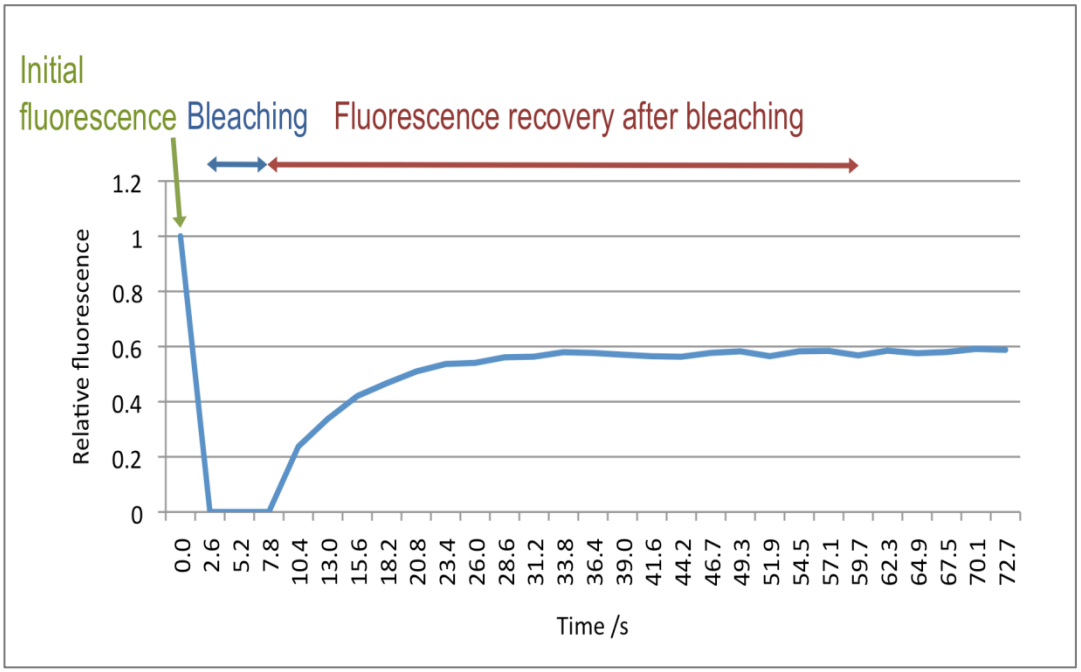

b)

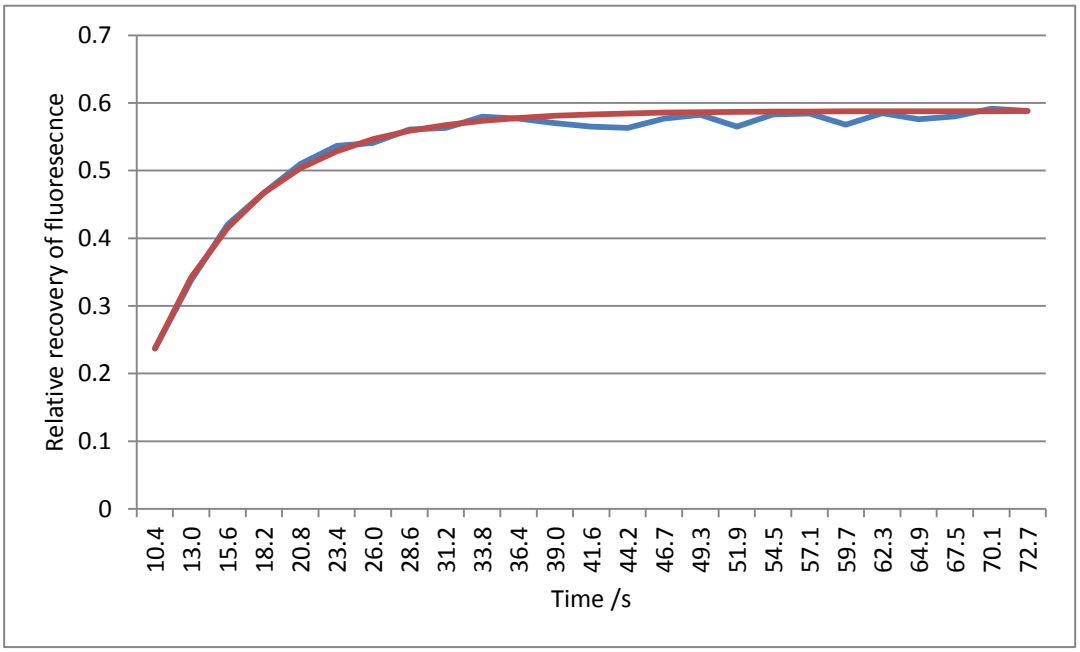

Figure 4.6: This shows data from a representative example of the bleaching process and analysis of the data a) Typical recovery of fluorescence curve seen during photo bleaching experiments. The graph shows an initial level of fluorescence followed by a sharp decrease of fluorescence during the bleaching phase. After this the levels of fluorescence begin to recover in an exponential fashion. b) The curve of recovery of fluorescence (blue) with overlaid predicted exponential (red). Mapping an exponential curve of predicted fluorescence recovery to the data allows analysis of rate of recovery.

This measurement of fluorescence in the ROI produces a curve of fluorescence recovery. By fitting an exponential curve to this data, using least squares regression, a constant can be found according to the following equation:

$$F(t)= F_{\infty}- (F_{\infty}-F_0)e^{-tkOFF}$$

where F_{∞} is the final level of fluorescence achieved after photo bleaching, F_0 is the initial level of fluorescence after photo bleaching and t is equal to time. K_{OFF} is the constant which represents rate of recovery of dissociation of the protein. The rate of turnover of the protein of interest (t ½) can be calculated as:

$$t\,½ = ln(2) / K_{OFF}$$

This value allows the comparison of rates of turnover of various proteins and provides insight into the likely function of the protein. A shorter t ½ is characteristic of a protein with a regulatory role, and a longer t ½ is more likely to be a structural protein, although further proof of this would be required.

	NET1c		NET1d	
	K_{OFF}	$t_{1/2}$ /s	K_{OFF}	$t_{1/2}$ /s
	0.06	11.97	0.10	6.77
	0.22	3.22	0.08	8.22
	0.11	6.45	0.05	12.86
	0.03	20.36	0.16	4.27
	0.05	15.38	0.01	48.14
	0.16	4.33	0.14	5.06
	0.01	66.15	0.07	10.39
	0.06	10.73	0.14	4.98
	0.03	20.56	0.09	7.37
			0.07	10.42
Average	0.08	17.68	0.09	11.85

Figure 4.7: Analysis of Fluorescence Recovery after Photobleaching for NET1c and NET1d actin binding domains associated with actin filaments.

The values of t ½ for both NET1c and NET1d actin binding domains are very small, in the order of seconds. This indicates a very high turnover rate of the protein. The recovery observed appears to occur at all points on the filament rather than moving along the filament from unbleached areas. This suggests that the recovery is from a cytoplasmic population rather than the movement of the NET1 proteins along the filaments. This indicates that, at least with respect to the interaction with actin

filaments, the protein plays a regulatory rather than a structural role in modelling the actin cytoskeletong eg by bundling filaments. It is possible that interactions with other proteins may be more stable and that actin binding is brief and perhaps controlled by other factors but more information is required to draw further conclusions. The apparent stabilisation of the filaments seen when the actin binding domain is transiently expressed within *N. benthamiana* leaf tissue would seem to indicate that the protein was capable of binding to and stabilising the filaments, which might be expected of a structural protein rather than a regulatory one. It is possible that the protein has a high affinity for the actin, such that even though turnover of protein is high, the filaments are still constantly coated in the NET1c or NET1d actin binding domain-GFP proteins, causing a stabilising effect on the filament network.

4.8 Presence of actin binding in other NET groups

4.8.1 Introduction

The NET superfamily in *A. thaliana* is made up of fifteen proteins. Thirteen can be arranged into four groups, with two proteins making a possible fifth group as they have the most divergent form of the NET actin binding domain and may not be true NET proteins (see Phylogenetic Analysis, Chapter 3). Within the four groups the actin binding domain is fairly well conserved and it seems logical to conclude that since actin binding is observed throughout the NET1 group, it is also likely to be conserved throughout the remaining groups as well. The scope of this project is focussed mainly on the Group 1 proteins but as proof of concept, the N-terminal actin binding domain of NET2a was tested for its actin binding capacity. (See also, Actin Binding Domain, Chapter Two).

4.8.2 Experimental data

J. Calcutt (Calcutt 2009) was able to prove that the NET1a retains capacity for binding actin with only the first 94 amino acid residues of the N-terminus of the protein, rather than requiring the 288 amino acids that were used in the first fluorescently labelled recombinant protein. The equivalent region of NET2a was 93 amino acid residues in length and consequently this section of the protein was used in further experiments, tagged with C-terminal GFP and using the previously discussed *A. tumefaciens* and *N. benthamiana* transient expression system.

NET2a(1-93)-GFP

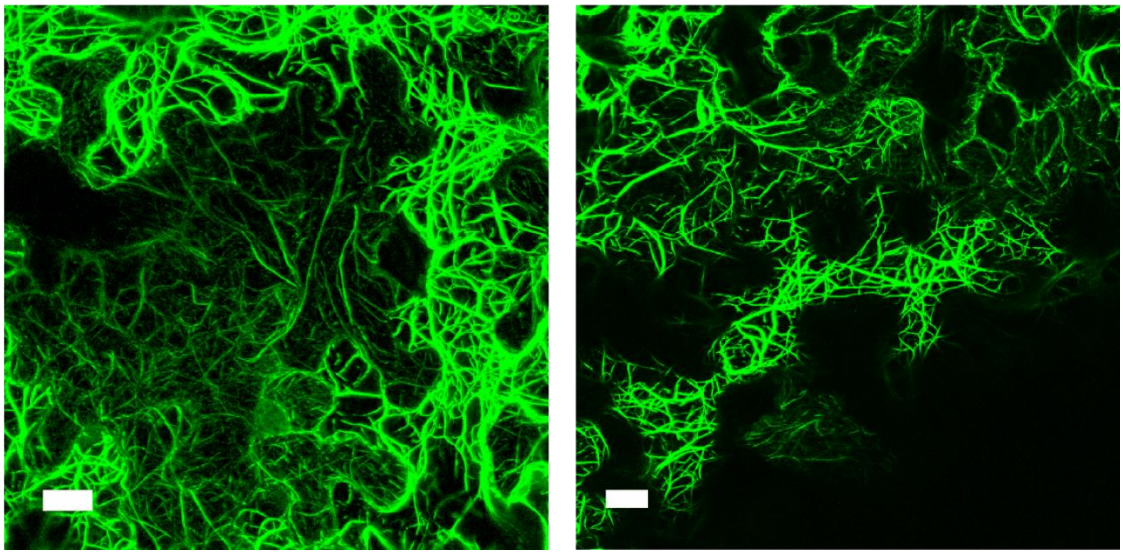

Figure 4.8: NET2a ABD with C-terminal GFP imaged using laser scanning confocal microscopy. GFP excited using 488 nm laser light. Scale bar equivalent to 20 μm.

Figure 4.8 shows the images produced when the NET2a-GFP construct alone was injected into the leaf. As expected, a filament network is visible, although in this case the filaments are rather thicker and perhaps therefore more bundled than is seen with NET1 proteins. The network appears ‘spikier’; filaments may be shorter and straighter than with NET1. This may result from subtle differences in the actin binding domains of the two groups.

4.9 Treatment of NET2a protein actin binding domain with anti-actin drugs and co-localisation with NET1a ABD

To demonstrate actin binding in a way consistent with the NET1 group, the same experiments of co-localisation with NET1a-DSRed and treatment with anti-cytoskeletal drugs were carried out.

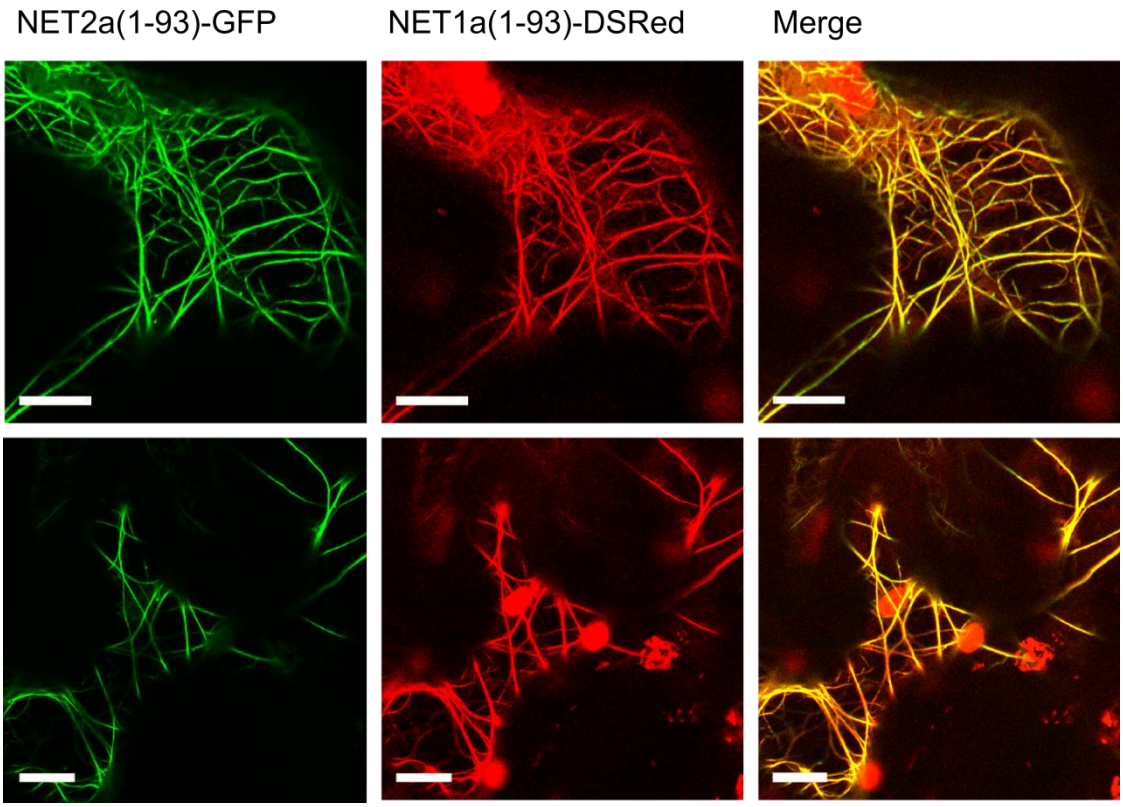

Figure 4.9: Co-localisation of NET2a ABD-GFP with NET1a ABD-DSRed to establish overlapping patterns of expression. Chloroplasts are seen here during excitation of DSRed as they were during co-localisation of NET1 proteins. The yellow colour of the merged images indicates that co-localisation of the two proteins is occurring. Scale bar equivalent to 20 μm.

Figure 4.9 shows the results of the co-localisation of NET2a-GFP and NET1a-DSRed. In this case the two NET proteins appear to co-localise perfectly, hence the almost entirely yellow images in the overlaid images where green and red fluorescence occur in the same place to produce a yellow colour.

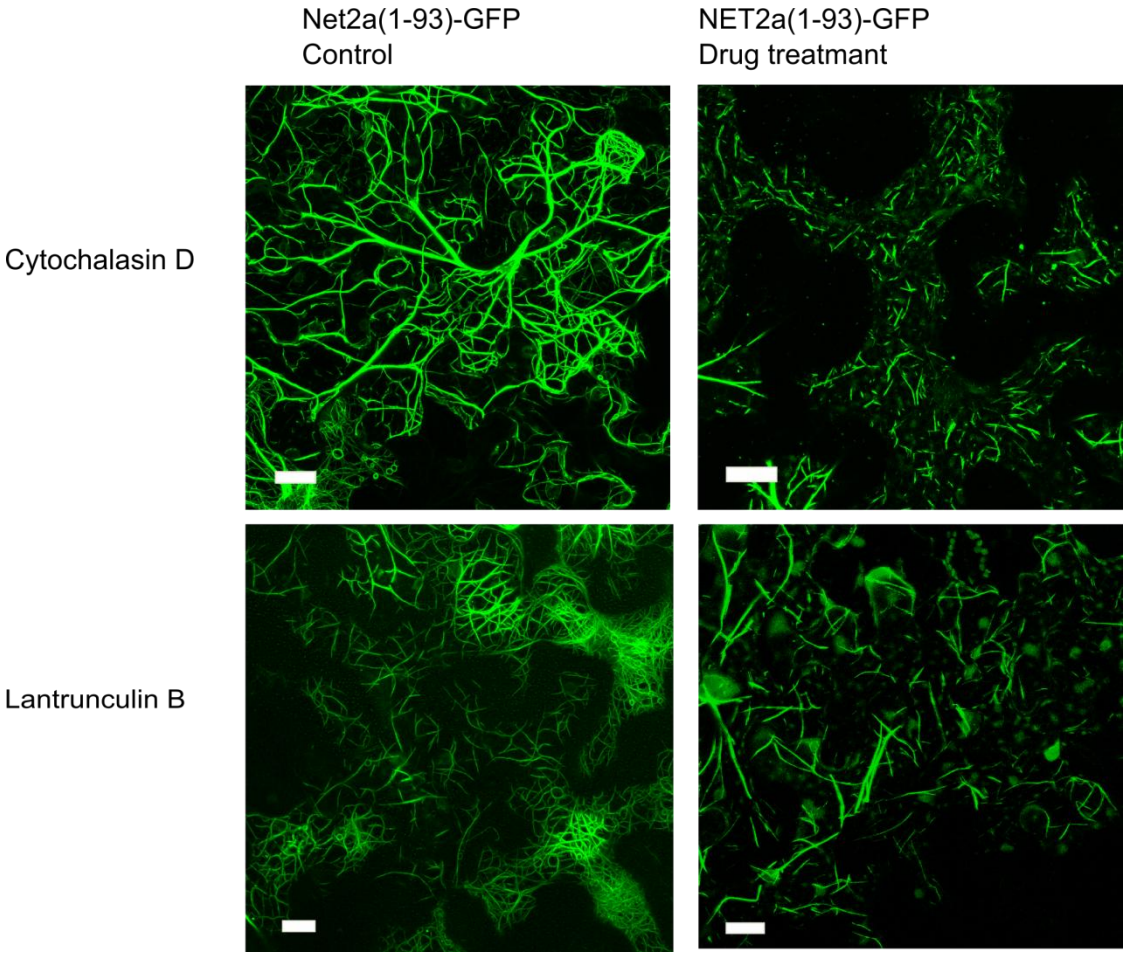

Figure 4.10: Images of leaf cells containing NET2a ABD-GFP 30 mins after treatment with 100 µM Cytochalasin D (top) and 50 µM Latrunculin B (bottom) to show the disruption of the filament network after treatment with anti-actin drugs, in comparison to the controls (left) which show no effect due to control treatment with DMSO. Scale bar equivalent to 20 µm.

Figure 4.10 shows the treatment of NET2a-GFP with anti-actin drugs Cytochalasin D and Latrunculin B. As with the NET1 proteins, the drugs result in the disruption of the actin, and therefore NET2a, filaments. The fragments of filaments here are seen as short sections of filament rather than the aggregates produced by the NET1 proteins. This may be a side effect of the thicker, more bundled filaments that are shown with NET2a. The anti-actin drugs are slower to have an effect on the filament network. It is interesting to note that the NET2a-GFP protein is produced so rapidly and in such quantity that it is essential that imaging be carried out 24 hours after infiltration of the leaf with the *A. tumefaciens* solution or the protein overwhelms the cells and causes initiation of cell death. In contrast, imaging of NET1 proteins is carried out after two to three days. The thickened filaments observed with NET2a-ABD may be due to this over-expression of the protein.

These experiments with NET2a can be seen as a proof of concept for actin binding throughout the remaining NET family groups. Although the project described within this thesis has gone no further in seeking proof of this, work carried out by the Hussey lab to date has shown that eleven out of the thirteen proteins are capable of actin binding via the N-terminal actin binding domain of the protein.

4.10 Yeast two hybrid experiment using the actin binding domain as bait

4.10.1 Introduction

The use of a yeast two hybrid screen is a useful tool in discovering the potential function of a protein interest by providing evidence of potential protein-protein interactions. The process is based on the transcription factor GAL4 which has been split and therefore rendered inactive. The protein of interest (or a section of the protein) is cloned into a vector containing part of the transcription vector, so that both these proteins are expressed as a chimeric fusion protein. The vector containing the bait protein also contains a gene that enables the yeast to produce tryptophan, so that the vector can be positively selected for once transformed into the *Saccharomyces cerevisiae.*

Assuming autoactivation does not take place (when the bait plasmid is capable of activating transcription without the presence of the second part of the transcription factor found in the prey vector); the yeast containing the bait plasmid can be mated with yeast containing a prey library. This contains a large variety of plasmids consisting of an *A thaliana* protein fragment joined to the second region of the transcription factor and a gene conferring the ability to produce leucine.

If an interaction between bait and prey occurs, the two regions of the transcription factor will be brought together to produce a functional protein. This in turn activates the expression of reporter genes, such as ability to grown on minimal media or generation of pigment, to allow detection of yeast colonies containing the interacting bait and prey.

During a library screen, once mating has occurred, any diploid yeast containing both a bait and prey vector which interact will be able to grow on a media lacking in tryptophan (due to the bait), leucine (due to the prey) and either histidine or alanine (due to activity of the reporter genes). It is also possible to select for colonies based on expression of the β-galactosidase gene. Extraction of the prey plasmid from the resultant colony and further testing of the veracity of the positive result in yeast will enable potential interactors for the protein on interest.

4.10.2 Experimental data

NET1a consists of an N-terminal actin binding domain and the remainder of the protein is made up of a series of coiled-coil domains. Coiled coils present something

of a difficulty within the context of a yeast two hybrid screen, due to a tendency for coiled coil domains to appear as false positives due to non-specific binding once in the yeast cell and out of the typical cellular environment. Coiled coil domains are also thought to increase chances of autoactivation when used as bait (Golemis *et al* 1999). For this reason, the 288 amino acid sequence from the N-terminus of NET1a was used for bait. The NET1a-ABD requires only 94 amino acids, so there is potential for further protein-protein interactions occurring without contradiction of the presumed interaction with actin.

Initially the ABD construct was tested for autoactivation to ensure that it would not cause activation of reporter genes without the presence of protein-protein interactions. Figure 4.11 shows the results of these tests. The –W plate, which contains yeast grown on minimal growth media lacking the amino acid tryptophan, is the positive control and shows well developed colonies as is expected, since this is the marker for the plasmid used for the constructs. The row of colonies labelled 'formin' acts as a further positive control, as it is a bait construct that has been used in a successful yeast two-hybrid experiment in the past. The bait is AtFH4ΔTM, the AtFH4 protein lacking the transmembrane domain (Deeks *et al* 2005). This allows comparison with the new bait construct in terms of successful growth of colonies and the presence of autoactivation at levels that may hinder the yeast two hybrid experiment.

The remaining images show the growth of the yeast colonies on different potential selection media. The -W-H plate (growth media lacking tryptophan and histidine) does show some yeast growth but this did not appear before the formin control so is likely to be a successful bait construct, and in the final screen 5 mM 3AT (3-Amino-1,2,4-triazole) was used as an inhibitor of histidine synthesis to further improve the accuracy of the results (this was not tested prior to the screen, but selection was sufficient in the absence of 3AT so a repeat test was not required). The -W-A plate (lacking tryptophan and alanine) similarly shows no colonies, demonstrating that either selection method is suitable for the final screen. The -W+X-α-gal (no tryptophan, addition of 5-bromo-4-chloro-3-indolyl-α -D-galactopyranoside) plate shows white colonies for both the bait construct and the formin control. In this particular selection plate, the lack of tryptophan in the growth media selects for yeast containing the bait construct and the X-α-gal allows blue/white selection of colonies, which contain a viable interaction between the bait and a prey vector by detection of

galactosidase activity. The NET-ABD bait is therefore suitable for all three selection methods.

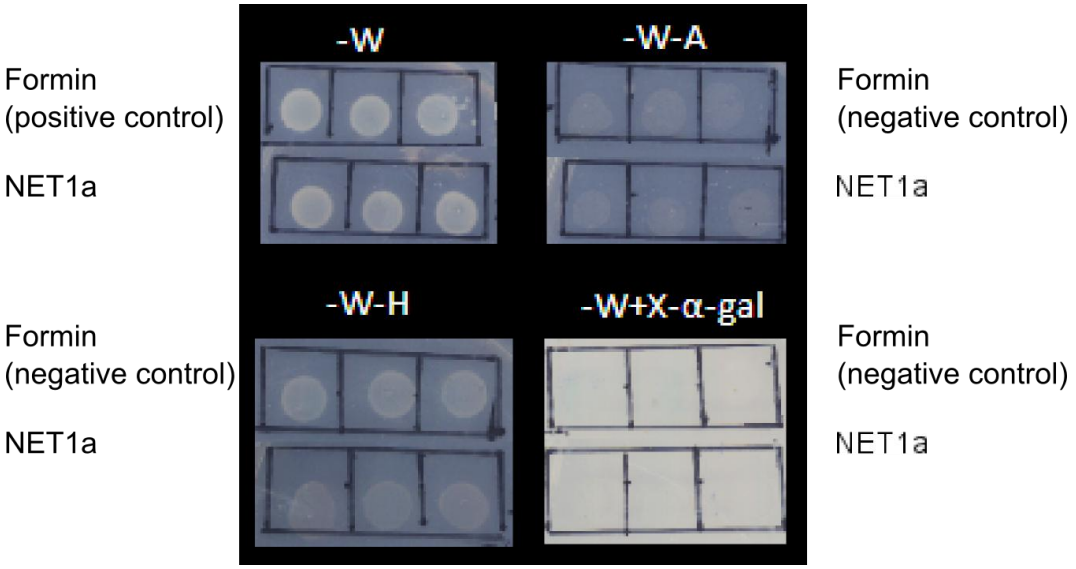

Figure 4.11: Culture plates showing the presence or absence of yeast colonies on different selection media. –W is a positive control plate showing growth of yeast containing the bait construct. –W-A, -W-H and –W+X-α-gal are the three types of selection used. Colonies labelled formin are the negative control and represent a previously tested non-autoactivating bait construct.

The NET1a amino acid sequence to the C-terminal end of the NET-ABD is too large to be cloned and used as a single bait construct, so an alternative solution was to clone the C-terminus as three overlapping sections. The first of these ran from amino acids 307 to 759. This was cloned in the same way as the NET1a-ABD and used for the same autoactivation tests. Figure 4.12 shows the results. With the -W plate, colonies are seen as expected, but colonies also appear on the -W-A plate. Yeast colonies were also observed on the -W-H plate before the appearance of colonies for the formin control. When the construct was used as bait on the -W+X-α-gal plate, blue colonies were observed. This demonstrates that this section of NET1a is highly autoactivating and cannot be used for a yeast two hybrid screen. As a result, the experiment has focussed on the use of NET1a-ABD as bait.

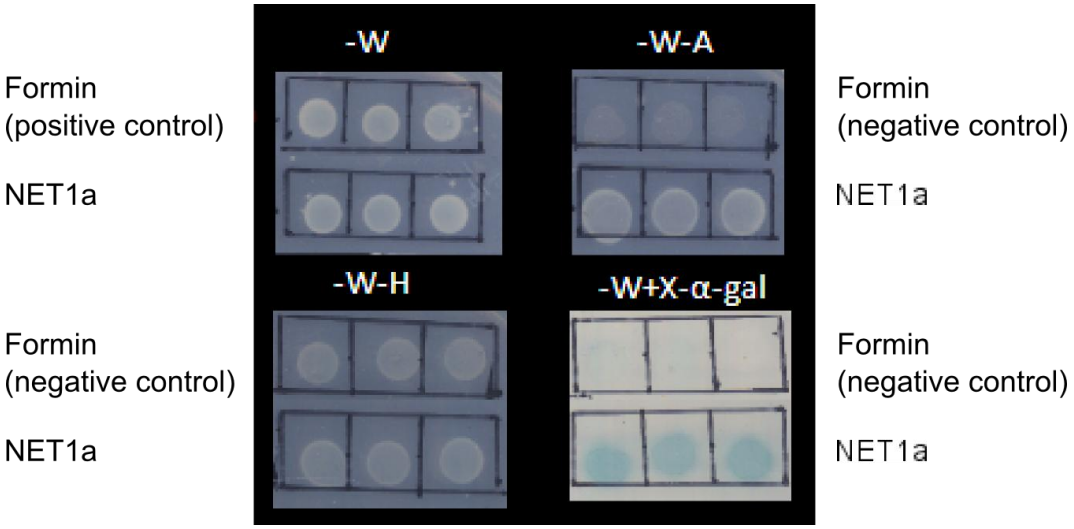

Figure 4.12: Culture plates showing the presence or absence of yeast colonies on different selection media, using a 452 amino acid section from the coiled-coil region of NET1a. –W is a positive control plate showing growth of yeast containing the bait construct. –W-A, -W-H and –W+X-α-gal are selection plates with autoactivation occurring.

The NET1a-ABD bait was used to screen a combination of an oligodT and random primer library. The efficiency of the mating was tested during this screen. The mating efficiency was 53% and approximately 8.3 x 10^6 diploid yeast would have been screened during the process. The selection used was a minimal growth media lacking tryptophan to select for the bait construct, lacking leucine to select for the presence of a prey construct and lacking in histidine to test for an interaction between bait and prey. 3AT was also added to improve this selection by inhibition of histidine which is possible at low levels without the presence of a valid interaction. The 'three dropout' selection media was used, as a compromise of stringency to balance the possibility of excessive false positives and the potential for false negatives, where successful protein-protein interactions do not produce a viable colony. After the appearance of colonies on the –W-L-H selection plates, yeast was streaked onto a second –W-L-H plate, a –W-L-H-A plate and a YPDA plate and a small volume of yeast cells were grown in liquid culture to allow extraction of the prey plasmid DNA. These plasmids were then sent to DBS Genomics for DNA sequencing to identify possible prey proteins and produce the results discussed below.

4.10.3 Results of the Yeast Two Hybrid Screen

The yeast two hybrid screen resulted in six yeast colonies containing potential interactors. Figure 4.13 shows these proteins. One of them, At3g47620 appeared

twice but has henceforth been dealt with as one protein as the behaviour of the two fragments of the protein found is identical in subsequent experiments. Some potential interactors are known proteins and some are unknown, however many of them did not stand up to further validation of the potential interaction.

Colony no.	Gene	Protein	Function
1	At4g37490	CYCB1	Cyclin dependent kinase
2 and 5	At3g47620	AtTCP14	Transcription factor
3	At3g21640	TWD1	FK506-binding protein, similar to PPIases
4	At4g29130	ATHXK1	Hexokinase
6	At4g27980	At4g27980.1	Similar to heat shock protein

Figure 4.13: The potential interactors found from the yeast two hybrid, using the NET1a-ABD as bait.

At4g27980.1 is an unknown protein with similarity to heat shock protein Hsp40. Heat shock proteins bind to a multitude of other proteins to protect them from heat damage and ensure correct folding. They are capable of association with many different proteins so are likely to be a false positive.

At4g37490.1 is a cyclin dependent protein kinase, similar to COP1 (Li *et al* 2005). While the presence of a kinase potentially interacting with a 'kinase interacting domain' presents a plausible scenario, NET1a does not contain a true kinase interacting domain (the KIP1 domain is not in fact the domain in PiKIP involved in interactions with the kinase, *see Chapter 3*) so the interaction becomes less likely. It is also known to be located to the cell nucleus whereas NET1a appears to be exclusively expressed in root tissue and has never shown a nuclear localisation. COP proteins, in particular COP9, have been shown to be common false positives in yeast two hybrid experiments, so the conclusion that this protein may not be a true interactor becomes more conceivable. (Nordgård *et al* 2001).

At3g47620.1 is a transcription factor that regulates seed germination, is expressed in embryonic vascular tissue and responds to giberellin and abscisic acid. (Riechmann *et al.* 2000) There may be a link to NET1a through the expression pattern in vasculature, although NET1a has not previously been associated with seed germination (Calcutt 2009).
While these three potential interactors do not suggest an obvious function for or relationship with NET1a, they require further analysis. The yeast two hybrid did, however, provide two potential interactors with a more obvious link to the known

properties of NET1a. The first was At3g21640.1: this is a 42 kDa FK506-binding protein with similarity to PPIases (peptidyl-prolyl cis/trans isomerases) in mammalian steroid hormone receptor complexes. It is located on the plasma membrane, which agrees with the known localisation of NET1a and is involved in leaf development, with a possible role in signalling, auxin response or vacuole transport. Mutants of this gene have the 'Twisted Dwarf' phenotype and show reduced size and disorientated growth in all organs. This does suggest a potential role in auxin signalling and growth (Geisler *et al* 2003), which had been identified as possible links to NET1a function through the use of mutant phenotypes (Calcutt 2009).

The second possible interactor is At4g29130.1, which encodes a hexokinase involved in glucose signalling (Balasubramanian *et al.* 2007). There may be a connection between this protein and F-actin, as it is thought to link the actin cytoskeleton to glucose signalling, but it has been shown to bind the actin directly so there is no role for NET1a as an intermediary. NET1a cannot be acting upstream of this protein in the pathway as direct protein interaction with glucose has already been found for At4g29130.1, leaving no current gap for the role of NET1a although it is possible that the pathway is more complex than the current model. In addition to this, NET1a has already been shown to bind actin filaments directly so a role upstream in a signalling pathway is less likely than a role downstream in a pathway, affecting actin directly.

The most likely cause for the positive result is that due to another property of the interacting protein: the hexokinase is also a structural homologue of F-actin, so NET1a may be able to bind to it in the same way it binds actin filaments (Balasubramanian *et al.* 2007). This does confirm the theory that this section of the protein is solely responsible for binding actin, and that it does so directly. The binding of a structural homologue may also suggest that the binding of the KIP1 domain is based on the physical structure of the domain rather than the effect of specific amino acid residues.

To confirm the results of the yeast two hybrid library screen, the rescued plasmids were returned to yeast and one-on-one mating experiments were carried out. Yeast containing the prey plasmids were mated with yeast containing either the empty bait plasmid or the bait plasmid with Construct 4. After mating, the diploid yeast were grown on -W-L-H media (lacking in tryptophan, leucine and histidine as used during the screen) or –W-L-H-A media (lacking in alinine in addition to tryptophan, leucine and histidine) to test for the consistent presence of an interaction as false positives

are a common problem during a yeast two hybrid library screen. This test of the potential interactors was repeated twice. Figure 4.14 shows the results of these experiments. 'No growth' has been used to indicate a complete absence of yeast growth on the plate, while 'Colony' has been used to denote a thick, white yeast colony. 'Small colony' indicates that growth of a yeast colony was only partial, leading to a very small or thin colony.

Colony no.	Gene	Dropout media	First mating test		Second mating test		Interaction
			Control plasmid	NET1a bait	Control plasmid	NET1a bait	
1	At4g37490	-W-L-H	Colony	Colony	No growth	Colony	Yes
		-W-L-H-A	No growth	Colony	No growth	No growth	Yes
2 and 5	At3g47620	-W-L-H	No growth	No growth	Colony	No growth	No
		-W-L-H-A	No growth	No growth	No growth	No growth	No
3	At3g21640	-W-L-H	No growth	No growth	Colony	No growth	No
		-W-L-H-A	No growth	No growth	No growth	No growth	No
4	At4g29130	-W-L-H	Colony	Colony	Colony	Colony	Unclear
		-W-L-H-A	Small colony	Colony	Colony	Colony	Unclear
6	At4g27980	-W-L-H	Colony	Colony	Colony	Colony	Unclear
		-W-L-H-A	No growth	Colony	No growth	Colony	Yes

Figure 4.14: Results of one-on-one mating tests carried out to verify the results of the yeast two hybrid library screen. Two repeats of this test were undertaken and each test is carried out on 3 drop out (lacking W, L and H) and 4 drop out (lacking W, L, H and A) growth medium. The empty bait vector was used as a negative control.

In both repetitions of this experiment, the interaction with the transcription factor At3g47620.1 and the NET1a-ABD is not present and colonies are more likely to appear with the control plasmid than with the bait construct. This is also true for the protein At3g21640.1, or TWD1, and these two potential interactors can be discounted as false positives in the initial screen.

The heat shock protein, At4g27980.1, produced colonies with both the bait construct and the control plasmid on the three drop out growth media, but on the four drop out media there is a consistent positive result for the bait and not for the control plasmid in both the first and second repetitions of the mating test. This suggests a positive

result for this protein, but as previously discussed, heat shock proteins are capable of binding to many proteins in a protective faculty rather than integration into a particular pathway or process within the cell. This doubt as to the validity of the binding of At4g27980.1 under normal cellular conditions is supported by the pattern of expression of the gene, which is entirely in above ground tissue and the embryo so unlikely to be expressed in the same cells as NET1a *in vivo* (Schmid *et al.* 2006).

The most promising interactor is the cyclin dependent kinase, which has consistently shown interaction with the bait but not with the control plasmid. The CYCB1 protein has also shown an overexpression phenotype of increased proliferation of root cells (Doerna *et al.* 1996), and a link to control of the cell cycle. Since actin shows reorganisation during the cell cycle (Yu *et al.* 2006), interaction between the actin binding protein NET1a and CYCB1 presents a possible link between these two processes. There is also a connection between the mutant phenotype shown by CYCB1 and the effects on roots seen on removal of the NET1a and NET1b proteins (Calcutt 2009). However, the disparate cellular localisations of CYCB1 and NET1a (to the nucleus and the periphery of the cell respectively) and the discovery of a long root rather than a short root phenotype which is caused by defects in cell elongation rather than cell division (see Chapter Six) must be considered and further validation and investigation of the interaction is required.

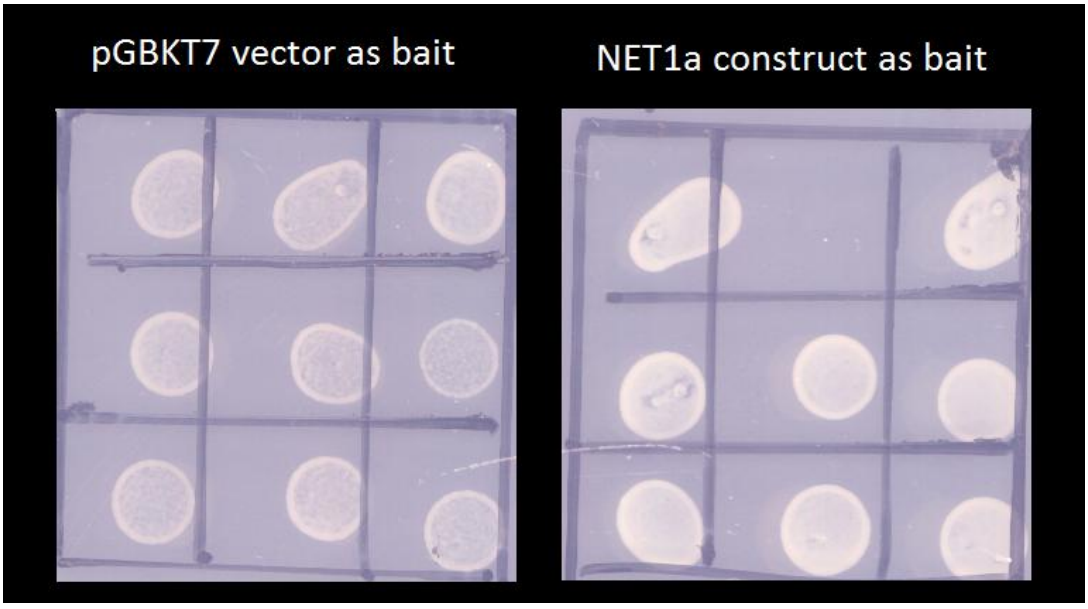

Figure 4.15: Growth of colonies on selection, showing decreased growth of yeast colonies containing the empty vector (the set of nine colonies on the left) which acts as a control for the one on one mating test and which should not show any growth in comparison to yeast containing the hexokinase bait (the set of nine colonies on the right) where growth of colonies would indicate a positive result if yeast growth occurred here but not in the control.

The final interactor to be considered is At4g29130, the hexokinase. The results of the one on one mating tests are unclear in this case, as growth of colonies was observed with both the NET1a bait and the control vector in every case. This may be due to some contamination or to an unknown property of the hexokinase prey. In some cases however it was noticeable that the growth of yeast containing the NET1a protein was more rapid and colonies were denser than those containing the control (see Figure 4.15). For this reason, the possibility of interaction is still present and must be further evaluated. The source of the protein-protein interaction is, however, unlikely to be due to functional properties of the bait and prey, and liable to be due to the structural similarity of the hexokinase to F-actin. The ability of NET1a to bind to a structural homologue is worthy of note as it indicates a reliance on structural properties of the F-actin rather than particular interactions or binding between amino acid constituents of the two proteins. As yet, structural predictions for the NET1a actin binding domain have not shown any essential residues or binding domains with the exception of the triple tryptophan at the N-terminus of the protein.

4.11 Conclusion

The N-terminal actin binding domains of the Group1 NET proteins show *in vivo* localisation to a filament network, which forms a net-like structure throughout the cell, in particular at the periphery of the cell. In all members of the NET1 group, the N-terminal actin binding domain of each protein has been shown to bind to the F-actin form of the actin cytoskeleton. Multiple experimental approaches have been used to establish this association to actin fibres, namely labelling of F-actin with the GFP-labelled NET1 actin binding domain and the subsequent disorder of the filament network upon treatment with anti-actin drugs. Co-localisation between the NET1 proteins and NET1a has also been used and demonstrates that the Group 1 NET proteins bind to nearly identical populations of filaments, with variation apparently due to variation between individual cells rather than differences between actin binding properties.

The NET1c and d actin binding domains cause stabilisation of filaments, as little movement of filaments is seen during transient expression of the actin binding domains with C-terminal GFP. The binding of the proteins is, however, highly dynamic, as recovery of fluorescence is seen after photobleaching. The role of these proteins may be to stabilise or tether actin filaments or to enable crosslinking between filaments but the interaction may be transient in nature. There may be a high turnover of the protein but a high affinity for actin, which would explain the constant decoration of all filaments but the high rate of turnover of the NET1c and d proteins. Further analysis is required to determine the exact role of the proteins. It is likely that the variable C-terminal domains of the NET proteins provide secondary functions beyond the actin binding capacity of the family.

Analysis of further groups of NET proteins has also established actin binding in these proteins, suggesting that the NET actin binding domain is universally capable of associating with F-actin. Since no homologous proteins have been previously identified and no homologues exist outside of the plant kingdom, it can be concluded that the N-terminus of NET proteins contains a novel, plant-specific actin binding domain.

A 288 amino acid sequence from the C-terminus of NET1a, containing the 94 amino acids of the NET actin binding domain was used as bait in a yeast two hybrid library screen. Several putative interactors were discovered during the screen and the

integrity of the interactions was further analysed through one-on-one mating tests. Two proteins continued to show a potential interaction with the NET1a actin binding domain. The first of these was a hexokinase, ATHXK1, which is involved in connecting glucose signalling to the actin cytoskeleton. While NET1a may have an as yet undiscovered role in this pathway, the interaction may also occur because the hexokinase is a structural homologue of F-actin and the NET1a actin binding domain appears to be capable of binding to F-actin directly (Calcutt, 2009). The second potential interactor is CYCB1, a cyclin dependent protein kinase. This shows the most reliable interaction with the NET1a actin binding domain and mutants lacking the protein show altered root growth, as do mutants lacking in NET1 proteins. There is also the potential for a role for NET1a in the reorganisation of actin, which occurs during the cell cycle. NET1a has not yet shown any link to the cell cycle and the mutant phenotype is a result of altered cell elongation rather than cell division (see Chapter Six). The subcellular localisations of the two proteins are not overlapping; so much further work would be required to identify how these proteins are related if the predicted interaction is indeed correct.

Chapter Five:

Analysis of the localisation and expression patterns of the NET1 group proteins

5.1 Introduction

The localisation of the actin binding domain of the NET1 proteins has been established using transient expression within *N. benthamiana* leaf cells, where the proteins have been shown to interact with actin filaments. This localisation is however only representative of the function of a small percentage of the whole protein, and the much larger C-terminal domains are likely to influence the localisation and function of the protein. To understand the role of the NET1 proteins beyond their ability to interact with the actin cytoskeleton, it is necessary to consider the localisation of the proteins within a cellular and whole plant context.

Affymetrix data can give insight into the expression of a gene within the plant, as discussed in Chapter 3. It can also have limitations, particularly due to contamination during the screening of a large volume of samples. Incorrect prediction of genes within the chromosome can also limit the usefulness of the data, as seen with the Affymetrix data for NET1a. Even when no obvious errors are noted, the localisation pattern must be confirmed by experimental means.

J. Calcutt (Calcutt 2009) used the GUS reporter gene to analyse expression of the NET1a promoter and found high levels of expression within the root vasculature and meristematic tissue. Some expression was also seen in the vasculature of the aboveground tissue. To continue this investigation, the activation of the promoters of NET1b and NET1d has been analysed using the same method.

To observe the subcellular localisation of NET1 proteins, polyclonal antibodies have been raised in rabbits and rats to NET1c and NET1d respectively. These have been used in immunological staining of wild type root tissue to demonstrate the localisation of the proteins within the cell.

5.2 Creation of stable *A. thaliana* lines containing NET1b and d promoter driven GUS reporter gene

5.2.1 Introduction

In order to study the expression of a particular gene in more detail it is possible to use a reporter gene to show gene expression. A construct is made such that the promoter region of the gene of interest is placed before a reporter gene and stably transformed into a plant line. In tissues where there is transcription of the gene of interest, the GUS reporter gene is also transcribed.

In this case the reporter gene is the GUS gene, which encodes the enzyme β-glucuronidase. This enzyme catalyses the cleavage of β-glucuronides and will cleave a variety of substrates to produce a substance which can be detected in the tissues where transcription is occurring. In this case X-Gluc (5-bromo-4-chloro-3-indolyl beta-D-glucuronide) is used and is cleaved by the enzyme to form glucuronic acid and 4-chloro-3-bromo-indigo, a blue precipitate, which can be viewed in the plant tissue using light microscopy. To produce this reaction, plant tissue is incubated in a buffer containing the X-Gluc reagent and both ferrocyanide and ferricyanide to ensure death of the tissue once it is placed into the buffer. This prevents atypical transcription of the protein of interest after removal of the tissue from the plant. (Jefferson et al. 1987) After staining an ethanol series is used to remove chlorophyll and clear the tissue for imaging.

5.2.2 Experimental data

To produce the stable *A. thaliana* GUS lines, the promoter regions of NET1b and NET1d were amplified (approximately 2 kb of the DNA upstream of the gene) and clonedinto a vector containing the GUS reporter gene. This was then stably transformed into *A. thaliana* using an *A. tumefaciens* transformation system involving dipping wild type plants into a solution of the bacteria and sucrose with a detergent (Silwet) allowing the bacteria to infect the flowers and developing embryos of the plant and transfer the GUS construct into the DNA of the next generation of plants. After transformation, antibiotic selection using kanamycin was used to identify the plants containing the construct. These T1 plants were allowed to proceed to generation T2 for analysis.

J. Calcutt (Calcutt 2009) used this method to study the transcription of NET1a and discovered that the protein is expressed within the root tissue. There is also some

expression within the vascular tissue of above ground tissue and embryos. The pattern of expression within the root is tissue specific.
NET1a transcription occurs in the vasculature of the root, restricted to the vascular cambium, and in the meristematic tissue at the root tip where it is apparently present in all cell files. It is absent from the very tip of the root below the meristem.

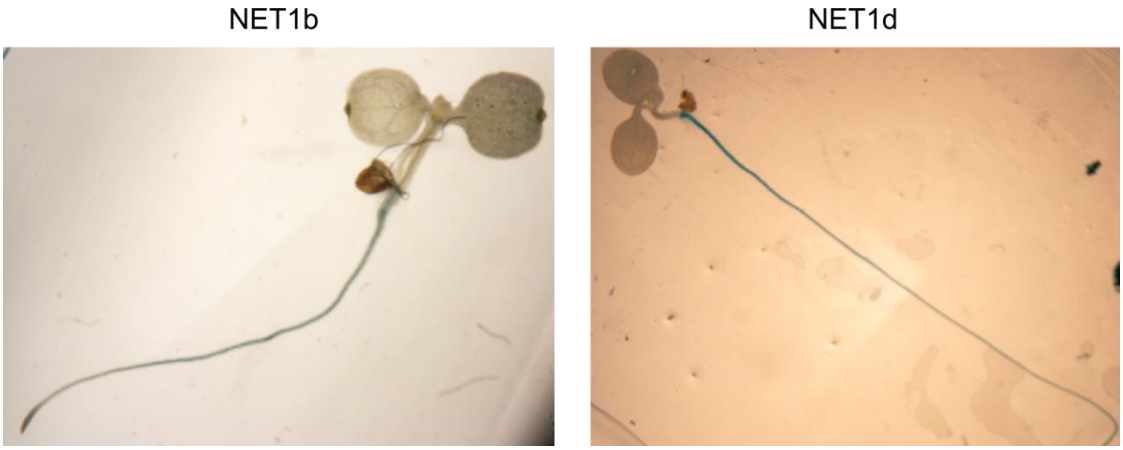

Figure 5.1: Images of GUS stained seedlings at approximately 2x magnification. a) NET1b seedlings three days after germination. b) NET1d seedlings three days after germination.

As shown in Figure 5.1, at three days after germination, the GUS histochemical staining shows expression of both NET1b and NET1d within root tissue, but not within leaf tissue. The pattern of transcription is not identical in the two genes. Examination of the root tissue at a higher magnification allows distinction of the variation between the genes. Figure 5.2 shows the two patterns of staining at higher magnification.

The expression pattern of these genes is incredibly interesting. NET1b shows a similar pattern of transcription to the NET1a gene, present in the centre of the root, possibly in the vascular tissue, but unlike NET1a it does not show the widening of expression to cover all cell files at the meristem. Instead the gene continues to be transcribed in the cell files at the centre of the root tissue to the root tip, past the area where NET1a expression ceases. It is not possible to see at this level of magnification whether the NET1a and NET1b genes are transcribed in the same or slightly different cell layers.

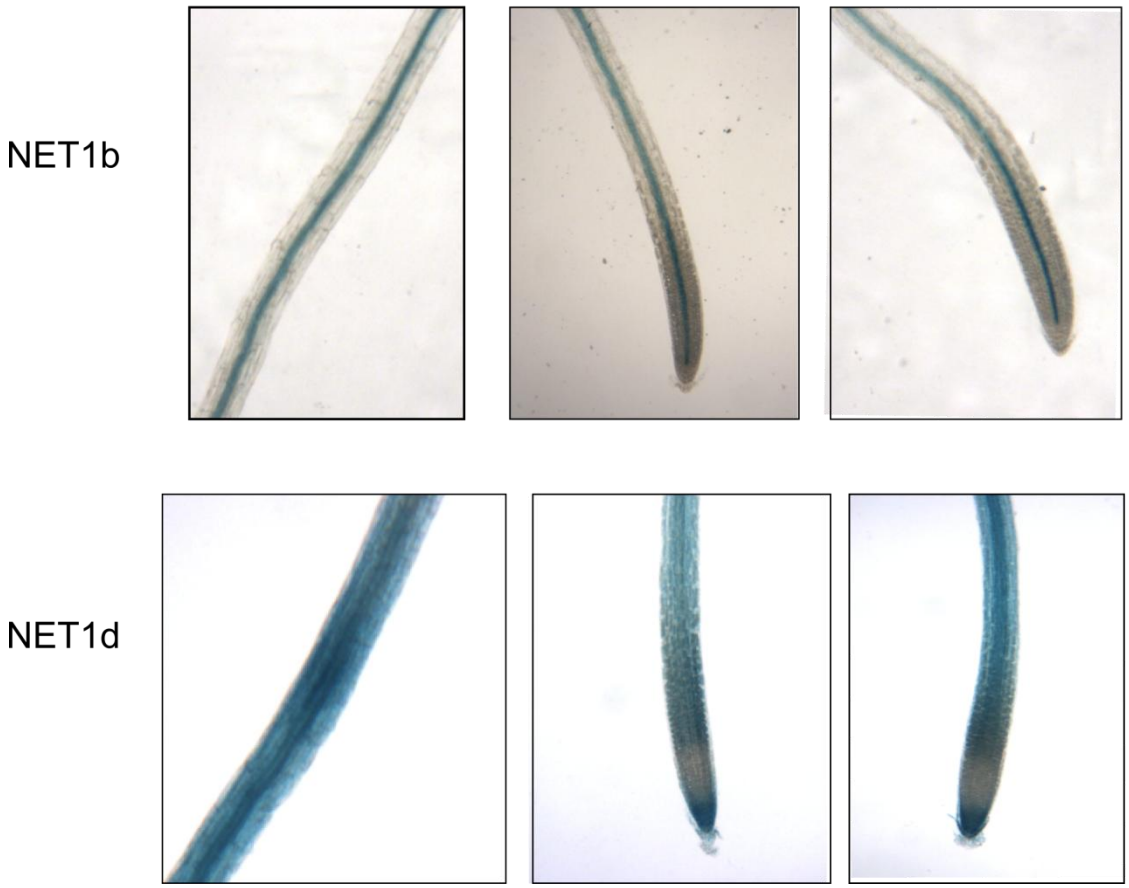

Figure 5.2: GUS histochemical staining of roots viewed at approx. 10x magnification. a) Expression pattern of NET1b at three days post germination. b) Expression pattern of NET1d at three days post germination.

NET1d shows another interesting pattern, expressing in the outer tissues of the root, in the epidermis and potentially in the vascular layers (some roots show darker staining towards the centre of the root) and showing expression throughout the whole root except within the meristematic tissue where no expression is seen. Expression resumes at the root tip, in the area where NET1a transcription does not occur.

NET1b		NET1d	
Line	Description of GUS staining	Line	Description of GUS staining
A	Vascular localisation	A	Epidermal staining, staining absent from meristem
B	Vascular localisation	B	Epidermal staining, staining absent from meristem
C	Vascular localisation	C	Epidermal staining, staining absent from meristem
D	Vascular localisation	D	Epidermal staining, staining absent from meristem
E	Vascular localisation	E	Epidermal staining, staining absent from meristem
F	No staining observed	F	Epidermal staining, staining absent from meristem
G	No staining observed	G	Epidermal staining, staining absent from meristem
H	Low level of expression, expected pattern observed	H	Epidermal staining, staining absent from meristem
I	Vascular localisation	I	No germination
J	Vascular localisation	J	Epidermal staining, staining absent from meristem
K	Vascular localisation	K	Pattern of expression typical of NET1c not NET1d
L	Expression seen in main root but not root tip	L	No germination
M	Pattern of expression typical of NET1d not NET1c	M	Epidermal staining, staining absent from meristem
N	Vascular localisation	N	Epidermal staining, staining absent from meristem
O	No staining observed	O	No germination
		P	Low levels of expression, expected pattern observed
		Q	Epidermal staining, staining absent from meristem
		R	Low levels of expression, expected pattern observed

Figure 5.3: Results of GUS histochemical staining at three days post germination in all lines containing NET1b promoter and NET1d promoter constructs. Staining was remarkably consistent between the lines, without large variation in the overall pattern of staining although levels of blue precipitate varied.

Figure 5.3 shows the appearance of GUS staining in a variety of different lines, as the location of the insertion of the GUS construct in the genome can cause variations in expression levels and patterns. In fact in this case, results seem to be very consistent between lines with only some small variations and one line for each construct which appears to show an identical pattern of expression to the other gene, and may be due to cross contamination during self pollination before analysis of the subsequent generation. For NET1c fifteen lines were analysed and ten showed the same pattern of GUS histochemical staining and analysis of eighteen NET1d lines produced fourteen lines with the expected pattern of GUS expression.

These expression patterns are particularly interesting because the NET1 proteins appear to cover all the tissue in the root in overlapping patterns of transcription of the genes. This fits well with the high structural similarity between the proteins and their possible ability to compensate for one another when one gene is absent (discussed in Chapter 6). The variation between the genes and expression patterns may be due to differences between the functions of cell files within the root, for example the presence of plasmodesmata pore units and symplastic transport of larger proteins and nucleic acids found in phloem and companion cells due to the enucleate nature of mature sieve elements in the phloem (Ayre *et al.* 2003).

NET1d NET1b

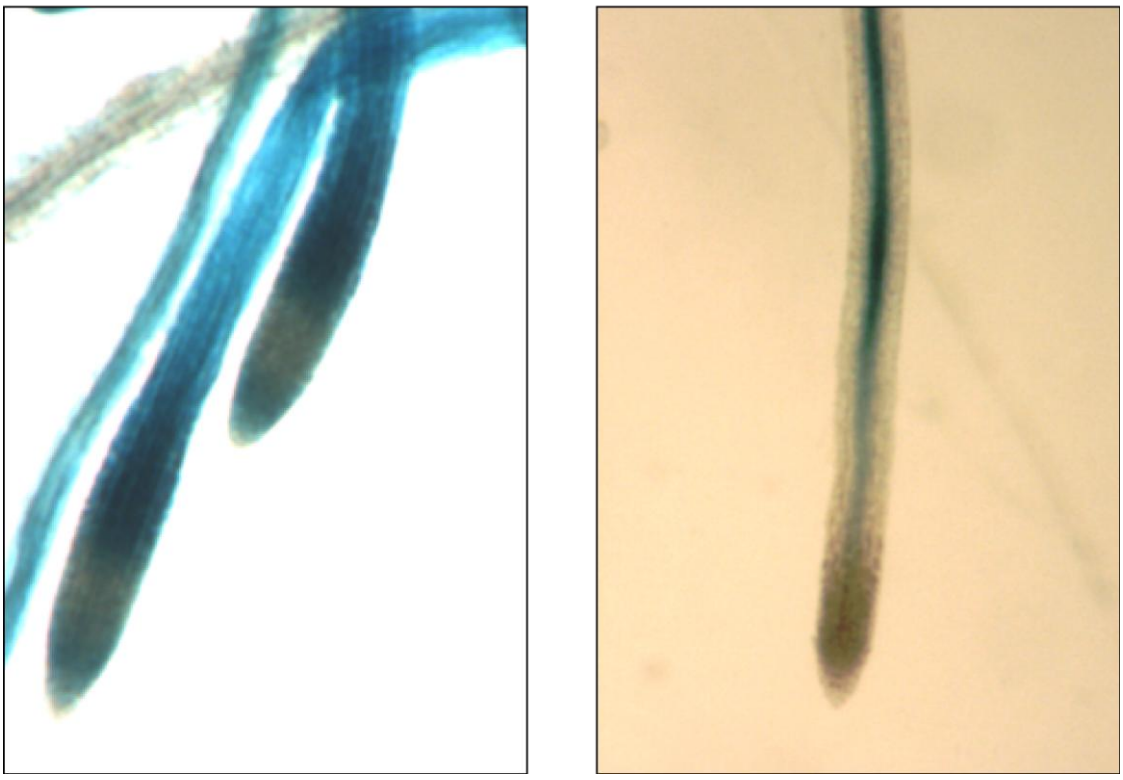

Figure 5.4: GUS staining in root tissue at twelve days post germination between 2x and 10x magnification in a) NET1d and b) NET1b

The expression of the two genes is largely the same at day twelve after germination compared to day three. The expression pattern in the roots is identical. While some expression in the leaves is seen, it is very variable and not consistent between lines and may be related to damage of the leaf when it was placed into the GUS buffer. The expression seen within the leaf is not specific to one particular tissue, unlike the expression of NET1a that is localised only to vasculature. Given the inconsistent

nature of leaf staining, the most interesting area of expression remains that found in the root.

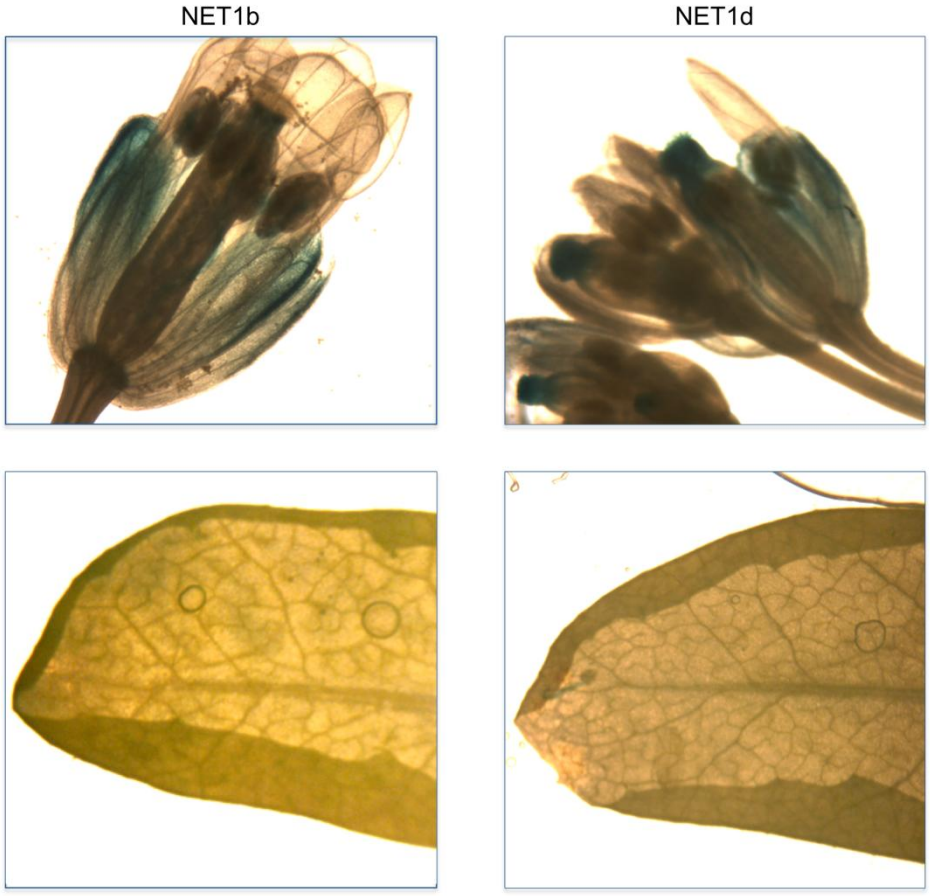

Figure 5.5: GUS histochemical staining within flowering shoots and leaves of a) NET1b and b) NET1d.

Flowering stems were used to show possible gene expression throughout flowering and silique formation. No staining was observed in leaves or siliques except at the base of the stem. This is likely to be a response to damage where the stems were cut, as are the small and inconsistent areas of expression in leaves. Some expression occurs within the stigma of both lines, with a diffuse pattern of expression also occurring in the sepals. This expression requires some further investigation but in general it appears that the expression pattern of NET1b and NET1d is located almost exclusively in roots.

5.3 Sectioning of NET1a, NET1b and NET1c roots after GUS histochemical staining

The pattern of overlapping GUS staining seen with NET1a, b and c promoter regions is a particularly interesting feature of the NET1 proteins. If the transcription of the proteins occurs in different tissues without overlap, it suggests a locational segregation of the proteins rather than a functional one (although functions may still be different even if they occur in different locations) while expression within the same tissues would suggest a role for more specific variations in the functions of the four proteins. Aspects of the staining patterns suggest both arguments. For example the darker staining of the centre of roots with the GUS gene under the control of the NET1d promoter indicates expression in the vascular tissue for all three proteins, whereas the presence of NET1a in the meristematic tissue compared to the complete absence of NET1d may indicate a mutually exclusive expression pattern.

To investigate the expression pattern further sectioning of the root was used. After GUS histochemical staining the roots of plants three days after germination were fixed using 2% paraformaldehyde Karnovsky's fixative (Karnovsky 1965) and taken through an ethanol series before embedding within Historesin and sectioned in 50 μm slices using an ultramicrotome. This fixation, embedding and sectioning, was carried out by C. Richardson, Durham University Microscopy and Bio-imaging Facility.

Figure 5.6 shows the results of the root sectioning. 50 μm sections were taken through the root tip and meristem and then through the root after the elongation zone. In cases where some GUS staining could be seen in the hypercotyl sections were also taken in this region.

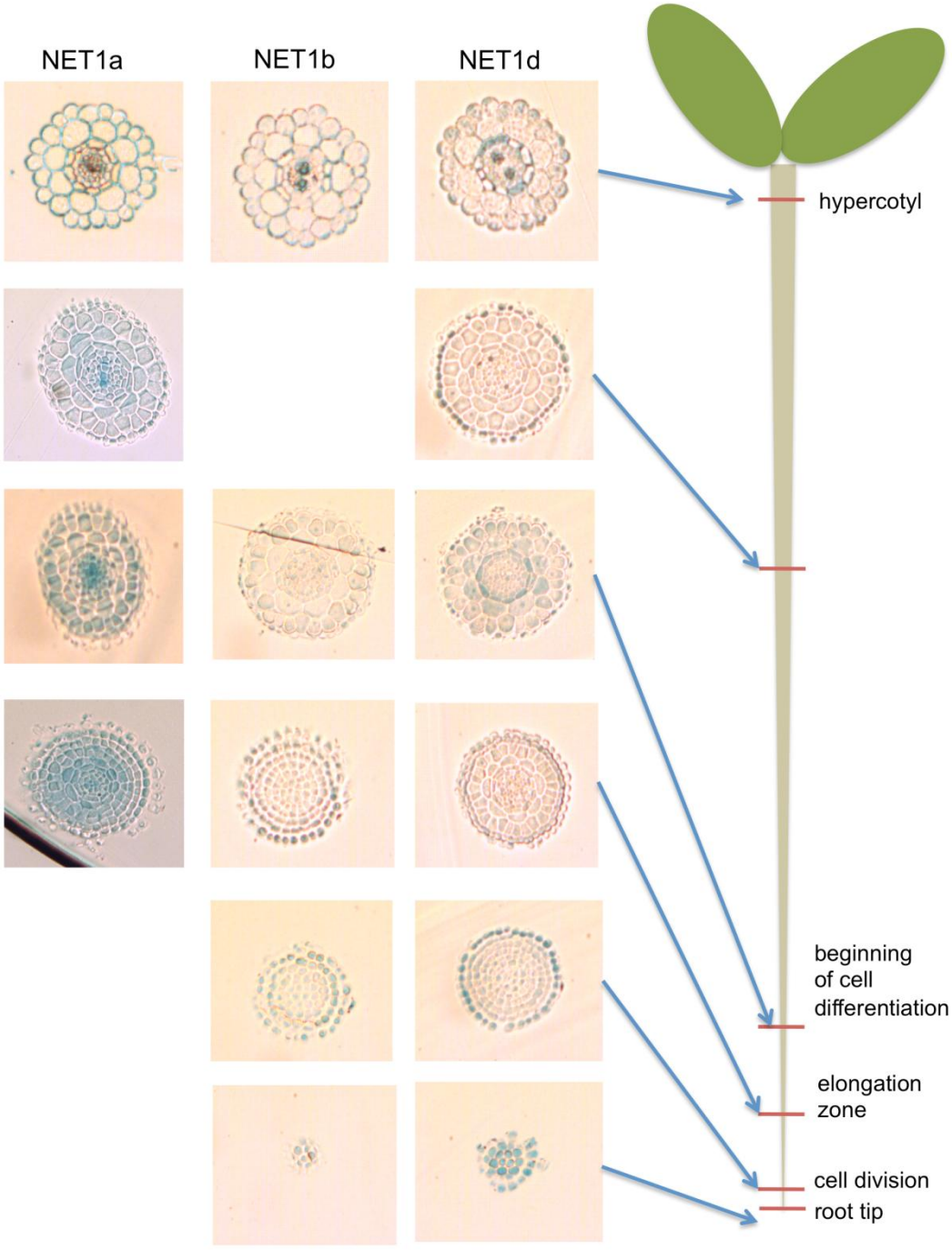

Figure 5.6: 50 µm sections of root tissue after GUS staining from NET1a, NET1b and NET1d. Sections are shown in order travelling down the root from stem on the left to root tip on the right. Sections were taken from the hypocotyls, half way down the length of the primary root, and from the elongation zone through the meristem to the root tip.

In roots where the promoter region of NET1a is used to drive GUS expression, some of the blue staining appears to have moved to all layers of the root tissue. It can be

observed however that this staining is in tissue which does not contain the blue compound in whole roots and the staining in these tissues is pale. Far darker staining can be observed within the stele of the primary root suggesting a vascular localisation.

In the meristematic and lower elongation or transition zones, dark blue staining is observed in all cell files. This is again as expected from GUS staining of the whole root where the outer cells of the root appear to be stained, although it does confirm that expression is in all cells at this area of the root development. The root tip does now show staining, or only a very faint blue colour as anticipated due to the staining of the whole root.

NET1b does not show as clear a pattern of GUS staining as NET1a. Whole root staining shows a central root stain with no changes throughout the progression of the root tissue from root tip to fully elongated cells. Unfortunately after sectioning the localisation of the stain appears far less specific and more diffuse. Some staining appears in all cell files in an irregular distribution. Staining appears inconsistent within the cells, with patches of darker and lighter staining. In some sections two central circles of blue staining are observed, suggesting vasculature, and possibly an association with xylem tissue. In other sections staining is less distinct and appears more in the cortex and epidermis. While the staining of whole roots appears to have a much narrower pattern of expression, which corresponds to the vascular localisation, it is possible that some expression also occurs in the cortex of the root.

The sections taken after staining of roots with NET1d promoter driven GUS expression show the most interesting result. The whole root staining results in a root where all tissues appear blue and the exact cell files showing expression cannot be distinguished. The root tip shows blue staining in all cells, which then disappears within the meristematic tissue where universal expression of NET1a is observed. After this region GUS staining reappears, but not in all cell files. GUS expression is located in the epidermal cells, forming a ring around the root tissue which results in the entirely blue root seen during whole root staining, but it also appears within the stele, in two distinct areas of expression, suggesting a vascular localisation, but not one which is identical to NET1a. Further up the root, further cell files show GUS staining, with a visible ring around the stele forming, possibly the endodermis. The epidermal localisation remains constant throughout the root.

Figure 5.7 shows a comparison of the areas of GUS expression within root tissue. Considering all three proteins, the GUS staining covers the majority of the root tissue. Staining appears in the root tip, meristem and in the remainder of the root. Expression of the NET1 proteins occurs in the vasculature, endodermis and epidermis. The major area lacking in NET1 expression is the root cortex, and it is possible that this may be the area of expression of NET1c, although this hypothesis would require analysis not currently possible due to the difficulty in cloning the promoter of this gene.

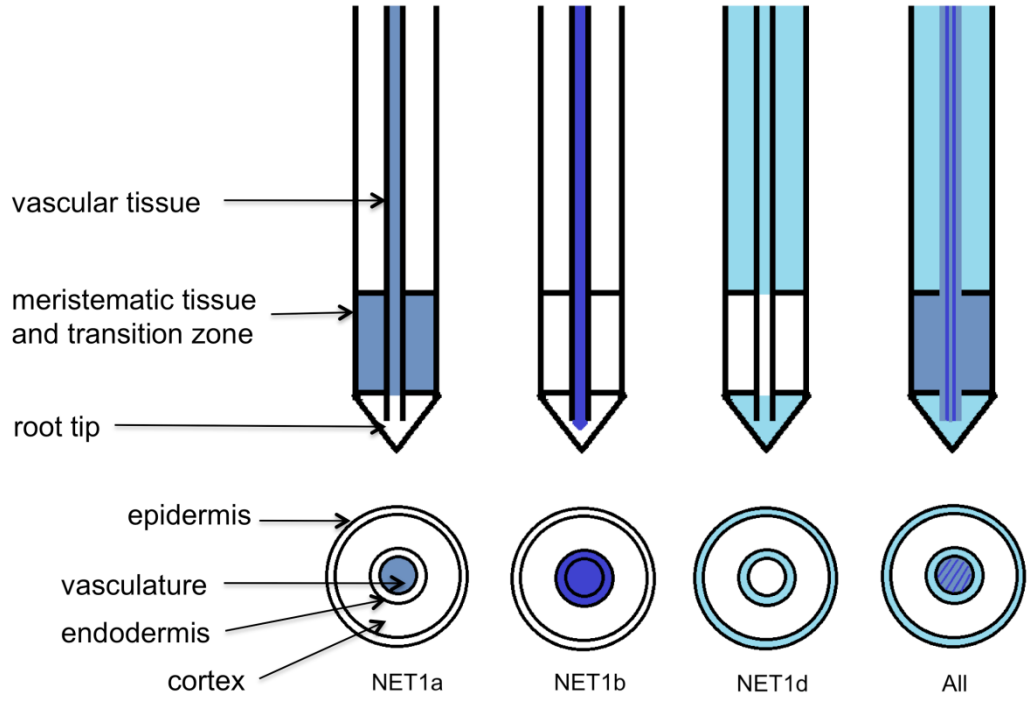

Figure 5.7: A comparison of GUS histochemical staining in NET1a, NET1b and NET1d promoter lines within a) the root tip and b) a cross section through the primary root.

5.4 Use of qPCR to identify tissues with NET1c expression

a)

Tissue	Level of expression in comparison to actin	Level of expression allowing for contamination found in H_2O control
Leaves	3.34×10^{-3}	3.5×10^{-4}
Roots	5.24×10^{-3}	2.25×10^{-3}
Flowers	2.28×10^{-3}	-1.70×10^{-4}
Seedlings	2.21×10^{-3}	-7.80×10^{-4}
Water only control	2.99×10^{-3}	0.00

b)

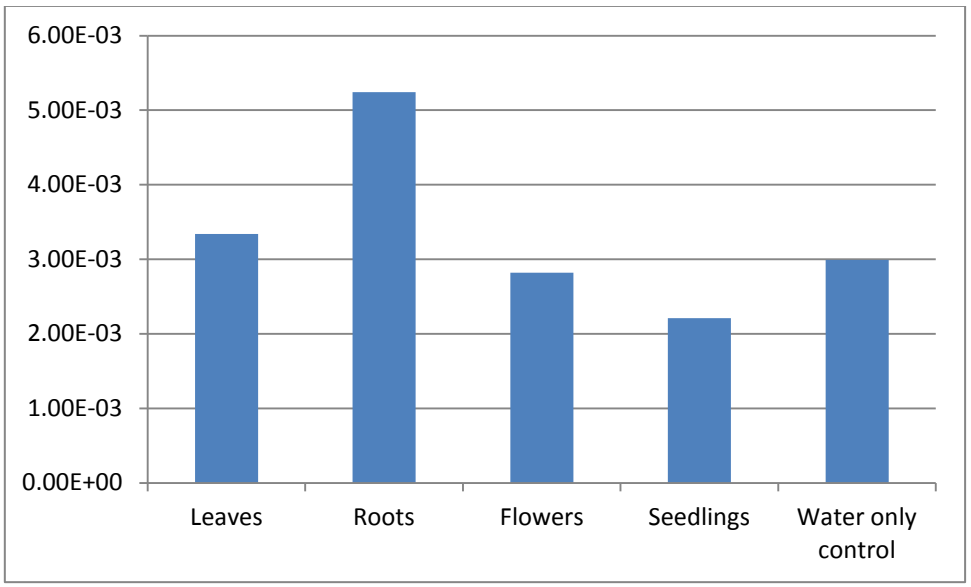

Figure 5.8: a) Relative levels of expression of the NET1c cDNA in different plant tissues, the value for expression is found by comparison between levels of expression of the NET1c cDNA to levels of actin cDNA found within the same tissue to allow quantitative comparison between samples. b) This graph shows a comparison of levels of expression of NET1c cDNA found in different tissues.

The promoter region of NET1c could not be amplified by PCR and cloned for use in a GUS reporter gene construct, possibly due to a secondary structure in that region of the chromosome or some error in the sequencing of the promoter region (although variation of primers was used without success), so GUS staining was not possible with this gene.

Affymetrix data for this gene is not particularly clear as levels of expression are particularly low or absent *(see Chapter 3)* and this gives the impression of a low level of expression throughout the plants. Some expression is observed but it is at a similar level in all tissues where expression is high enough to be recorded in

Affymetrix data. Due to the overlapping expression patterns of the three remaining NET1 proteins it is desirable to know if the root focused localisation also holds true for NET1c.

To provide some evidence of expression levels, the technique of quantitative PCR was used. This process relies on RNA extraction from plant tissue to provide a cDNA template for the PCR that is representative of the mRNA population of the tissue. Primers are then designed to amplify a short region of the gene of interest. The SYBRgreen DNA polymerase mix (Sigma-Aldrich) is used in the qPCR reaction to allow measurement of the level of DNA transcript present in the reaction mix. The ability to measure DNA levels quantitatively is reliant of the properties of the SYBRgreen fluorescent dye which undergoes a conformational change when bound to a double stranded DNA molecule to a form which is capable of fluorescence. As the PCR reaction continues, the level of DNA of the gene of interest increases, and the fluorescence emitted by the SYBRgreen molecule enables measurement of this increase. As DNA increase is on an exponential scale, the earlier the detection of increased fluorescence, the greater the quantity of the gene of interest in the original cDNA sample. This allows comparison of the levels of a gene of interest, in this case NET1c within a variety of tissues.

While lacking the specificity of a GUS assay, the use of qPCR does allow distinction between levels of expression in different areas of the plant. For this assay tissue samples were taken from wild type *A. thaliana* plants at two days and twelve days post germination. Tissue was also taken from the roots, leaves and whole flowers of mature plants.

The results of the comparison of expression can be seen in Figure 5.8. While some levels of expression are detected in all tissues, the level of cDNA transcript found in root tissue is highest. Each tissue sample was used in three reactions to improve accuracy of data due to the possibility of contamination (a single contaminating copy of the cDNA of the gene of interest would give rise to a fluorescent signal in time) although the raw data from the experiment showed similar responses for each sample. Some level of contamination was found in the samples containing only water, suggesting that there is a background level of contamination which is relatively consistent in all samples. The level of expression found in other tissues may therefore be even lower. Figure 5.8 shows that the majority of samples have a similar

level of expression to the negative controls containing water. This may indicate that the majority of expression is found within root tissue.

While an exact understanding of the localisation of NET1c has proved unobtainable, it appears that the protein is expressed in root tissue, possibly within the epidermal layers and root cortex based upon the pattern of antibody staining. This supports a theory of the NET1 group as four novel actin binding proteins expressed in root tissue with gene specific expression patterns covering the root tissue in an interconnected pattern.

5.5 Cellular localisation of NET1a, discovered by J. Calcutt

J. Calcutt (Calcutt 2009) was able to clone the NET1a gene in its entirety, with 2 kb of promoter region, into the pMDC107 expression vector which allowed expression of the gene under the native promoter with a C-terminal GFP tag. This was then stably transformed into *A. thaliana* by use of an *A. tumefaciens* transformation vector, which caused the T-DNA vector containing the NET1a gene to integrate into the genome of the plant.

Since this vector expresses in a way subject to the controls of the native promoter, and contains the whole gene, the localisation of this gene is assumed to be that of the native protein. In the case of NET1a this construct indicated that the protein localised to root tissue (Calcutt 2009). The protein localised to the crosswalls of root cells and unpublished work by F. Cartwright (Durham University) showed that this was in fact a punctate pattern around the edges of the cell, with occasional filamentous localisation present. Antibodies were raised against NET1a and NET1b and immunological staining showed both proteins localising to the same area of the cells as the NET1a-GFP fusion protein. The NET1b antibody produces a very similar pattern to NET1a although with a reduced filamentous localisation compared to NET1a.

This localisation suggested a role for the protein in the communication between cells. The pattern is reminiscent of that seen with plasmodesmata; links between cells where the cytoplasm is continuous with the adjacent cell to allow communication and transport between them. This pattern is also consistent with the presence of NET1a on the side walls of cells as well as the apex. Work carried out by the Hussey lab found a colocalisation of this punctate pattern of GFP with aniline blue staining, which is indicative of the presence of callose. This has indicated a plasmodesmal localisation for the NET1a protein.

During the course of this project attempts were made to clone the remaining NET1 genes under their native promoters. NET1d and NET1b were successfully cloned but could not be stably transformed into *A. thaliana*. It is possible that plant growth conditions were a factor in preventing recovery of the plants after the transformation process or that the construct itself is unstable. When attempting to clone NET1b, NET1c and NET1d under a 35S promoter the gene was frequently found to be truncated of to have sections of the coding sequenced excised. The length of the genes and therefore the plasmid containing the genes may be a factor which

increases the likelyhood of damge to the plasmid sequence. When cloning NET1c under the native promoter, amplification of the gene was highly problematic. Cloning of the actin binding domain was possible, as was cloning C-terminal half of the protein but the promoter region could never be amplified. This problem also prevented the creation of a line containing the GUS reporter gene driven by the NET1c promoter. The difficulty is thought to have been caused by a secondary structure in the DNA of the promoter region.

5.6 Production of polyclonal antibodies against specific regions of NET1c and NET1d to enable immunological staining

Polyclonal antibodies were raised in rabbits and rats to NET1c and NET1d respectively. Short sections of each protein were used, selected for lack of homology between the NET1 proteins so that specific localisations could be examined. The pGAT4 Gateway vector was used to add a His tag to the antigens during expression. Figure 5.9 shows the regions of the proteins used as antigens.

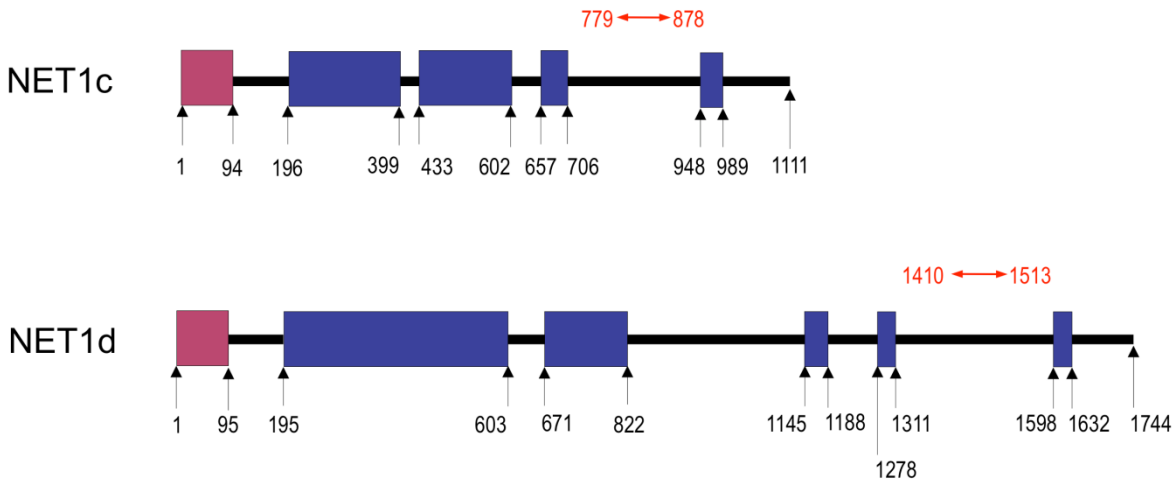

Figure 5.9: The proteins NET1c and NET1d, with the region used as an antigen for raising polyclonal antibodies shown in red.

These protein fragments were expressed in *E. coli* and purified before injection into the animals to cause immune response. A pattern of repeated 'boost' injections was used to ensure a sustained response and then blood samples were taken from which the blood serum could be extracted. This serum contained the antibodies raised to the gene of interest.

To assess the binding of these antibodies, Western blotting was used. Whole plant protein extract was separated according to protein size using SDS gel electrophoresis and then transferred to nitrocellulose membrane for Western blotting.

The antibodies raised against NET1c and NET1d were used as the primary antibody to probe the Western blot, testing the antibodies raised in each of the two rabbits and three rats used. An antibody raised against NET1a by J. Calcutt (Calcutt 2009) was used as a positive control and to provide an indication of protein size.

Figure 5.10 shows the results of the Western blotting. When the anti-NET1d antibodies are used, it is possible to see that a protein band appears at roughly the same size as NET1a in the samples from all three rats, which is the expected size of the NET1d protein (predicted size 200 kDa, compared to 195 kDa for NET1a). The blot using antibody from Rat 2 is very faint. Some smaller protein bands are seen, but this may be due to degradation of protein to produce protein fragments also bound by the antibody. While these are not desirable, they should not present a significant problem with antibody specificity and the antibodies with the strongest signal were chosen for further use. In this case, antibodies from Rat 1 and Rat 3 were used.

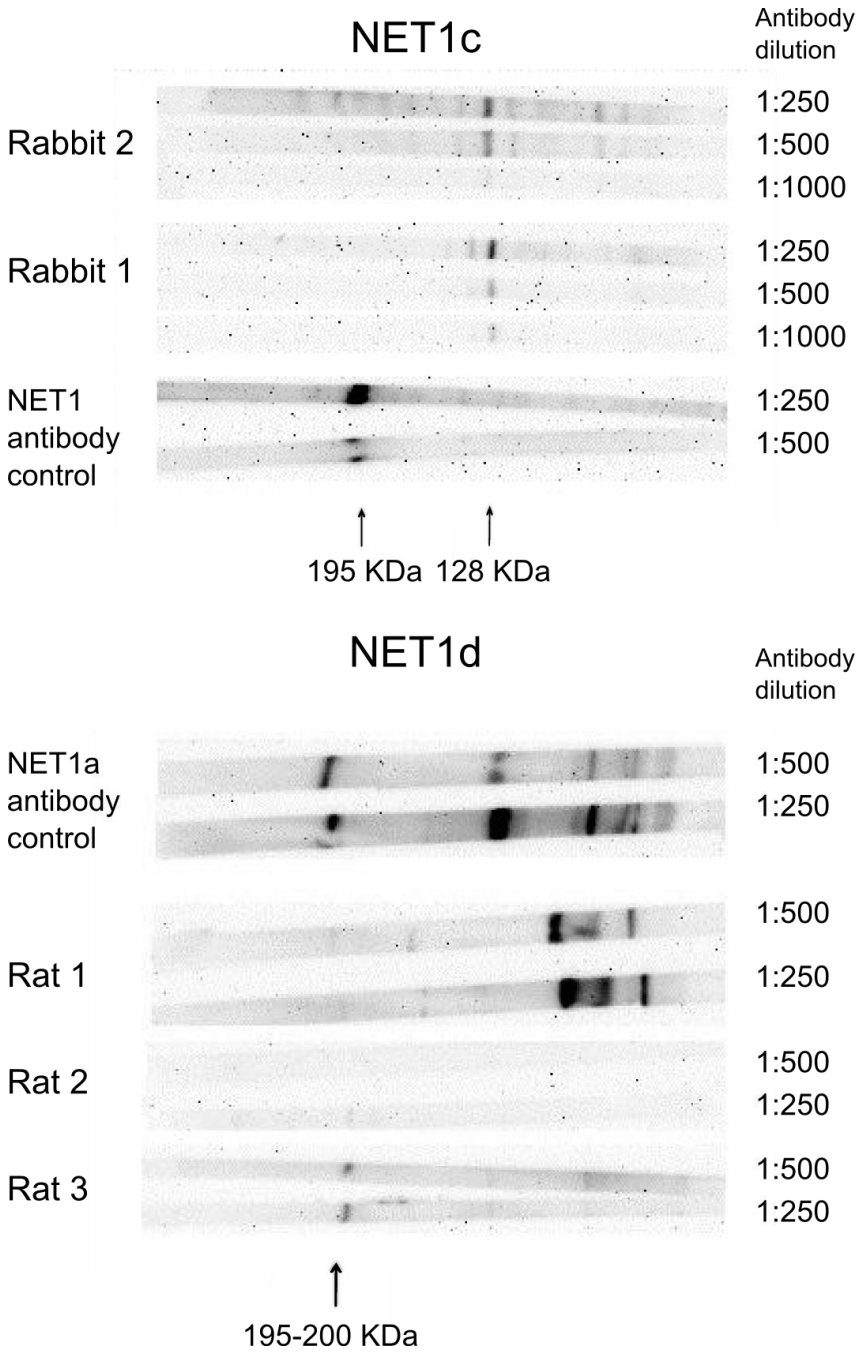

Figure 5.10: Western blotting used to probe whole plant protein extract with polyclonal antibodies raised against NET1c and NET1d. a) Blot using two rabbit antibodies raised against NET1c with the primary antibody used at 1:1000, 1:500 and 1:250 dilutions. b) Blot using three rat antibodies raised against NET1d, with the primary antibody used at 1:500 and 1:250 dilutions.

When the anti-NET1c antibodies were used to probe the Western blot, a band significantly smaller than the 195 kDa NET1a protein was observed. This is consistent with the predicted size of NET1c of 128 kDa. For Rabbit 1 this appeared to be only band present, with some faint bands seen at a lower molecular weight, a promising result for this antibody. For Rabbit 2 however, some faint bands were seen

at a higher molecular weight than the expected band for NET1c. This was only seen at the highest concentration of primary antibody. At lower concentrations only the expected band was seen, so for future use the antibody is used at 1:300 dilution rather than 1:500 to avoid possible non-specific binding.

The specificity of the antibodies does require final confirmation through the use of whole protein extract from plants lacking the NET1c and NET1d genes and observation of the absence of the band predicted to be due to the binding of the antibodies to the NET1c or NET1d proteins. Staining of root tissue utilising these antibodies was carried out as a primary investigation of potential protein localisation, and all results discussed within the remaining sections of this chapter require final confirmation. This would involve immunological staining of root tissue from knockout mutants lacking the NET1c or NET1d proteins to demonstrate absence of staining in the absence of the protein of interest.

5.7 Immunological staining of roots to identify subcellular localisation of NET1c and NET1d

Six-day-old wild type Col0 *A. thaliana* seedlings were used for immunolabelling. After fixation in a 3.7% paraformaldehyde solution the seedlings were incubated with the primary antibodies at a dilution of 1:300. Both Rabbit antibodies were used and Rats 1 and 3. In order to visualise the location of the antibody binding, secondary antibodies were incubated with the roots at a dilution of 1:200 overnight. Anti-rabbit Alexa546 and Anti-rat Jackson TRITC were used. This enabled imaging of the labelled plants using an SP5 Leica Confocal Microscope. Fluorescence was excited using the 543 nm laser line and emission was detected in the range 565-700 nm with peak emission at 576 nm for TRITC and 573 nm for Alexa-546. This experiment was intended as an initial examination of potential subcellular localisation and all results presented here are preliminary data requiring confirmation through replication of experimental procedure and use of pre-immune serum to ensure that the pattern of staining observed is related to the introduction of the NET1 antigens and subsequent production of antibodies against the proteins of interest.

Figure 5.11 shows the images obtained from probing the roots with anti-NET1c rabbit polyclonal antibodies. The fluorescence appears in a pattern of small, punctate dots surrounding the cortex of the root cells. While this might initially appear to be protein aggregates, the consensus between the two antibodies, the consistency of the size of the areas labelled by the antibody and the total absence of the antibody deeper within the cell suggests that this may be a genuine localisation. This punctate pattern surrounding the cell is very reminiscent of the pattern of localisation seen with the NET1a-GFP construct and subsequent colocalisation with callose discussed previously, although NET1a shows a greater localisation to the apex of the cell, whereas NET1c tends to appear on the side walls and binding to the apex of the cell is seen to a lesser extent. This protein may also be associating with plasmodesmata in the cell walls or with another cell membrane structure with a similar localisation.

No antibody staining is observed in the leaves or hypocotyls of the plant, which is in agreement with the protein expression pattern predicted using the quantitative PCR. It is also noteworthy that antibody staining is seen in the epidermal and cortical cell files, suggesting that the NET1c protein may be expressed in these cells, perhaps completing the universal expression of at least one NET1 protein in all root cells. This

is the first indication of a localisation of NET1c of greater specificity than the level of a whole tissue.

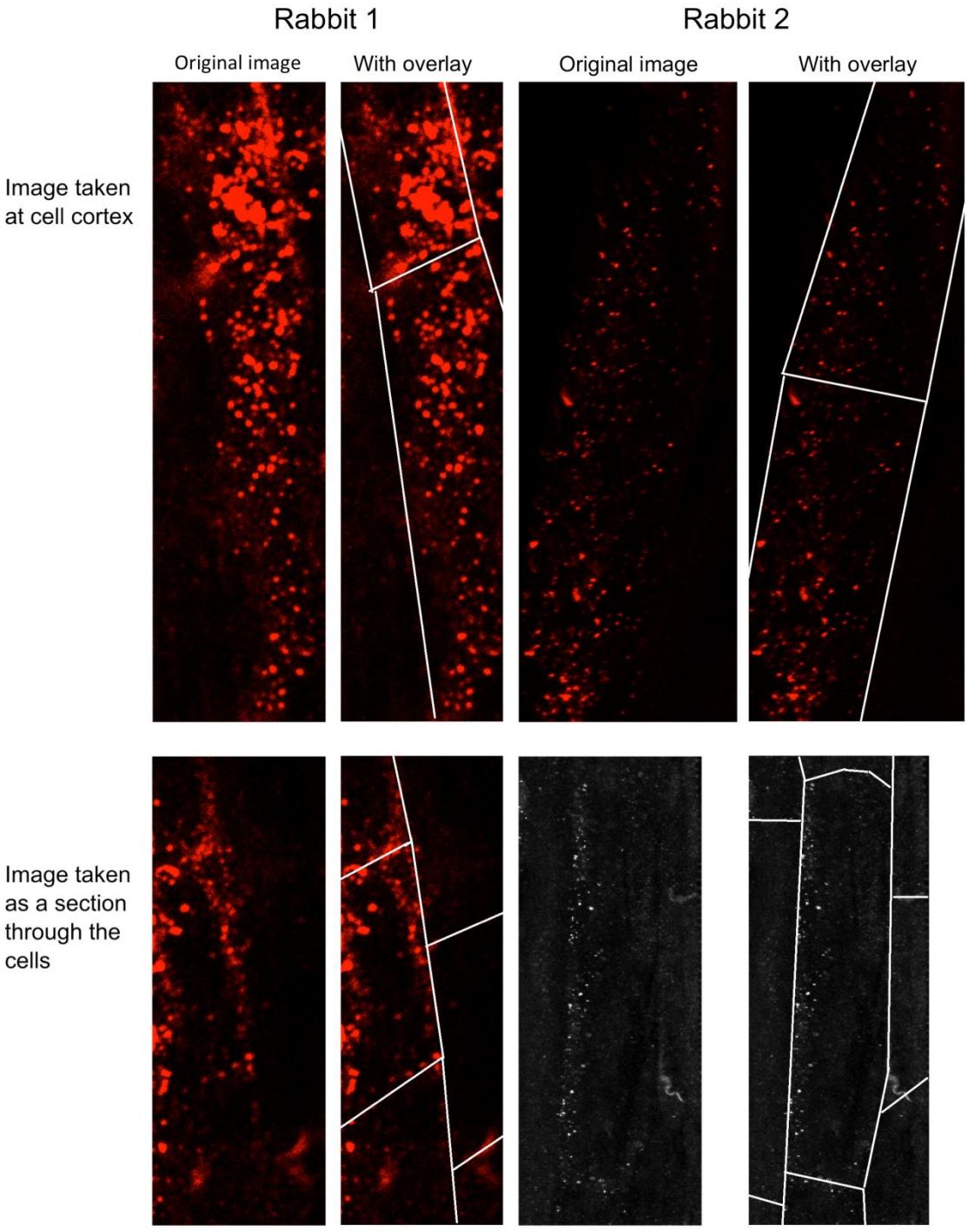

Figure 5.11: Immunolabelling of wild type A. thaliana roots with a) Antibody Rabbit 1 and b) Antibody Rabbit 2 against NET1c, using anti-rabbit Alexa546 as a secondary antibody and imaged using a Leica SP5 confocal microscope. In the absence of any markers of cell boundaries or other cell structures due to the failure of the intented counterstaining, overlays of the cell outlines have been created using brightfield images and placed over a duplicate of the image to indicate cell dimensions more clearly.

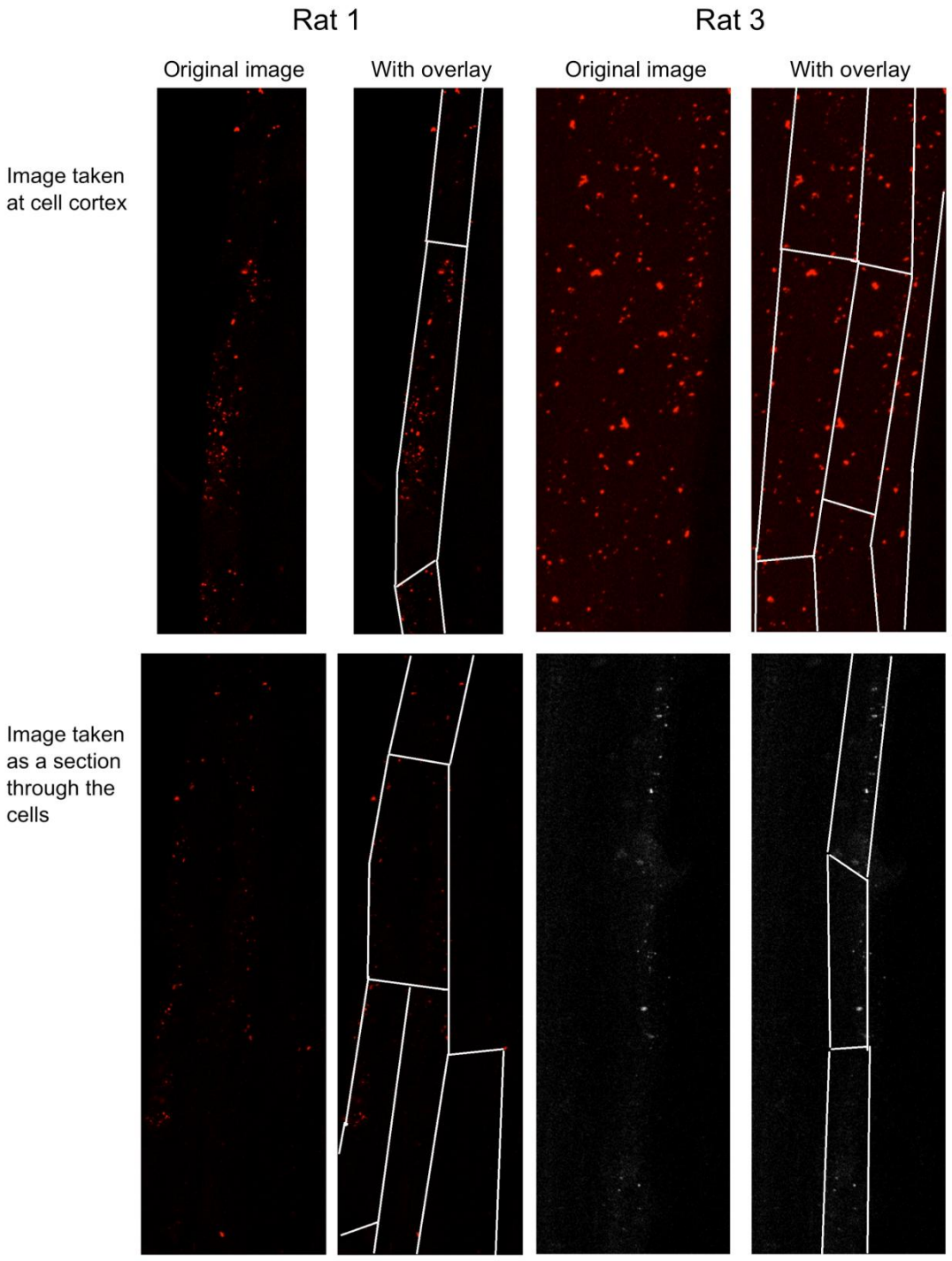

Figure 5.12: Immunolabelling of wild type A. thaliana roots with a) Antibody Rat 1 and b) Antibody Rat 3 against NET1d, using anti-rat TRITC as a secondary antibody and imaged using a Leica SP5 confocal microscope. In the absence of any markers of cell boundaries or other cell structures due to the failure of the intented counterstaining, overlays of the cell outlines have been created using brightfield images and placed over a duplicate of the image to indicate cell dimensions more clearly.

Figure 5.12 shows seedlings immunolabelled with anti-NET1d raised in rats. The pattern of localisation is initially similar to that observed with anti-NET1c. The

fluorescence forms a punctate pattern at the periphery of the root cells. The areas of antibody labelling are, however, slightly larger on average and more diffuse in their overall pattern of localisation. It is probable that NET1c and NET1d associate with different cell membrane or cell wall structures, or with different populations of the plasmodesmata.

The NET1d immunolabelling is located solely within the root tissue, and an interesting feature of the staining is the absence of any fluorescence in the meristematic tissue of the root. This coincides with the pattern of GUS staining observed for this protein, and provides further evidence of the specificity of the immunolabelling and veracity of the punctate localisation.

5.8 Conclusion

Use of GUS histochemical staining to identify areas of transcription of NET1b and NET1d has demonstrated a root localisation for three of the NET1 proteins, with a possible overlapping and complimentary pattern of gene expression. While use of a GUS assay was not possible for NET1c, quantitative PCR has been used to show higher levels of expression within root tissue. These data indicate that the NET1 proteins are root-specific actin binding proteins segregated by expression pattern. The high homology between the proteins suggests that this may allow compensation by other NET1 proteins when one is absent (see Chapter Six) due to transcriptional control.

Use of polyclonal antibodies to probe cellular localisation results in a punctate pattern at the periphery of root cells for both NET1c and NET1d, a pattern shared with data obtained using NET1a-GFP expressed under the native promoter by J. Calcutt (Cacutt 2009), suggesting that the NET1 proteins share some functional similarities within the group. The proteins may share the plasmodesmal localisation of NET1a or they may bind to a distinct population of plasmodesmata or to other cellular structures with a cell wall or cell membrane localisation. The proteins may act to tether or regulate the presence of actin filaments at the membrane either for structural or functional reasons.

Further work is required to confirm and ascertain the cause of these punctate expression patterns for the proteins NET1c and NET1d. The localisation shown in the initial experimental work using immunological staining must be confirmed through replication of the data and use of serum obtained from the animals prior to immunisation with the antigen to confirm that the staining observed is not an artefact of the staining process or a naturally occurring antibody to another plant protein. Staining for cellular features such as plasmodesmata in conjunction with immunolabelling might assist in discovering any possible link to specific structures within the cell. Use of stains such as aniline blue could help to demonstrate any possible link to plasmodesmata. The antibodies against NET1a, NET1c and NET1d were raised in different species. This allows the co-labelling of multiple NET1 proteins in the same cell, which could be utilised to identify any overlap in expression patterns between the NET1 proteins.

Chapter Six:

Investigation of the effect of the mutation of the NET1 proteins and possible roles for NET1 proteins *in vivo*

6.1 Introduction

The NET1 proteins have been shown to be actin binding proteins with a novel actin binding domain at the N-terminal end of the protein. NET1a has also been shown to localise in a punctate pattern to the periphery of the root cells, and this localisation is the same as that of the plasmodesmata, which also surround the outside of the cell. Actin is known to associate with the structure of the plasmodesmata through an unknown mechanism; therefore a potential role for the NET1 proteins is in forming and maintaining this connection in a purely structural capacity. It is possible, however, that this is not the role of the proteins or not the entirety of the role the proteins play in this location.

To obtain a more complete hypothesis of the role of the NET1 proteins, it is necessary to consider the effect of the proteins *in vivo* under their native conditions, as well as in a transient expression system. It is also important to consider what effect the proteins may have on the plant as a whole organism or on a particular tissue where the proteins are expressed. This is conventionally carried out through the use of mutations of the gene, which then produce a mutant phenotype, or physical effect upon the plant as a result of the mutant genotype. Mutations may be over-expression mutants, where the protein is expressed constitutively in the plant or at a higher than usual level, or they may be mutations which prevent the protein from operating normally, either by affecting the function of certain domains or causing the complete absence of the protein due to lack of transcription or translation.

In this case, ‘knock out’ mutants, which render the entire protein absent or non-functional, were used in preference to overexpression mutants. An absence of the gene can produce a more dramatic effect than increased levels of expression which may be modified by post transcriptional control. Over-expression also demands the cloning of the protein so that plant genome can be modified to contain the gene with a

constitutive promoter. The large size of the NET1 proteins resulted in frequent mutations of the genes during cloning, which could potentially affect the mutant phenotype obtained.

The knockout mutants of NET1 proteins have been analysed to quantify the level of gene expression remaining and the phenotype of the resulting plants has been studied. Plants containing multiple mutant genes have been created and studied under a variety of environmental conditions.

6.2 Creation of insertion mutants by NASC

6.2.1 Introduction

The Nottingham Arabidopsis Stock Centre (NASC) provides insertion mutants created by SIGnAL (the Salk Institute Genomic Analysis Laboratory). Mutant lines are created by insertion of a large section of T-DNA into the plant genome using Agrobacterium tumefaciens. PCR, amplifying outwards from the T-DNA insert can provide some of the sequence of the gene where the T-DNA has been inserted, and this gives the identity of the gene which has been disrupted.

Due to the large size of the insert, and the presence of several stop codons within its sequence, insertion of this section of DNA into a gene usually renders it non-functional. Transcription is less likely and translation may be truncated. If the plant is homozygous for this mutation, it is possible that the protein may be completely eliminated.

6.2.2 Experimental data

Figure 6.1 shows the insertion lines available for the NET1c and d proteins, and the location of the insertions. For greatest likelihood of absence of the protein, and therefore for greatest interest when studying the mutated plants, the mutant allele should contain an insert into the coding area within an exon. It is possible for mutations of the promoter or an intron to cause a defect of the protein but an exon is more certain.

Each insertion mutant results in a different allele of the gene. It is desirable to have several different alleles of the gene to establish a genuine phenotype. This is due to the nature of the creation of the mutant lines. The T-DNA insert appears in the gene of interest, but differences in the location may change the level of effect on the gene. It is also possible that the insertion of T-DNA may happen more than once within the genome of the same plant, leading to a phenotype that is not related to the gene of interest. In view of this, several lines were ordered from NASC for analysis.

Three potential lines were available for NET1c: SALK_069202, SALK_142711 and SALK_139608. Of these, only SALK_139608 was located within the gene of interest. SALK_069202 and SALK_142711 were located some distance away from the start of the gene, possibly within the promoter region. An insertion into the promoter may prevent transcription, but the further the location of the insert from the gene the less likely this is to occur and these two inserts are more than 2000 bases away from the

beginning of transcription. For this reason, these lines were examined for mutant phenotypes but not used for any further crosses or analysis. The third line, SALK_139608 was the most likely to cause a non-functional protein. Plants from this line were grown on vertical plates so that both above and below ground tissue could be observed. In both cases the tissue appeared normal. Germination rates were as expected and no different to that of wild type Col-0 *A. thaliana* grown simultaneously. Bolting, flowering, seed setting and senescence were all as for the wild type plant. No obvious phenotype was observed.

One SAIL (Syngenta Arabidopsis Insertion Library) line was also ordered, SAIL 879-B08. This line was also from a T-DNA insert library and was used to confirm the absence of any mutant phenotype in the absence of NET1c since only one SALK allele was available. It was examined according to the same method as the SALK alleles and produced no visible phenotype.

A greater number of T-DNA insert alleles were available for NET1d: SALK_032339, SALK_032243, SALK_151290 and SALK_033948. Of these, three have very similar SALK numbers and they appear to be inserted into the same location in the genome. This can occur when tissue from one true T-DNA insert line contaminates other lines. In this case, all three SALK lines were ordered and analysed for the presence of the insert, by genotyping PCR (as described below). Only SALK_033948 was used in subsequent analysis. This allele results from an insertion of T-DNA into the exon of the gene, while SALK_151290 is found in the predicted promoter region. To provide two alleles for analysis, GK_106H05 Gabi-Kat was ordered from NASC. This is a T-DNA insert line created by the Max Planck Institute and contains a T-DNA insert into the second exon of the NET1d gene. These three lines were analysed using the same conditions as were used for the NET1c mutants. As with the NET1c lines, the NET1d plants showed no visible differences to wild type plants.

Four SALK lines had been ordered previously for the analysis of NET1a and NET1b (Calcutt 2009) and these had also been crossed to form two double mutant combinations (referred to as NET1a/NET1b-A and NET1a/NET1b-B). The ‘A’ combination of alleles comprises a cross between the SALK_081081 line with a T-DNA insertion into NET1a and SALK_003809, which contains a mutation in NET1b. The other double mutant was created by crossing SALK_109591 and SALK_142729, with mutations in NET1a and NET1b respectively. The location of these insertion mutations is also shown in Figure 6.1.

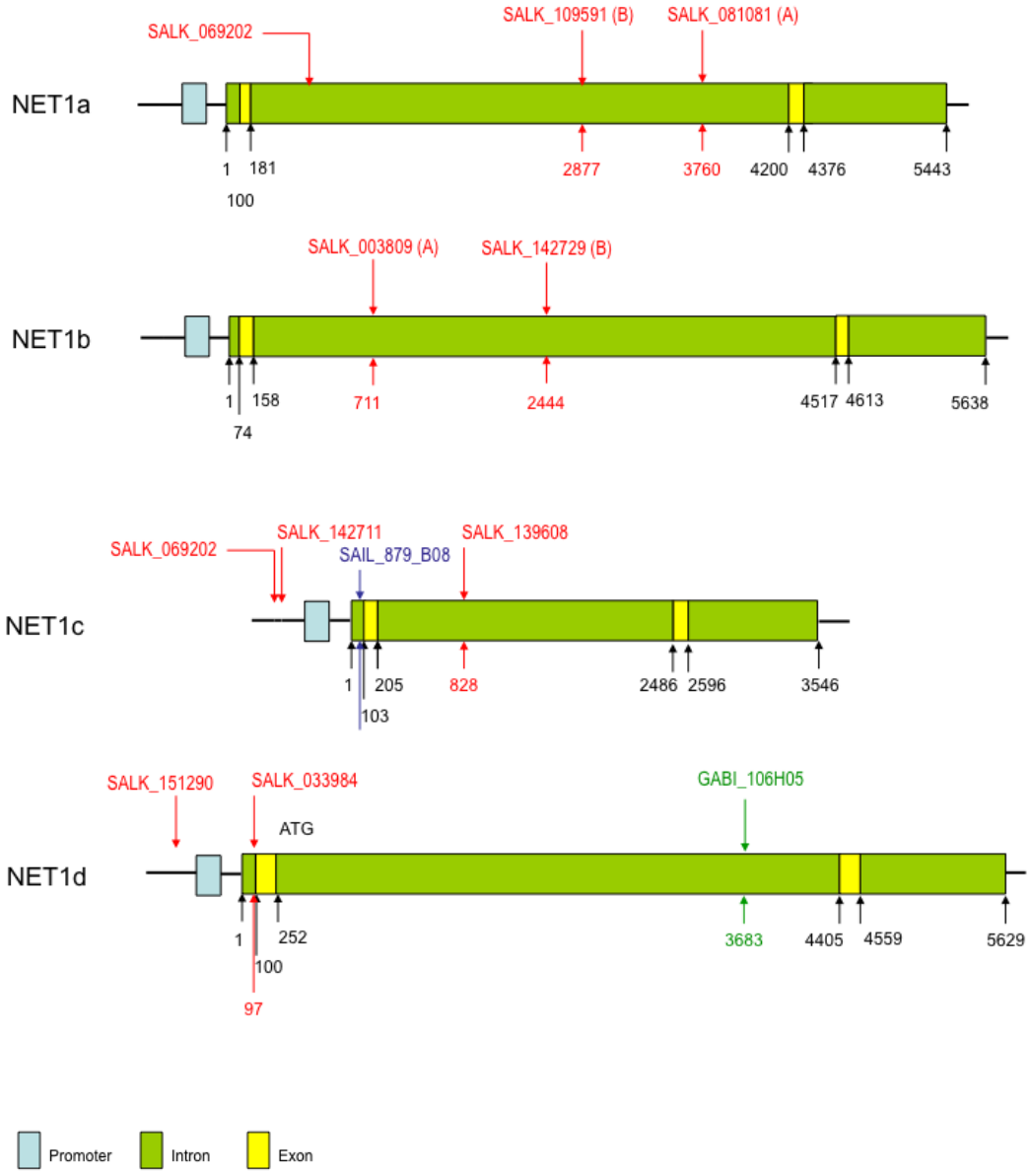

Figure 6.1: Location of SALK, SAIL and GABI line inserts into the NET1 genes, based on sequencing from the left border of the T-DNA insert carried out by the Salk Institute Genomic Analysis Laboratory.

6.3 Genotyping of mutant plants to establish homozygote lines

To identify whether a plant contains the mutant allele or not, the process of genotyping is carried out using the polymerase chain reaction (PCR) to amplify a fragment of DNA specific to each mutant allele from the genome of the plant in question. The genomic DNA is extracted from a leaf of the plant using the Edwards' method of gDNA extraction (Edwards 1991) and is then used as the template of a PCR. Two combinations of primers are used: one pair of primers binds to a section of the unmodified gene, with one on either side of the location of the insertion of the T-DNA (the location is available due to sequencing of the genome next to the insert DNA by NASC). If the plant genome contains a wild type copy of the gene, this PCR reaction will produce a DNA fragment that can be seen using agarose gel electrophoresis. If an insert is present in the gene, the distance between the two primers is too great for synthesis of a DNA fragment so no band of DNA will be seen on the agarose gel.

The second pair of primers consists of one of the wild type primers, and a primer that matches part of the border of the insert (the wild type primer used is determined by the direction of the insert). In this case, the PCR reaction will only amplify a DNA fragment if the insert is present in the gene. This will identify any plant containing the mutant allele. By using both sets of primers with each template the genotype of the plant can be identified. Azygous plants will show only the wild type DNA fragment, heterozygotes will produce a DNA fragment in both reactions and homozygous plants will show only the insert band.

Homozygous plants are required for analysis of a mutant phenotype as loss of a single copy of a gene is unlikely to cause much of an adverse effect upon the plant due to presence of a wild type allele which can compensate for the absence of the other allele, and transcriptional control may increase protein synthesis. Multiple mutant alleles are also necessary as it is possible for two T-DNA insertions to occur in the same line, and a mutant phenotype may be caused not by the gene of interest, but by a second and hidden insertion event. Two different alleles will show the same absence of the gene of interest but any secondary insertion of T-DNA will not be in the same location in the different lines, so at least two alleles must show the mutant phenotype.

For the purposes of mutant analysis described in this chapter, the homozygous plants were first identified by conventional genotyping as described above. An internal control in the form of primers to a housekeeping gene that produce a larger band than that of the insert or wild type fragment is normally used to establish that the reaction is working. Without this it is more difficult to establish that a PCR with no fragment amplified is due to an absence of that form of the gene, rather than a failed reaction.

The primers used in the genotyping of the alleles for NET1c and NET1d were only possible to design such that the internal control primers failed to work under the conditions necessary for the wild type and insert primers to function due to incompatible annealing temperatures. Repetition of the PCR was used, but another method was also carried out to confirm that the plants identified as homozygotes did in fact contain two copies of the non-functional mutant allele and no copies of the wild type gene.

Conventional genotyping was used to identify mutants in NET1c and NET1d lines. SALK lines for NET1a and NET1b have already been identified and a double mutant line lacking both NET1a and NET1b has been created and identified by conventional genotyping (Calcutt 2009). Mutant lines from all four NET1 proteins have also been analysed using quantitative PCR to quantify levels of transcription of the gene of interest remaining in mutant lines.

6.4 Quantification of levels of expression in the mutant lines

6.4.1 Introduction

To analyse the most promising of the mutant allele lines, quantitative PCR was used. In this experiment, RNA was extracted from seedlings 1-2 days post germination which were homozygous for the mutant allele. The RNA was used as a template for cDNA, using an oligodT primer to amplify mRNA with a 3' poly-A tail. This cDNA represents proteins produced by the cell at this stage of development, and this was used as a template for a PCR reaction, where SYBRgreen DNA polymerase mix enabled the quantification of the level of product produced. This is possible due to a change in the properties of the SYBRgreen fluorescent dye once it has bound to double stranded DNA. The complex absorbs light at 488 nm and emits light in the green part of the visible spectrum. As amplification proceeds in the PCR, the levels of dsDNA increase and so does the corresponding emission of light from the SYBRgreen/dsDNA complex in a log scale. The speed of this increase and the point at which the increase is detected can be measured and used to compare the levels of DNA initially found in the samples.

With the presence of primers for another A. thaliana gene (in this case for G-actin) and a water control with no cDNA present, the relative levels of the gene in wild type and mutant seedlings can be compared. This is useful as it not only identifies presence or absence of the mutant allele; it also shows the extent to which the mutant allele causes an absence of the gene of interest. While insertion lines usually prevent the production of the protein, some transcription may still occur and a qPCR reaction shows to what extent this is taking place.

6.4.2 Experimental data

Figure 6.2 shows the results of the analysis of the mutant alleles for the NET1 family. Although some transcript is still found in the NET1c SALK mutant during the analysis of the single mutant, once this allele has been crossed with the NET1a/NET1b-A double mutant the level of transcript has decreased to less than 10% of the wild type level. Both 'A' and 'B' combinations of the double mutant show transcription levels of NET1a and NET1b of less than 15% and when the level of NET1b is analysed in the triple mutant only 6% of the wild type level of expression of the gene remains.

Although transcription has not been completely eradicated by the insertion mutations, levels are low enough for these alleles to be considered to have removed the gene

from the plant. It is possible that levels of cDNA detected are due to contamination of samples during preparation of the RNA, or low level synthesis of the gene containing the insertion. This form of the gene may be non-functional as a result.

These data confirm that the alleles selected for further analysis are deletion mutants lacking the required genes and have the added effect of confirming that the double mutant is homozygous for both mutant alleles; and therefore that the conventional genotyping has been accurate.

Levels of transcription for the NET1c SAIL mutant are the only exception to this reducing of the levels of gene transcription. The mutant allele seems to have an increased level of transcription to 77% above the wild type expression. While it is possible that the gene has been rendered non-functional by the T-DNA insert and the increase in gene level due to a strong promoter within the insert, the SAIL allele has not been used in future crosses or analysis after the initial analysis of the single mutant.

Mutant	Primer	Azygote: actin comparison	Mutant: actin comparison	% of azygote level of transcript still present in mutant
NEt1c SALK	NET1c	6.52 x10-4	2.10 x10-4	32.21
NET1c SAIL	NET1c	6.52 x10-4	1.16 x10-3	177.91
NET1d GABI	NET1d	3.67 x10-2	7.16 x10-3	19.51
NET1a/NET1b A	NET1b	2.86 x10-2	4.14 x10-3	14.48
	NET1a	1.80 x10-2	2.84 x10-6	0.02
NET1a/NET1b B	NET1b	2.80 x10-2	4.49 x10-4	1.60
	NET1a	1.80 x10-2	1.44 x10-4	0.80
NET1a/NET1b /NET1c	NET1c	9.65 x10-4	9.30 x10-5	9.64
	NET1b	3.35 x10-2	2.13 x10-3	6.36
	NET1a	1.64 x10-2	3.76 x10-4	2.29

Figure 6.2: Results of quantitative PCR showing the levels of cDNA transcript in azygote and mutant cDNA relative to actin cDNA at two days post germination. Comparisons are made between the azygote lines and the NET1c and NET1d single mutants, the NET1a/NET1b double mutants and the NET1a/NET1b/NET1c triple mutant. Percentage values show the level of cDNA transcript present in the mutant tissue as a percentage of the level found in wild type tissue.

6.5 Analysis of plants lacking one NET1 gene

The affymetrix data, localisation of NET1a-GFP *in planta* and the use of the GUS reporter gene to show the localisation of promoter activations, show that the NET1 proteins are localised to the roots of the plant. For this reason, it was anticipated that any mutant phenotype resulting from the mutation of the NET1 proteins would appear in the root tissue.

Initial studies of the single mutants (NET1a and NET1b mutants were in studies by J. Calcutt (Calcutt 2009) and NET1c and NET1d within the current project) showed no obvious aberrations within any part of the plant. For the NET1c and NET1d alleles both above and below ground tissue appeared normal, as did germination rate, flowering, seed formation and senescence. Even when grown on a vertical plate to show more detail of the developing root system, the plants did not appear significantly different from azygous plants grown simultaneously under identical environmental conditions.

Tissue from the alleles was examined under 10 x magnification and compared with tissue from azygous plants. Embryos and roots at 12 days post germination were examined to observe any possible root phenotypes, but no variations were observed. Root hairs and trichomes were also compared but appeared normal in all mutant lines. The mutant and azygote plants were of similar size throughout development, without observable differences in size or area of leaves or in the length of roots.

The NET1 proteins show a great deal of similarity to each other within the group. This suggests that one protein might have a very similar function to another. In the root, expression seems to be highly segregated, so it is possible that difference in function may be partly due to location and activation of promoter, rather than inherent structural differences between the proteins. It is not implausible to suggest that if one protein is absent from a cell, another protein from the same group might compensate.

In light of this possible compensatory effect and the lack of a visible mutant phenotype within the plants containing a single mutant protein, the plants containing mutants for NET1a were crossed with plants containing the single mutant for NET1b. This was carried out by J. Calcutt (Calcutt 2009), who then allowed the plants resulting from this cross to self pollinate to produce a segregating population which contained a double mutant. This NET1-a/NET1-b mutant was then screened using

genotyping. In the course of the current project, the qPCR technique described above was used to confirm the absence of both NET1a and NET1b transcript within this mutant. (See Figure 6.2 above).

6.6 Analysis of the NET1a/NET1b double mutant

Initial work done by J. Calcutt (Calcutt 2009) suggested that this double mutant might have no phenotype or that a slight shortening of the roots might occur. This data however was based on use of seeds from two different generations of plants, such that the azygous controls had not been grown synchronously with the mutant plants. The variation between different generations of plants, both in terms of quality of seed due to growth conditions and health of the parent plant and the environmental conditions the germinating seed is subjected to, causes significant differences in plant size and corresponding root length. This is shown by the root length data within this chapter, where seeds grown under different conditions may vary by several centimetres in length by twelve days post germination. This makes an accurate comparison impossible in this case.

In order to establish whether the mutant roots showed a genuine phenotype in comparison to the azygous plants, single mutants of NET1a and NET1b (NET1a-A and NET1b-A), the NET1a/NET1b-A mutant and the azygous plants were grown simultaneously and allowed to self pollinate and produce seeds under the same environmental conditions. Seed was collected, dried and placed on vertical 25 mm petri dishes containing ½ MS agar. Approximately 15 seeds were placed on each plate, about 1.5 cm from the top of the plate. Five plates were prepared for each mutant or azygote line.

The plates containing the seed were incubated at +4 ^{o}C for three days to ensure that germination would be synchronised and then the plates containing the seeds were transferred to 16 hours light at 20 ^{o}C and 8 hours dark at 18 ^{o}C. The length of the primary root was measured on days 3, 6, 9 and 12 post-germination. Roots were measured using scans of the vertical plates, and ImageJ (Abràmoff 2004) was used to trace the primary root and then measure the length of the root using a known distance for comparison (a ruler included in all scans of the plates). The data from this experiment can be seen in Figure 6.3. While this data represents one analysis of primary root length, the azygote and double mutants have been used as controls in subsequent root length assays and have shown results consistent with the data presented here.

a)

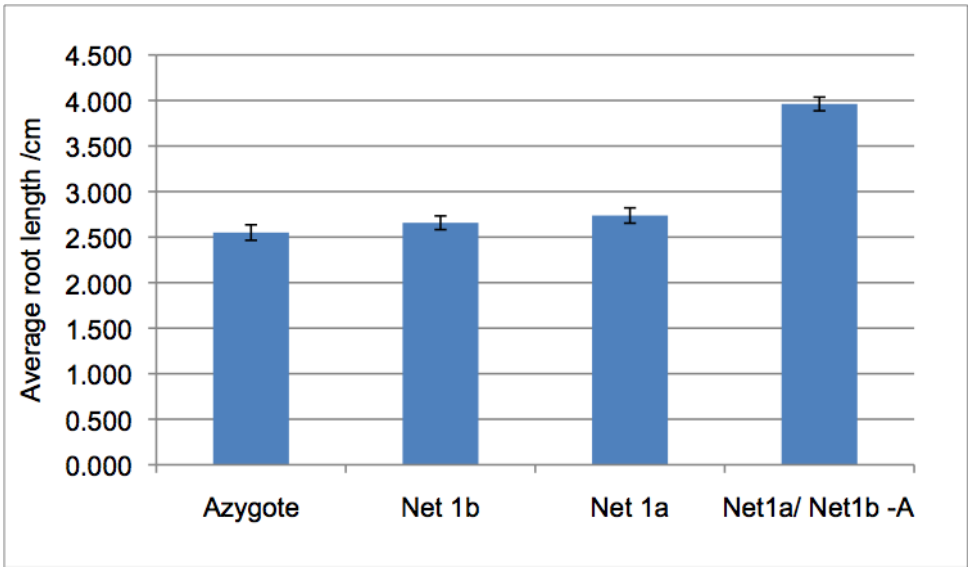

b)

		Day 3	Day 6	Day 9	Day 12
Azygote	Average length /cm	0.95	1.94	2.26	2.55
	Standard error	*0.03*	*0.06*	*0.07*	*0.09*
NET1b	Average length /cm	0.73	1.76	2.29	2.66
	Standard error	*0.03*	*0.06*	*0.08*	*0.08*
NET1a	Average length /cm	0.92	1.89	2.38	2.74
	Standard error	*0.03*	*0.05*	*0.08*	*0.08*
NET1a/NET1b-A	Average length /cm	1.07	2.28	3.16	3.96
	Standard error	*0.04*	*0.08*	*0.12*	*0.15*

c)

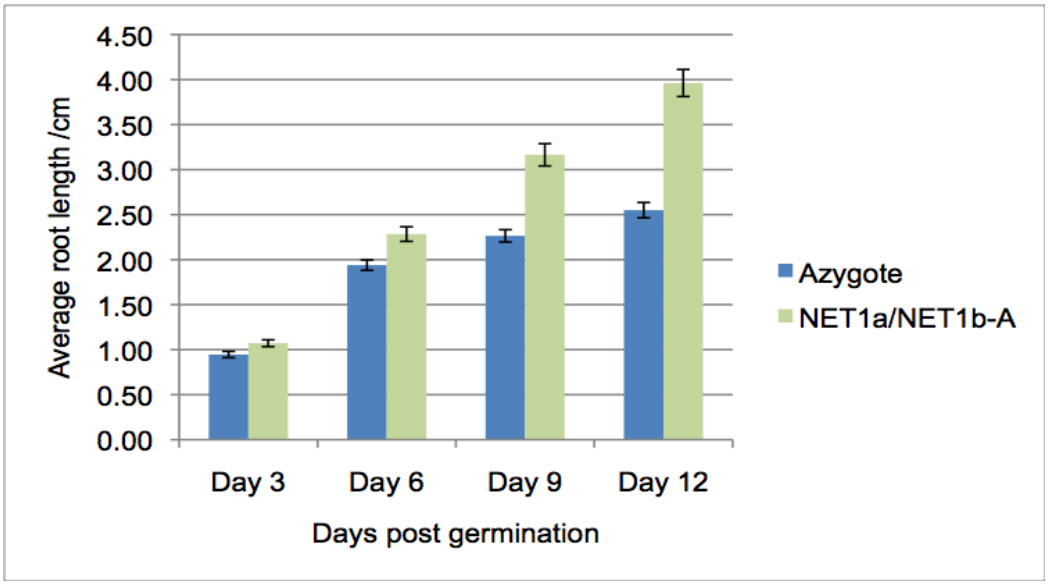

Line compared to azygote at Day 12	Number of plants	p-value for significance of increase in root length
NET1a	72	0.13
NET1b	68	0.35
NET1a/NET1b-A	76	5.91×10^{-13}

Figure 6.3: a) Results of the analysis of primary root length in Azygote-A, NET1a, NET1b and NET1a/NET1b-A alleles. b) Increase in primary root length over time in Azygote-A and NET1a/NET1b-A. c) The significance of variation in root length between the alleles, calculated using a two tailed T-test.

Figure 6.3 illustrates that the plants containing only a single mutation of one NET1 gene do not show a significant difference in the length of the primary root. The azygote plants have an average root length of 2.55 cm, the NET1a mutant has an average length of 2.74 cm and NET1b-A has an average length of 2.66 cm. The double mutant however shows a very significant increase in root length of 55% as average root length increases from 2.55 cm to 3.96 cm. The use of a two tailed t-test to analyse the significance of the change in root length produces p-values of 0.13 and 0.35 for the two single mutants NET1a and NET1b respectively. These values are not considered significant. For the purposes of this analysis, significance was determined as a p-value of <0.01. The increase in the length of the primary root of the double mutant compared to the azygote has a significance value of 5.91×10^{-13}. This is a highly significant value and demonstrates that the long root phenotype is a true phenotype demonstrating a difference in root physiology, not due to random variation in root length.

When the mutant and azygote lines are compared over time, it is possible to see that the increase of root length begins to appear before Day 9, even if the difference in average root length is small and not statistically significant. The phenotype observed in the NET1a/NET1b-A mutant is based on a cumulative effect within the plant. This theory agrees with the presence of the NET1 proteins from one to two days post germination, as seen during qPCR, since development of a phenotype at Day 9 without previous apparent effect in the plant may imply the synthesis of the protein begins at that stage of development.

This assay was repeated using the mutant NET1a/NET1b-B and an azygote line (Azygote-B) that had also been grown under identical environmental conditions for a generation. This pair of mutant alleles shows the same long root phenotype. The phenotype is not so severe – as shown in Fig 6.4, the root length increases by 24% rather than 55% as seen with the NET1a/NET1b-A combination of alleles. The increase in root length is however still present and the p-value for these results is significant, at 0.0043. The increase in p-value in comparison to NET1a/NET1b-A may be due to the smaller sample size used in this assay. The population size for 'B' was only 55 plants in comparison to an average of 72 plants per line for 'A'.

Data is shown here from all four stages of root comparison. The mutant phenotype causes a noticeable difference in root length from nine days after germination, but a slightly increased average root length is apparent at six days post germination. This trend again implies a cumulative phenotype that requires a certain passage of time to develop into a significant root length difference.

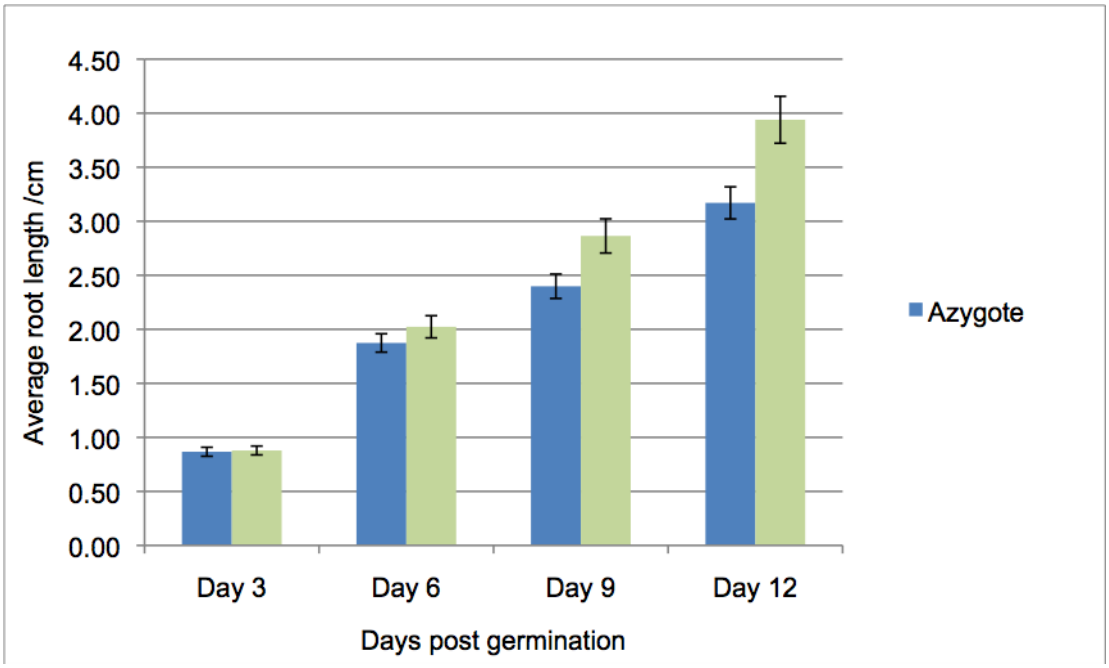

		Day 3	Day 6	Day 9	Day 12
Azygote	Average (cm)	0.87	1.87	2.40	3.17
	Standard error	*0.04*	*0.09*	*0.11*	*0.15*
NET1a/ NET1b -B	Average (cm)	0.88	2.02	2.86	3.94
	Standard error	*0.04*	*0.10*	*0.16*	*0.22*
Significance		0.8387	0.2644	0.0183	0.0043

Figure 6.4: Results of the analysis of primary root length of Azygote-B and the NET1a/NET1b-B double mutant at days three, six, nine and twelve after germination. The significance of this increase in root length is also shown.

This mutant phenotype is particularly interesting for two reasons. Firstly it does appear to confirm that the NET1a and NET1b proteins can in some way compensate if the other is missing, hence the need for two mutant alleles to be present before the plant will show a discernable phenotype.

Secondly, the phenotype appears to be a gain of function. The primary root appears longer without any other visible detrimental effect on the plant. Development after twelve days continues to be normal and the plants are capable of flowering, setting seed and producing the next generation of plants without adverse consequences. When the long root phenotype is seen, the above ground tissue does not seem significantly smaller than the same tissue in the azygote plants. Since a gene that inhibits growth logically ought not to have been retained through a long period of

evolution in plants, and also have been retained in several divergent forms, there must be another effect on the plant, one which cannot be seen but which in some way requires control during normal growth.

The fact that the root phenotype only appears after nine days of growth post germination suggests that whatever acts as the underlying cause of the phenotype is either cumulative (and requiring time before it appears at a perceptible level in the root), or it is linked to a stage of development that occurs at nine days. The former is more likely as the quantitative PCR used to determine levels of transcription of the gene in the mutant was carried out at no more than two days post germination. In the wild type plant, the NET1a and NET1b proteins were already present seven days before the presence of the phenotype in the mutant, so the corresponding absence of protein in the mutant plants from two days post germination suggests a cumulative effect before a visible phenotype is observed.

6.7 Analysis of the NET1a/NET1b/NET1c triple mutant

The results with the double mutant were obtained from using a plant missing two genes of one pair of highly homologous genes. To continue the investigation of the phenotype, a triple mutant was made, between NET1a, NET1b and NET1c. This was a cross between the NET1a/NET1b-B combination and NET1c allele SALK_139608. NET1b and NET1c are present on the same chromosome so crossover of chromosome 1 must occur between these two genes in order for the triple mutant to occur in a homozygous form. This also reduces the probability of a triple mutant occurring.

Dr MJ Deeks (Durham University, UK) calculated the genetic map distance of NET1b and NET1c to be 36.24 and used the Haldane formula to calculate that the recombination frequency between the two genes would be 25.8%. Using this it is possible to calculate what percentage of the segregating F2 population of the proposed triple mutant would be.

If the three genes are present on separate chromosomes, the expected number of plants homozygous for all three genes would be 1 in 4^3, or 1 in 64 plants. The requirement for recombination of one chromosome reduces this probability by 74%. This results in a final probability of a triple mutant of 1 in 256 plants, or 0.39%. In view of this low probability, after crossing the seed from the dried siliques was germinated and grown so that self pollination occurred to produce a segregating F2 population. 1000 plants from this population were germinated on vertical agar plates and allowed to grow to twelve days post germination. A selection of plants was taken including those with the longest and shortest roots. Within the group of plants with longer roots, a plant was found which was homozygous for NET1b and NET1c alleles but heterozygous for the NET1a allele. This plant was allowed to self pollinate and the next generation screened again. This resulted in the NET1a/NET1b/NET1c triple mutant homozygous for all mutant alleles.

The mutant was crossed, selected through conventional genotyping and quantitative PCR and allowed to grow to the next generation in synchrony with an azygous line as before. Root lengths were then analysed and the results can be seen in Figure 6.5 which shows a comparison between the triple mutant line, azygote and double mutant plants grown under the same conditions. Results of the quantitative PCR are shown in Figure 6.2. In Figure 6.5 data is also shown comparing the NET1c SALK allele with

the azygote line, demonstrating that the NET1c line is not the cause of the shortened root. Variation between the NET1c mutant and the azygote plants in terms of average root length was found not to be statistically significant, so any changing of the length of the primary root observed in the triple mutant line is due to the absence of a third NET1 gene.

In the data presented in Figure 6.5 the triple mutant no longer shows the long root phenotype seen with the double mutant and shows instead a slightly shortened primary root in comparison to the azygote line. Using a two-tailed T-test for two samples of unequal variance, the p-value for the variation between the triple mutant and the azygote is 4.3×10^{-4}. This is a statistically significant shortening of the root and represents a change in the observed phenotype. It could have been anticipated that a further loss of a NET1 protein would result in a greater lengthening of the primary root if the NET1 proteins had a purely regulatory effect on root growth. Other factors must be significant in the determination of root length. It is possible that at this point, the balance between the positive effects of the mutation and the negative effects of the lack of the NET1 genes are such that the plant shows a detrimental effect due to the mutation. The exact nature of the positive and negative effects cannot yet be determined. If this trend of increasing loss of NET1 proteins leading to greater negative effect on growth is the case it might be expected that a quadruple mutant would perhaps show a further shortened root or a more generally disrupted growth phenotype but the large time scale needed for the crossing and screening of such a mutant has so far prevented the analysis taking place. Due to the severity of the decrease in root growth caused by the removal of a third NET1 protein from the genome it is possible that a quadruple mutant removing all NET1 proteins would prove to be lethal.

a)

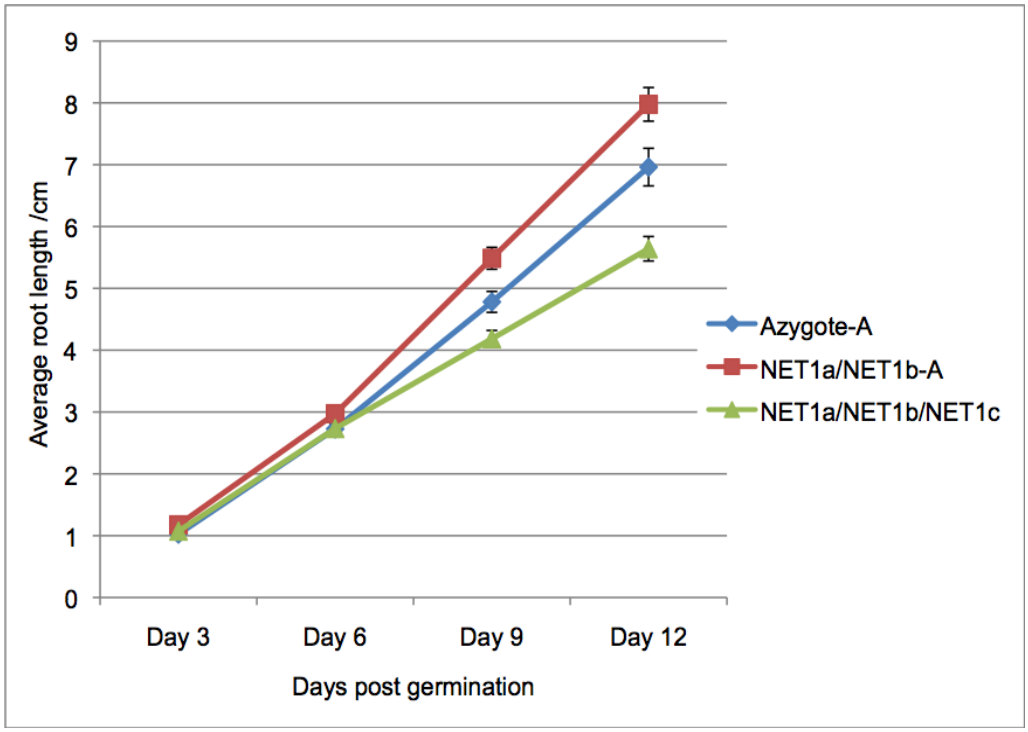

		Azygote-A	NET1a/ NET1b-A	NET1a/NET1b /NET1c
Day 3	Average root length /cm	1.03	1.18	1.07
	Standard error	*0.04*	*0.04*	*0.03*
Day 6	Average root length /cm	2.73	2.97	2.73
	Standard error	*0.09*	*0.10*	*0.08*
Day 9	Average root length /cm	4.78	5.49	4.19
	Standard error	*0.17*	*0.18*	*0.13*
Day 12	Average root length /cm	6.96	7.98	5.64
	Standard error	*0.30*	*0.27*	*0.20*

b)

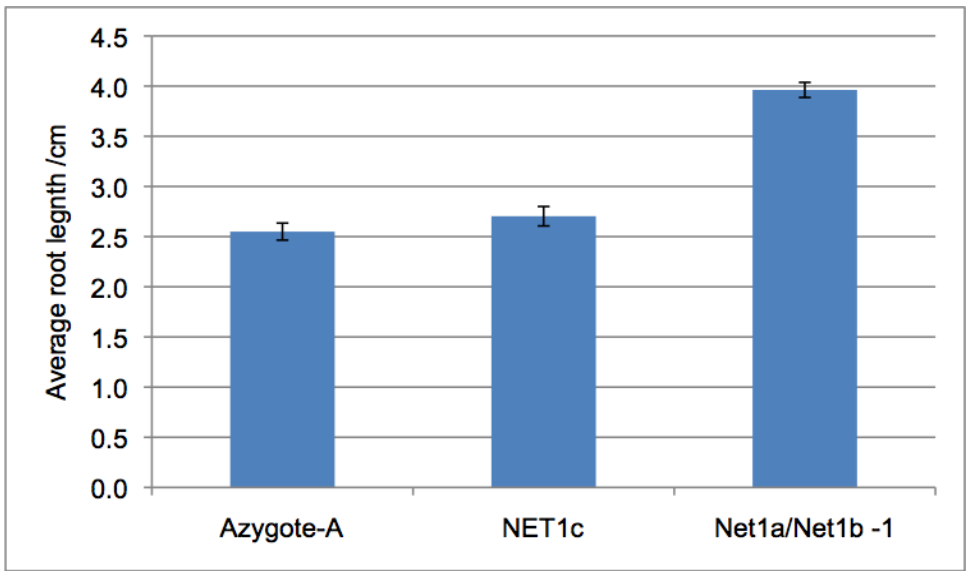

	Azygote-A	NET1c	Net1a/Net1b -1
Average root length /cm	2.55	2.70	3.96
Standard error	0.085	0.096	0.075

Figure 6.5: a) Analysis of the primary root length of the NET1a/NET1b/NET1c triple mutant in comparison to Azygote-A and the significance of this variation in root length. b) Comparison of NET1c with the Azygote and Double mutant. NET1c single mutants have an average primary root length equivalent to that seen in wild type plants. The p-value for variation between the Azygote population and the NET1c population is 0.24. This variation is not significant and is due to normal variation between roots.

The next obvious stage, arising from the work carried out with the mutant phenotype of the primary root, is to discover the underlying cause of the phenotype. This cause has not yet been completely understood but there have been several approaches taken to establish the underlying process which, if they do not provide an answer, prove what is *not* occurring to cause a longer root.

6.8 Analysis of cell size in the NET1a/NET1b-A mutant compared to azygote cells

6.8.1 Introduction

The long root phenotype found in the NET1a/NET1b double mutants is an unusual one as removal of a gene usually has a detrimental effect upon the plant. The phenotype is also ambiguous in its exact cause. A longer or shorter root can be caused either by a difference in rate of cell division, in cell elongation or in a combination of both. While the difference to the whole root is the same, on a cellular level these different underlying phenotypes imply very different causes of the phenotype. For example, the over expression of CYCB1 causes an increase in root length due to increased cell proliferation rather than cell elongation (Doerna et al. 1996) due to disruption of the cell cycle leading to increased cell division. Cell elongation however can be caused by factors such as disruption of auxin signalling (Luschnig et al. 1998).

6.8.2 Experimental data

To identify the cause of the long roots seen in the mutant plants, seeds from both NET1a/NET1b-A and the corresponding azygote lines were placed on vertical plates containing ½ MS growth medium and, after three days of vernalization at +4 ^{o}C, allowed to grow to nine days post-germination under the normal growth conditions used for analysis of the plant phenotypes. The roots were then fixed in a 3.7% formaldehyde solution. To image the root, 55 µM calcofluor was used to stain the cell walls of the root cells. 405 nm laser light was used to excite the fluorescent dye and fluorescence emission detected in the range 409 – 487 nm. Images of the whole root were taken using a Leica SP5 laser scanning confocal microscope.

Once images of the epidermis of the root were obtained, cells that had passed the elongation zone, at the stage of formation of secondary roots, were measured by manually tracing the length of the cell using ImageJ. This measurement was repeated for ten to fifteen cells within the root, and repeated for approximately 20-25 roots for each genotype. Cells to be measured were chosen as a row horizontally across the root to avoid any bias in selection of cells.

Figure 6.6 below shows the results of the analysis of the cell size in the mutant and azygote plants. The mutant plants show a clear increase in cell size, with an average of 130.8 µm compared to 99.2 µm in the azygote. The standard error for these measurements is small due to the large value of n (233 for the smallest population)

although root cells can be rather variable in size: the mutant population shows the largest standard error of 2.9 (2sf). The significance of these data has a p-value of 8.29×10^{-18}. The low number represents a very highly significant difference between the size of mutant and azygote cells.

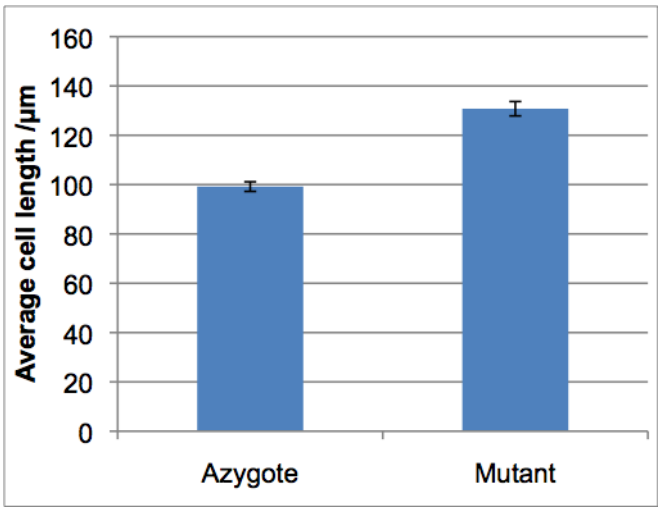

	Azygote	Mutant
Average cell length/µm	99.2	130.8
Number of cells	233	236
Standard deviation	29.83	44.74
Standard error	1.95	2.91
Percentage difference %		31.84

Figure 6.6: A comparison of cell length in Azygote-A and NET1a/NET1b-A primary roots.

This work demonstrates that the long root phenotype seen with the mutation of NET1a and NET1b is caused by an increase in cell size of approximately 31.8%. The increase is of a similar order of magnitude to the difference in whole root length usually seen (50% for double mutant combination A and 20-30% for double combination B), so the variation in cell size is likely to be the cause of the phenotype: cell division is unlikely to be making a significant contribution to the elongated roots although it is possible that a small rise in cell number could be a contributing factor.

6.9 The effect of auxin on root growth in the NET1a/NET1b-A mutant

Defects in root growth and a protein localisation to the apex of root cells suggest a possible link to proteins such as the PIN proteins, which are involved in auxin signalling (Krecek *et al.* 2009). For this reason, the effect of exogenous auxin has been studied, using the synthetic auxin 2,4-Dichlorophenoxyacetic acid (2,4-D).

Previous work on the Net1a/Net1b double mutant (Calcutt 2009) demonstrated that variation of auxin concentration had an effect on the predicted short root phenotype, appearing to both exacerbate and rescue to phenotype. The work carried out here was intended to clarify this initial data.

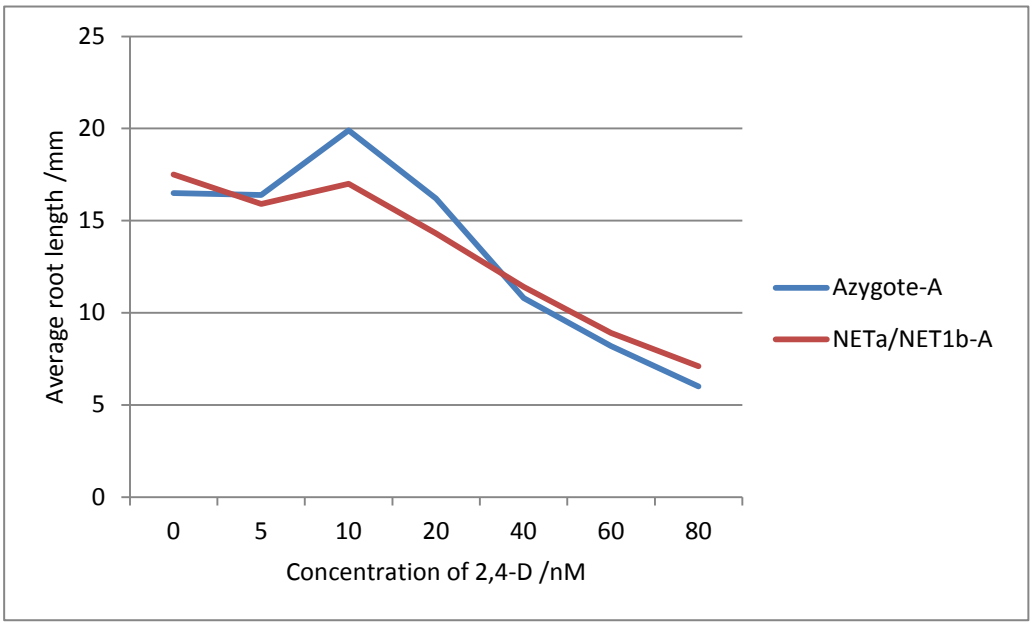

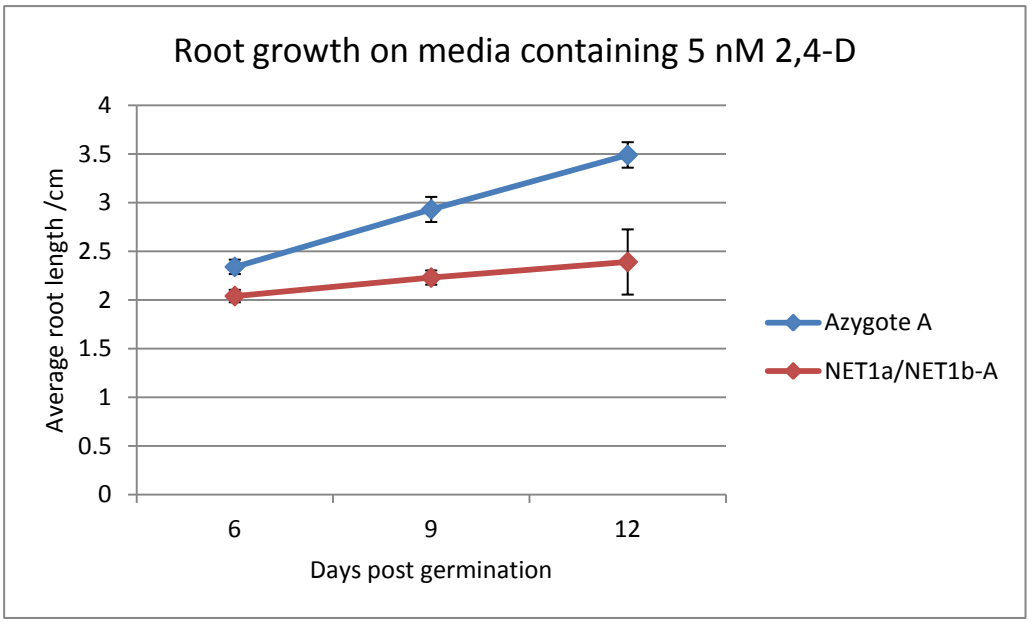

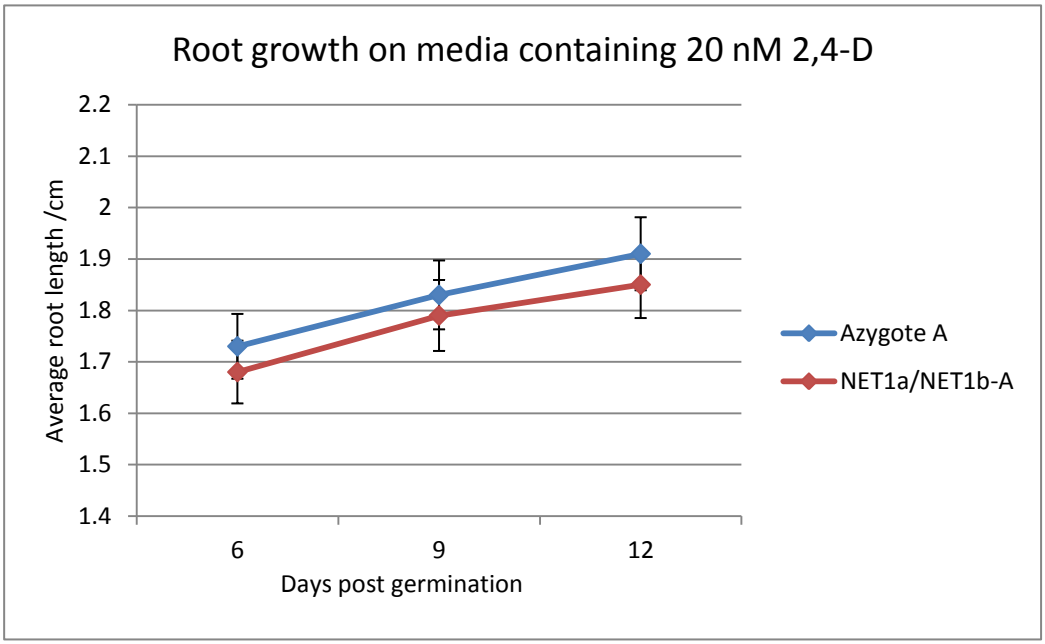

Days post germination	Average root length with 5 nM 2,4-D /cm		Standard error	
	Azygote A	NET1a/NET1b-A	Azygote A	NET1a/NET1b-A
6	2.34	2.04	0.074	0.064
9	2.93	2.23	0.129	0.073
12	3.49	2.39	0.131	0.335

Days post germination	Average root length with 20 nM 2,4-D /cm		Standard error	
	Azygote A	NET1a/NET1b-A	Azygote A	NET1a/NET1b-A
6	1.73	1.68	0.063	0.061
9	1.83	1.79	0.067	0.069
12	1.91	1.85	0.071	0.065

Figure 6.7: a) The initial analysis of the effect of auxin concentration on primary root length in azygote and double mutant A using 2,4-D as a source of synthetic auxin. Measurements were taken twelve days after germination. b) The effect of 5 nM and 20 nM 2,4-D on primary root length of Azygote-A and NET1a/NET1b-A at days 6, 9 and 12 post germination.

Initial analysis of the effect of auxin was carried out using a small sample size of approximately 20 – 25 seedlings per concentration of 2,4-D in order to test the range of responses to varying concentration of auxin. High concentration of auxin reduces

root growth significantly and work by J. Calcutt (Calcutt 2009) shows variation in the response of the root to high and low auxin concentration.

While not statistically significant, the pattern of average primary root length variation with increasing levels of auxin found shows an interesting response (see Figure 6.7 a). Initially, as with previous analysis, the mutant line has a greater average root length than the azygote line. At low concentrations of auxin however, the phenotype is reversedsuch that the mutant now displays a primary root shorter than the azygote rather than demonstrating the long root phenotype. This is most marked at 10 and 20 nM 2,4-D. At greater 2,4-D concentrations the average root length of both lines begins to decrease and the mutant line once again shows a longer root length than the azygote plants. For further analysis, two concentrations of 2,4-D were chosen: 20 nM at which point the phenotype has been reversed, and 5 nM where the initial analysis showed almost equal average root lengths in both lines.

Once a statistically significant sample size is used for this analysis it becomes apparent that the pattern discovered with the smaller sample size is not replicated exactly. At 5 nM 2,4-D the preliminary assay showed a slightly longer root for the azygote line, but it was almost equivalent to the mutant line. When a larger sample size was analysed the azygote line has a significantly longer primary root than the mutant line. The p-value from a two-tailed t-test of the significance of the data at twelve days after germination is 6.91×10^{-11}, a highly significant value. The phenotype does appear to respond to changes in external auxin concentration, which not only removes the long root phenotype, but also causes the reversal of the phenotype to produce a significantly shorter root.

With seedlings grown on media containing 20 nM 2,4-D a further shortening of the primary root in comparison to the azygote line was expected. However this result was not observed with the statistically significant population size. No significant variation in primary root length was found between the azygote and mutant, although the average root length was greater in the azygote line.

Attempts to analyse root length at higher auxin concentrations were unsuccessful due to highly stunted root growth so the pattern of resuming long rooted phenotype at high concentrations observed in the preliminary assay could not be established in a significant population size. The response to exogenous auxin is very variable, resulting in roots of almost normal length or of too short a length to be accurately

measured. A very large population would be required to provide understanding of the effect of a high concentration of auxin on the primary root of the NET1a/NET1b mutant. At present the exact nature of the relationship is unclear. It is however certain that the application of auxin does have some effect on the phenotype and causes a shortening of the root beyond that observed in wild type plants.

This eradication of the expected phenotype may be due to defects in auxin signalling or auxin transport. The cell is likely to be capable of responding to auxin levels, as an insensitivity to auxin would not result in a decrease in root length, so any direct relationship between the mutation of NET1a and NET1b and auxin response is likely to be due to incorrect levels of auxin reaching the root cells.

It is also possible to hypothesise that the effect of exogenous auxin is similar to that effect seen when a third NET1 protein is mutated in the plant. The balance between gain and loss of function in the NET1a/NET1b double mutant may be disrupted by the addition of external stress as well as stress within the root caused by the loss of NET1c in the triple mutant. This may explain the variability of response to auxin observed in the assays. While seedlings from both mutant and azygote lines are subjected to stress from the environmental conditions of the assay, the mutant plants may be less resilient and less able to demonstrate resistance to external stress.

Further work is required to determine more accurately the effect of higher concentrations of auxin and to determine whether the effect of the increasing auxin concentration on root length is directly as a result of a malfunction of auxin signalling within the double mutant root or indirectly, a result of increased environmental stress upon the root to which the plant has decreased resistance.

6.10 Effect of sucrose concentration on root growth in the NET1a/NET1b-A mutant

It was conjectured that since the growth of the root appeared to be involved in the formation of the phenotype that the transport of nutrients to the root of the plant might be too rapid leading to increased cell growth and a disruption of osmotic regulation. Analysis of root length on media containing sucrose by J. Calcutt (Calcutt 2009) showed an apparent increase in the primary root length of the double mutant, suggesting that sucrose concentration and osmotic stress might exacerbate or reduce the phenotype.

Figure 6.8 shows the result of the growth of the roots on media containing a variety of concentrations of sucrose. ½ MS media contains no sucrose, ½ MS10 contains 10% sucrose and MS-Ple contains 45% sucrose (Müller *et al.* 2004). Roots on the ½ MS media are the longest for both mutant and azygote and slightly shorter for ½ MS10 but in both cases, the mutant roots are longer than the azygote to the extent that the mutant roots grown on ½ MS10 media are longer than wild type roots grown on ½ MS. The highest sugar concentration in the MS-Ple media (Müller *et al.* 2004) results in an interesting and unexpected change of phenotype. Not only are the roots of both lines very stunted in their growth due to the high osmotic stress, but the mutant is actually shorter than the azygote. This reversal of phenotype may be similar in nature to the decrease of root length seen with the NET1a/NET1b/NET1c triple mutant and the alteration of the phenotype with application of external synthetic auxin. The high concentration of sucrose present in the Pleiade media creates an environmental stress upon the plant and it may be that the level of stress exceeds that which the plant can accommodate, just as the loss of the third NET1 gene appears to change the balance of the mutant phenotype from gain of function to a loss of function.

It would be interesting to study the effect of increasing sugar concentration on the root phenotype, perhaps using a gradient of increasing sucrose concentration to pinpoint the level of sucrose, which causes the mutant to lose the increased root length phenotype.

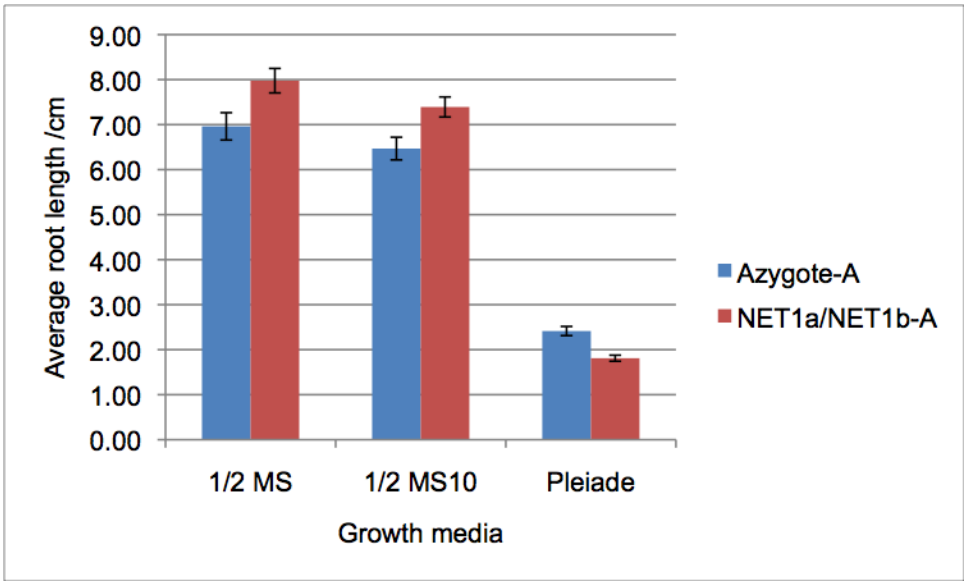

Growth media		1/2 MS	1/2 MS10	Pleiade
Azygote-A	Average root length /cm	6.96	6.47	2.41
	Standard error	0.30	0.25	0.10
NET1a/NET1b-A	Average root length /cm	7.98	7.39	1.81
	Standard error	0.27	0.22	0.07
Percentage increase in root length		14.58	14.28	-25.01

Figure 6.8: The variation of root length between Azygote-A and NET1a/NET1b-A at twelve days post germination on growth media containing differing concentrations of sucrose.

With a possible link to transport of sugars as the cause of the phenotype, Lugol staining was used to discover the localisation of starch within the root. While an increase in sugar would be expected to be metabolised in growth rather than converted to increased starch storage, this was examined as at high sugar concentrations as the mutant no longer shows increased growth. Mutant and azygote roots were immersed in Lugol stain for five minutes, washed in distilled water and mounted on a slide with two drops of Hoyer's solution to clear the root tissue for imaging. This process was undertaken at day three and day nine post germination, ie at time points before and after the emergence of the mutant phenotype.

When Day 3 plants were analysed, both mutant and azygote plants showed the pattern of starch grains located in the root tip that is typical of the expected distribution of starch within the root. These starch grains are present in wild type roots and were once thought to be involved in gravitational sensing to enable gravitropism although their exact role is now unclear (Staves *et al.* 1997). This is as

expected since the plants do not yet show signs of the long root phenotype seen later in development.

Figure 6.9 also shows the roots of Day 9 plants. The azygote plants show a pattern of starch staining highly similar to that observed at three days post germination. The root tips shown in Figure 6.9 from the azygote lines are therefore considered to be representative of these and the Day 3 plants.

When considering the mutant lines, for the most part the distribution of starch appears normal, with some slight aberrations that appear in both mutant and azygote, apparently at random which may be due to damage of particular root tips or of differences in the level of staining. The only notable result was in one particular experiment, where mutant roots show a pattern of starch staining that suggests localisation of starch within the rest of the lateral root, particularly around the edges of the cells. This was initially thought to be an interesting possible cause of the phenotype but it has not subsequently been replicated, so may have been an artefact of those particular roots or of environmental conditions particular to that assay. It has not been seen again and has never appeared in the control roots so although it is unlikely, it is possible that the localisation of starch may be a factor in the long root phenotype.

Starch staining was also carried out after a long period of light deprivation, caused by wrapping plates in tinfoil for 24 hours before staining for starch. This did not have a discernable effect on the Lugol staining, except to make it more likely that the expected starch grains would be missing from the root in both mutant and azygote. The results of this staining are shown in Figure 6.9.

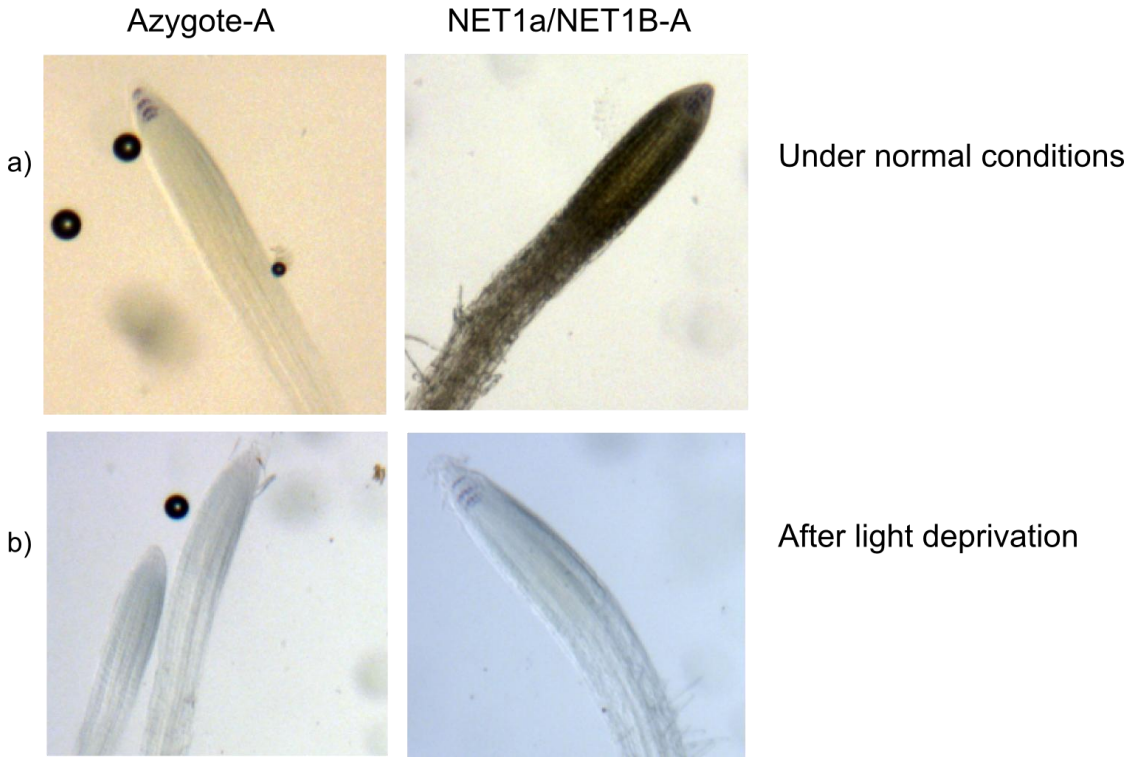

Figure 6.9: Lugol staining of Azygote-A and NET1a/NET1b-A roots to show starch distribution in the root tip of the primary root. a) Roots at nine days after germination, when the longer root phenotype can be observed. Roots were stained after growth in normal light conditions. b) Roots stained at nine days post germination after light deprivation for 24 hours

6.11 Conclusion

For each of the four NET1 proteins, there is now at least one mutant allele for a non-functional version of the gene and homozygous lines have been obtained for each of these mutants. These 'single' mutants have been analysed and no observable mutant phenotype can be found.

When an *A. thaliana* plant is lacking functional copies of both NET1a and NET1b, a long root phenotype is seen and this is consistent between two allelic variants of the double mutant. This elongation of the root tissue is due to an increase in cell size and therefore cell elongation rather than increased cell division increasing cell numbers. The phenotype may therefore be caused by errors in signalling or in the transport of nutrients, as an increase in the level of sugars transported to the root might increase growth of cells without causing increased cell division.

If it is the case that NET1 proteins are linked to plasmodesmata then whole plant effects of the absence of these genes may be due to the transport of molecules through the symplastic route via plasmodesmata and elongation of cells suggests that they are nutrient rich rather than suffering from a lack of phloem transport and unloading in the cells. Increasing concentrations of sucrose appears to impact the severity of the phenotype but any increase in sugar levels is not reflected in an increase of starch. It would be interesting to observe the effect on primary root length when seedlings were grown on a more complete gradient of sucrose concentration.

If the phenotype is related to a defect in plasmodesmatal function this could be analysed through the comparison of rate of transport of a substance in the roots of mutant and azygote plants. One possible technique would be the use of fluorescein, which can be introduced to the root through incubation and then photobleached in one section of the root tissue. Recovery of the fluorescence will be indicative of the rate of transport of the fluorescein and therefore rate of symplastic transport and would allow comparison of mutant and azygote (Rutschow *et al* 2011).

Defects in the signalling pathway might also account for the phenotype given the effect of auxin concentration on primary root length, but the effects of auxin on the mutant phenotype are unclear. Clarification of this effect would require further analysis of the effect of auxin on primary root length, perhaps with a larger sample size to compensate for the shortening of the root caused by high concentrations of

auxin, or variation of the concentration of auxin to further understand the reversal of the phenotype and whether this persists at high auxin concentration. While analysis of mutant phenotypes caused by removal of NET1 proteins has shown that they have a plant-wide impact and cause changes which are compatible with the known plasmodesmatal localisation and function, an exact function of the proteins has not yet been discovered.

Chapter Seven:

Discussion

7.1 Results of the analysis of the NET1 proteins

This project was begun with the knowledge that the protein NET1a, discovered as an unknown protein associated with a filament network (Escobar *et al* 2003), was in fact a novel, plant-specific actin binding protein. NET1a and the related protein NET1b had been shown to contain an N-terminal actin binding domain and a series of long coiled coil domains. Both proteins were shown to localise to the transverse walls of cells within the root, and NET1a displayed a punctate pattern of localisation that was thought to be co-localised with plasmodesmata. Absence of NET1a or NET1b from the plant was not seen to cause a visible phenotype, but absence of both genes was thought to result in a slight shortening of the primary root (Calcutt 2009). The remaining proteins of the NET1 group in *A. thaliana*, NET1c and NET1d had not yet been analysed although they were also predicted to contain the NET actin binding domain.

The experimental analysis of the NET1 proteins described within this thesis has shown, through use of transiently expressed constructs labelling the N-terminal region of the NET1c and NET1d proteins tagged with GFP, that both the remaining NET1 proteins are capable of association with the actin cytoskeleton. While the filaments observed during expression of the NET1c and NET1d actin binding domain appeared to be highly stabilised and show reduced movement of the actin filaments, assessment of the recovery of fluorescence after photobleaching indicated that turnover of the protein was high (recovery was seen after seconds). This result indicates that while the transient expression of the protein can be used for assessment of actin binding capability, the behaviour of the protein and the actin cytoskeleton is not indicative of the behaviour of these proteins under less perturbed conditions where expression of the NET1 proteins would be much lower. The protein is also likely to be expressed in a selective manner and to be maintained in particular subcellular locations to avoid disruption to actin filaments. The protein may be trafficked to or tethered to the correct area or interact with regulatory proteins to prevent non-specific actin binding.

No protein interactors beyond the actin cytoskeleton had been found for NET1a, so in order to establish a potential link between this protein and others a yeast two hybrid process was used to screen an *A. thaliana* cDNA library. It was hoped that this might establish a link between NET1a and a particular function, process or structure within the cell. The N-terminal region of the protein was used as bait owing to autoactivation occurring when the C-terminus of the protein was used. Two interactors were found: the first was a hexokinase AtHXK1, which was already known to be part of a signalling process linking glucose signalling to the actin cytoskeleton (Balasubramanian *et al.* 2007). Since the interactions of this protein with proteins upstream and downstream in the signalling pathway are known, it is possible that this interaction is due to the structural similarity of the hexokinase with F-actin although a role in glucose signalling cannot be ruled out.

The second potential interactor for NET1a is a cyclin dependent kinase, CYCB1 which has been linked to control of the cell cycle (Doerna *et al* 1996). During the cell cycle the actin cytoskeleton undergoes a process of reorganisation (Yu *et al* 2006) so it is possible that NET1a is connected with this process. This would also explain the expression of NET1a in meristematic tissue where cell division is occurring. However the subcellular localisation of the proteins is not complimentary as NET1a is found at the cell cortex and CYCB1 is located to the nucleus. Another factor rendering the link between these proteins currently inconclusive is the overexpression phenotype of the CYCB1 protein. This causes an increase in cell proliferation (Doerna *et al* 1996), and while initially it was believed that this was in agreement with the decrease observed in root growth when NET1a and NET1b were not present, this does not agree with what is now known about the phenotypes occurring due to absence of expression of NET1 genes.

Absence of one NET1 protein from a plant line was not seen to cause an observable phenotype. This has been demonstrated by analysis of NET1c and NET1d knock out lines to complete the observation of NET1a and NET1b single mutant lines (Calcutt 2009). Assays have been carried out to determine the effect of a double mutant lacking both NET1a and NET1b and, when seed from both mutant and azygote lines is obtained from the same generation of plants and a statistically significant sample size is used, a long root phenotype is observed. This gain of function phenotype is an interesting one and the exact cause of the elongation of the root is unknown. Measurement of individual cells in the root has established that the phenotype is due to cell elongation rather than cell division. This reduces the likelihood of interaction

with CYCB1 but may indicate disruption of signalling pathways (Luschnig *et al.* 1998) or changes in conditions such as an increase in the availability of sucrose leading to increased growth. Interestingly, a link has been established between the presence of an intact actin cytoskeleton and cell elongation (Baluška *et al* 2001) although the exact mechanism is unknown.

The underlying cause of the increase in cell elongation is still unknown and requires further investigation to establish a potential function for the NET1 proteins, although the response of the phenotype to various environmental conditions has been tested. The phenotype may respond to increased levels of sucrose or to exogenous auxin but the exact relationship between these external conditions and the growth of the root has not been established. A gain of function phenotype is particularly interesting, because the absence of the protein of interest appears to benefit the plant; and the detrimental effect of this absence, which is expected to occur as a gene inhibiting the plant would not be expected to be retained within the plant genome, is unknown. The function of the protein therefore becomes more difficult to establish. A protein, which inhibits cell growth may be beneficial to the plant in a number of ways not immediately obvious from the physical changes occurring in the plant tissue.

Another interesting feature of this phenotype is its rescue and even inversion to a short root phenotype under several different conditions, including the absence of the third NET1 gene, NET1c, which causes a shortening of the root phenotype. This also occurs when the plant is exposed to high concentrations of sucrose in the growth media or the application of synthetic auxin. These may represent a direct consequence of errors in auxin signalling or sucrose transport but it is possible that this shortening of the primary root may be due to the hidden negative effects of the absence of functional NET1 genes which is only significant when the plant is undergoing environmental stress. The removal of NET1c may also cause stress within the plant as the ability of the NET1 proteins to compensate for the absence of one of the group diminishes.

The ability of the NET1 proteins to replace one another is likely to be due to the high levels of homology between the protein structures, and the lack of any discernable phenotype when only one of the proteins was removed from the plant. The increasing appearance of a mutant phenotype as greater numbers of the proteins are absent suggests this may be the case. The punctate pattern of subcellular localisation observed with all four of the NET1 proteins (observed through use of antibodies and

immunofluorescence in the case of NET1c and NET1d) indicates the possibility of similar functions for the four proteins.

When the expression patterns of the genes are assessed by use of the GUS reporter gene driven by the NET1 promoter regions a very interesting pattern of expression is observed. The transcription of NET1 genes in roots appears to be segregated according to tissue type, shown for example by the absence of NET1d from all meristematic tissue in the presence of NET1a expression in the same tissue. As data could not be obtained using the promoter region of NET1c the expression data is not complete for all four genes but the data obtained from the three NET1 genes does indicated that NET1 expression may be present in all cell files in the root tissue. This presents an intriguing theory of four highly similar proteins providing subtly different functions within cells depend on cell type. The lack of phenotype may be due to an ability of the genes to compensate to some extent but may equally be due to effects occurring in some cells in the root. A more in depth analysis of the effect of the mutation of individual NET1 genes on cell physiology would be interesting to attempt in future.

At present the NET1 proteins remain in need of further experimental analysis to definitively answer the question of their function within plant cells. The current knowledge does, however, provide insight into the potential relationship between the four genes and suggests that the proteins may play an interesting role in the plant. There are many unanswered questions regarding the actin cytoskeleton in plants to which the NET1 proteins may be the answer. While a single theory of NET1 function cannot be proposed with the data found during this project, some theories on the role of these proteins can be suggested and will be discussed below.

7.2 Potential roles for the NET1 proteins

7.2.1 NET1 proteins as structural proteins

An important feature of the NET1 proteins is the series of long coiled-coil domains. These domains, which are based on a series of α-helical domains twisted around each other to form a coiled coil, are very stable structures by nature of their design (Burkhard *et al* 2001). The helices are held together by interlocking groups of hydrophobic residues inside the coiled coil structure with more hydrophilic residues found on the outside of the coils and this stabilises the conformation of the domain (Walshaw and Wooflson 2003). These coiled-coil domains have been shown to have many different functions within animal and fungal cells, but comparatively fewer have been studied in plants (Rose and Meier 2004). The ability of the domains to form protein-protein interactions and frequently to form dimers or oligomers is reflected in the roles they play within the cell. They are commonly found as structural proteins, including the Structural Maintenance of Chromosomes (SMC) proteins (Melby *et al* 1998); tethering or stabilising other proteins; forming networks, such as the intermediate filaments formed from coiled-coil protein dimers (Qin *et al* 2009); or even participating in signal transduction as in the HelixTM2 and Helix C domains of VirA which play a role in the infection of host plants by *Agrobacterium tumefaciens* (Wang *et al* 2002), where coiled-coil proteins may be an active component of the signalling pathway or used as anchoring proteins to tether components of the pathway to the correct location.

The NET1 proteins contain the N-terminal NET actin binding domain but do not contain any further identifiable domains other than coiled-coils. This suggests that the function of the protein may be to interact with the actin cytoskeleton and then anchor the filaments. Since the localisation of the NET1 proteins *in vivo* is to the periphery of the cell, the NET1 proteins may be connecting the actin cytoskeleton to the cell membrane. In particular the known localisation of NET1a and NET1b to the transverse walls of the root meristem can be linked to the presence of longitudinal actin filaments in the same location and thought to be utilised in cells undergoing rapid elongation (Baluška *et al* 2001), a process which connects this localisation with the expression pattern of NET1a in the root tissue of the meristem and lower elongation zone where cells are preparing for a stage of rapid growth.

Coiled-coil domains have been previously shown to anchor structures to membranes in plants, for example CHUP1 which anchors to the chloroplast membrane and also

interacts with actin (Oikawa *et al* 2003) in the process of chloroplast movement in response to blue light levels. No complete picture has yet been found of the proteins which anchor actin to the cell membrane directly in plants although it is known that connections between actin, the cell membrane and the cell wall occur (Baluška *et al* 2003). The lack of a transmembrane domain in the NET1 proteins indicates that a membrane bound protein is required as an interactor of NET1a to locate it to the cell membrane.

Another potential function for the NET1 proteins in a structural role is in the organisation of actin. The ability of coiled coil domains to dimerise allows them to form a rod unit with a functional domain at either end, enabling the bundling or crosslinking of proteins (Burkhard *et al* 2001). Proteins that bundle actin filaments are usually short proteins, enabling the two actin binding domains to bring the individual filaments close together. The NET1 proteins are much longer and so they would more probably occur as crosslinking proteins (Rose and Meier 2004). A mesh of actin filaments is found at the transverse walls of root cells (Baluška *et al* 2001), but the NET1c and NET1d proteins do not localise to this region as frequently as NET1a, which is the more likely candidate for a cross-linking protein. The NET1b, c and d proteins are localised very close to the cell wall and only NET1a shows fine filaments in addition to the punctate pattern along the cell membrane. A cross-linking protein is unlikely to be found only on the membrane: a role in the anchoring of actin filaments to the membrane appears more likely.

7.2.2 NET1 proteins in signalling

A number of features of the NET1 proteins are applicable to a function as a protein within a signalling pathway. As discussed above, coiled coil proteins can be involved in signal transduction by anchoring the components of the pathway together or acting as components of the pathway themselves (Wang *et al* 2002). A signalling role might also account for the effect of increased sucrose or auxin concentration on the mutant phenotype. The proteins are also localised at the cell membrane, perhaps co-localising with transmembrane receptors at the start of the signalling pathway. The NET1 proteins do not contain any domains that could interact with others in a signalling pathway, such as phosphorylation sites, so the predicted function would be as an adaptor protein, linking actin to the pathway and potentially connecting the cytoskeleton to the proteins upstream of this in the signalling pathway.

When a protein is shown to localise in a punctate pattern to the transverse walls of a cell, one of the potential causes of such a pattern is a PIN protein. These proteins are involved in auxin signalling between cells and the response of the NET1 mutants to auxin indicates a potential link. The PIN proteins are, however, almost exclusively located to the transverse walls, which the NET1 proteins are not (Krecek *et al* 2009). NET1c and NET1d are rarely located on those walls and are mainly found in the longitudinal walls, while NET1a and NET1b have the potential to locate to both. While the possibility of an auxin signalling link still exists, a co-localisation with the PIN proteins is unlikely.

7.2.3 NET1 proteins as plasmodesmal proteins

A very useful key to producing model of NET1 protein function is the recent co-localisation of NET1a with aniline blue staining of callose, a marker of plasmodesmata (Dr TJ Hawkins, Durham University). The punctate pattern at the periphery of the cell characteristic of all NET1 proteins is typical of plasmodesmal occurrence in the cell wall.

These cell wall structures are the connections between adjacent cells that allow transport of molecules via intracellular transport and under the control of the diameter of the plasmodesmal pore (Aaziz *et al* 2001). Smaller molecules can move by diffusion, while larger molecules such as proteins may be excluded or require some conformational change of the channel to allow movement between cells, an example of this being the KN1 transcription factor (Lucas *et al* 1995). The basic structure of the plasmodesma channel is that of a membrane bound tube through the cell wall, with a continuous cytoplasmic sleeve connecting the cytoplasm of the adjacent cells (Roberts and Oparka 2003). A strand of the endoplasmic reticulum runs through the centre of the structure (Ding *et al* 2002) and other globular proteins, many currently unknown, are associated with this desmotubule and are also found in the cytoplasmic sleeve. Recently over a thousand plasmodesmata associated proteins were discovered by use of nano-liquid chromatography (Fernandez-Calvino *et al* 2011), overcoming the previous problems caused by the location of plasmodesmata within the cell wall which renders plasmodesmal proteins inaccessible for analysis. The discovery of these proteins provides a rich source of potential interacting proteins for the NET1 group.

The actin cytoskeleton is known to associate with the plasmodesmal structure and may also be involved in determination of the size-exclusion limit or SEL (Ding *et al* 1996). When actin filaments are lost, due to treatment with anti-actin drugs, the neck region of plasmodesmata is widened (Ding *et al* 1996), and the SEL increases twenty fold in *N. tabaccum*. Conversely the stabilisation of actin filaments greatly reduces the occurrence of symplastic transport. If the NET1 proteins are involved in the association of actin to plasmodesmata they may have an impact on transport between cells. This could explain the elongated cells observed in the NET1a/NET1b double mutant. Increased transport due to lowered regulation of transport could increase levels of photoassimilates in cells leading to increased growth or disrupt cell-to-cell communication with a similar effect. If this is the case the cells might also be less resilient to stress owing to a lack of control over symplastic transport or errors in distribution of substances required for normal growth. The disruption of starch staining observed in the double mutant may be due to this potential build up of photoassimilates and their conversion to starch molecules for storage although much further investigation to confirm this disruption is required.

The pattern of localisation at the cell cortex varies between NET1 proteins. This may indicate that the NET1 proteins associate with different populations of plasmodesmata. Not all plasmodesmata are equivalent as populations of the structure are formed at different stages in development, from the first formation of primary plasmodesmata during cell plate formation by incomplete cytokinesis in cell division (Lucas *et al* 2009) to the formation of secondary plasmodesmata later in cell development (Ehlers & Kollmann 2001). NET1a, with an expression pattern highest in the meristematic tissue and a subcellular location to the transverse walls might localise to primary plasmodesmata, whereas the NET1d protein which appears in tissue with more developed cells after the meristematic and transition zones localises more to longitudinal walls so may represent a population of secondary plasmodesmata developed to connect adjacent cell files.

A second distinction might also be occurring between simple and branched plasmodesmata. Simple plasmodesmata are single channels through the cell wall as described above, but branched plasmodesmata appear to have several channels connected by cytoplasmic sleeve links in the middle lamella and are thought to represent a more advanced form of plasmodesmata structure (Oparka *et al* 1999). It is also possible that there are distinctions in populations of plasmodesmata' which have yet to be discovered but which are associated with different NET1 proteins. A

comparison of NET1 localisation in the same cell would assist in defining whether NET1 proteins display an overlapping or mutually exclusive pattern of association with plasmodesmata.

7.2.4 NET1 proteins in association with other membrane structures

While a localisation to plasmodesmata is beginning to be established for NET1a it is possible that the NET1 proteins are not all associated with this structure. Other features of the cell membrane may also be responsible for a punctate pattern of localisation. The cell membrane is far from homogenous in structure and areas of altered membrane composition such as lipid rafts may produce the pattern observed with the NET1 proteins (Bhat and Panstruga 2005). A NET1 protein involved in signal transduction may localise to a region of membrane containing receptor proteins or the NET1 proteins may be localised to areas of the membrane bound proteins such as the H^+-PPase AVP1, shown to localise to the plasma membrane in a punctate pattern through the use of immunogold labelling experiments (Paez-Valencia *et al* 2011).

If co-localisation of the three remaining NET1 proteins to plasmodesmata is not found to occur, continuation of yeast two hybrid analysis might reveal protein interactors for the NET1 proteins that may help to understand the localisation. Once possible interactors were identified, attempts could be made to co-localise with other structural markers or antibodies specific to the putative localisation of NET1a.

7.3 The NET1 proteins in relation to research on the NET protein family in *A. thaliana*

Research into the NET protein superfamily is a developing area of research and analysis of the NET1 group, containing the founding member of the family, has been in the greatest depth in comparison to the other three groups which make up the family. One particularly notable feature common to the majority of NET proteins is their punctate subcellular localisation. The NET proteins have been found to surround various membrane bound features of the cell (for example one of the members of Group 4 has been observed surrounding the vacuole (TJ Hawkins, Durham University, UK)). The NET2 proteins, only divergent from NET1 proteins in Angiosperms, show a very similar localisation to the NET1 proteins as they are found in punctate dots along the membrane, in a pattern resembling beads on a string (M Dixon, Durham University, UK). The membrane bound by NET2 proteins is the membrane of the pollen tube rather than the cell, but there is a similarity between the two proteins.

In light of the common theme of NET proteins localising to membranes, support can be given to a hypothesis of NET1 proteins as proteins which are capable of linking together the actin cytoskeleton and the cell membrane. The presence of other protein adaptors is likely as the NET1 proteins contain no transmembrane domains, but the potential identity and quantity of these is unknown. The NET1 proteins may also be responding to the presence of certain structures within the membrane, as with NET1a and plasmodesmata. The Group 2, 3 and 4 proteins are not associated with membranes which contain plasmodesmata so whether NET1 proteins universally associate with plasmodesmata or whether structure with which they associate varies remains to be discovered.

The most recent research to be carried out on the NET1 group by F Cartwright (Durham University, UK) has explored a potential connection between the NET1a protein and the endoplasmic reticulum (ER). A construct containing the C-terminal domains of the protein (in effect the protein without the presence of the actin binding domain) has shown co-localisation with ER markers. The centre section of NET1a has previously been discovered to localise to the ER (Calcutt 2009) so a model can be predicted whereby the N-terminus of NET1a associates with actin, the centre section associated with the ER and the C-terminus is free to bind to a further protein or structure. This adds an extra dimension to the proposed theory of association of

NET1a with plasmodemata. The endoplasmic reticulum is associated with plasmodesmata as a modified strand of ER, known as the desmotubule, runs through the cytoplasmic sleeve of the channel (Ding *et al* 1992). An association between this structure and the actin cytoskeleton in the context of the plasmodesmata is therefore a plausible location for the NET1a protein as a structural protein maintaining the cohesion between components of the plasmodesmata.

In addition to the colocalisation of these three structures in plasmodesmata, actin and myosins are known to control the structure of the ER network through association of the ER with actin filaments (Ueda *et al* 2010) so while NET1a may connect the actin cytoskeleton with the ER at plasmodesmata there is an additional possibility that another NET1 protein may link these two on the surface of the ER membrane. Investigation of the localisation of the C-termini of the NET1 proteins may provide insight into the level of association with the ER or whether NET1b, NET1c and NET1d are to be found in other cellular structures.

While analysis of the C-terminal domains of the NET1 proteins is a project for future analysis, investigations of the detailed structure of the NET actin binding domain have begun and initial results have been interesting. A feature of NET proteins is the presence of a rare triple tryptophan at the N-terminal end of the domain. Work by F Cartwright (Durham University, UK) has shown that NET1a-GFP with a mutated form of this WWW sequence (replacing tryptophan with glycine) shows maintenance of the subcellular localisation, but an increased motility that suggests that the sequence is required for stabilisation of NET1a binding. The amino acid sequence preceding the triple tryptophan has also been noted as an area for further investigation as the region varies between groups but is more highly conserved within them. Experimental work could be carried out to exchange these regions and observe any changes in localisation. These areas could perhaps function as a targeting sequence, stabilised by the triple tryptophan and allowing an association of the N-terminus of NET proteins with a subcellular localisation in addition to binding of actin filaments. This model would render the C-terminal long coiled-coil domains free to associate with a further protein or proteins (multiple proteins are likely considering the length of this region) or to dimerise and create a protein capable of cross-linking actin filaments together at a defined location.

The lack of homology of the NET1 proteins to any other known protein and the incomplete knowledge of the exact structure and components of the plasmodesmata

allow huge scope for the prediction of models of NET1 function. Only further experimental analysis can support the hypotheses but the results of this subsequent analysis are likely to prove exciting.

7.4 Areas of further research

To fully understand the function of the NET1 proteins further analysis is required. Directly in relation to the analysis described in this thesis are several experiments that are needed to confirm or further understand the results obtained to date. These relate in particular to the localisation of the proteins. Further analysis of the expression of NET1c in root tissue would assist in understanding the relationship between the four proteins and any cells within the root which lack NET1 proteins or which show an expression of more than one of the group. This could be carried out using the expression of four different fluorescent proteins, the expression of each one driven by the promoter region of one of the four NET1 proteins. For a more specific subcellular localisation the NET1 genes should be expressed in a stable *A. thaliana* line under their native promoters and labelled with C-terminal fluorescent proteins. The NET1a-GFP line already exists and has proved useful in understanding the behaviour of NET1a under native conditions.

The subcellular localisation of the NET1 proteins to the periphery of the cells analysed through use of antibodies and immunofluorescent labelling requires further confirmation as the antibodies have not yet been tested on tissue from the mutant lines which lack the NET1 proteins. A lack of staining in these mutants would confirm that the localisation observed is genuine and not an artefact of the staining process. Use of tissue from a line lacking only the NET1 protein of interest would also test the specificity of the antibodies, which is necessary in this case due to the great similarity between the staining patterns.

In addition to this assessment of the validity of the results it would be interesting to investigate any co-localisation between the staining pattern and presence of plasmodesmata in order to establish whether all four NET1 proteins are associated with the same structures at the plasma membrane. Plasmodematal stains such as aniline blue could be used to establish this co-localisation. If this was not the case alternative markers for structures showing similar punctate patterns, such as lipid rafts, could be used to identify the cause of the presence of the NET1 protein at the membrane.

The variation in pattern of the proteins, with NET1a and NET1b appearing mainly at the transverse walls and NET1c and NET1d at the longitudinal walls may be due to association to distinct membrane structures for each individual protein but it may also

be caused by association with different populations of plasmodesmata (either primary or secondary, simple or branched). The NET1a, NET1c and NET1d antibodies were raised in different organisms so immunofluorescent labelling can be used to distinguish between the proteins within the cell. This would demonstrate either overlapping or mutually exclusive association with the punctate areas.

If a plasmodesmal link is established the effect of the loss of the NET1 proteins on plasmodesmata could be assessed. The method described by Rutschow (Rutschow *et al* 2011) uses fluorescein, introduced into the root and then photobleached in an area of the root to measure the rate of recovery and therefore the rate of transport through the symplastic route. This could be used in the NET1 knock out mutants to assess the consequences of loss of NET1 proteins on transport through plasmodesmata.

The phenotype present in the NET1a/NET1b double mutant line represents another area where greater analysis is possible. Assessment of root length in the presence of sucrose concentration and increased auxin levels could be investigated further to discover the concentration at which the phenotype is rescued but not converted to a shortened root phenotype. The effects of other external stresses such as increased or decreased temperature or light levels could also be investigated. In view of the hypothesis that the mutant phenotype is only possible in healthy seedlings and that stress of any kind on the plant will cause a loss of the increased root length it would be interesting to establish whether this occurs with all stress conditions or only with those which have some bearing on the function of the NET1 proteins.

7.5 Conclusion

The NET1 proteins are a group of novel, plant-specific actin binding proteins found in *A. thaliana,* which belong to the NET protein superfamily. The four proteins are structurally similar: they possess an N-terminal actin binding domain through which the protein associates with F-actin filaments and a long series of coiled-coil domains. All four proteins are found in root tissue with each gene displaying a unique pattern of expression in different cell files and regions of root tissue. On a subcellular scale, all four proteins display a punctate localisation to the periphery of root cells, although NET1a and NET1b locate more frequently to the transverse walls and NET1c and NET1d to the longitudinal walls although the immunolabelling requires confirmation and use of pre-immune serum to confirm that the observed staining is not an artefact or reaction to another plant protein occurring within the organism used.

The absence of one NET1 gene within a mutant *A. thaliana* line does not produce a mutant phenotype but a lengthening of the primary root is observed in a double mutant line lacking both NET1a and NET1b. This phenotype can be rescued or even altered to a shortening of root length when external stresses are applied to the root and the change in root growth has been shown to be caused by an increase in cell elongation rather than an increase in cell division.

The function of the four proteins is unknown at present although some models of NET1 functions can be suggested, for example as a structural protein linking the actin cytoskeleton to the plasma membrane. The hypothesis with most supporting evidence, particularly in the case of NET1a, is that of the NET1 proteins providing a link between the actin cytoskeleton and plasmodesmata and the endoplasmic reticulum based desmotubule which runs through the centre of the plasmodesmal structure (Ding *et al* 1992). Confirmation of this interaction must still be established, for example by use of aniline blue stain to label plasmodesmata.

Since actin has been linked to control of the SEL of plasmodesmata (Ding *et al* 1996), the role of NET1 proteins in this process may be particularly interesting. Determination of SEL and the selective transport of molecules through plasmodesmata has been studied in relation to herbicide transport (Concenco and Galon 2011) and proteins such as PDLP5, which confers resistance to pathogens by closure of plasmodesmata, have been found to show a connection between SEL and plant immunity to pathogens (Lee *et al.* 2011). NET proteins have been discovered in

crop species so if the association between NET1 proteins and plasmodesmata is confirmed, there is a potential for a significant area of research.

Should the relationship between the NET1 proteins and plasmodesmata prove to be incorrect this family of proteins would still present a significant step in understanding the control of the plant actin cytoskeleton. Far less is known about the control of the cytoskeleton in plant cells compared to animals or fungi. The processes and structures which use the actin cytoskeleton in plants are not always equivalent to those found in animals so the scope for plant specific proteins which model or utilise the actin cytoskeleton is clear.

References

Aaziz R, Dinant S and Epel BL (2001) Plasmodesmata and plant cytoskeleton. *Trends in Plant Science* 6,326-230

Abràmoff MD, Magalhães PJ, Ram SJ (2004) Image Processing with ImageJ. *Biophotonics International*, 11(7), 36-42

Allwood EG, Anthony RG, Smertenko AP, Reichelt S, Drobak BK, Doonan JH, Weeds AG and Hussey PJ (2002) Regulation of the pollen-specific actin-depolymerizing factor LiADF1 *Plant Cell* 14(11), 2915-2927

Allwood EG, Smertenko AP and Hussey PJ (2001) Phosphorylation of plant actin-depolymerizing factor by calmodulin-like domain protein kinase. *FEBS Letters* 499, 97-100

Altschul SF, Madden TL, Schäffer AA, Zhang Z, Miller W and Lipman DJ (1997) Gapped BLAST and PSI-BLAST: a new generation of protein database search programs. *Nucleic Acids Research* 25, 3389-3402

Arber S, Barbayannis FA, Hanser H, Schneider C, Stanyon CA, Bernard O and Caroni P (1998) Regulation of actin dynamics through phosphorylation of cofilin by LIM-kinase. *Nature.* 393. 805-809

Axelrod D, Koppel DE, Schlessinger J, Elson E and Webb WW (1976) *Mobility measurement by analysis of fluorescence photobleaching recovery kinetics.* Biophysical Journal, 16(9) 1055-1069

Ayre BG, Keller F and Turgeon R (2003) Symplastic continuity between companion cells and the translocation stream: long-distance transport is controlled by retention and retrieval mechanisms in the phloem. *Plant Physiology* 131(4), 1518-1528

Balasubramanian R, Karve A, Kandasamy M, Meagher RB and Moore BD (2007) A role for F-actin in hexokinase-mediated glucose signalling. *Plant Physiology* 145, 1423-1434

Baluška F, Jasik J, Edelmann HG, Salajová T, Volkmann D (2001) Latrunculin B-induced plant dwarfism: plant cell elongation is F-actin dependent. *Developmental Biology* 231, 113-124

Baluška F, Samaj J, Wojtaszek P, Volkmann D and Menzel D (2003) Cytoskeleton-plasma membrane-cell wall continuum in plants: emerging links revisited. *Plant Physiology* 133, 482-491

Bhat RA and Panstruga R (2005) Lipid rafts in plants. *Planta* 223, 5-19

Blanchoin L, Boujemaa-Paterski R, Henty JL, Khurana P and Staiger CJ (2010) Actin dynamics in plant cells: a team effort from multiple proteins orchestrates this very fast-paced game. *Current Opinion in Plant Biology* 13, 714-723

Brandizzi F. Fricker M. and Hawes C. (2002) A greener world: the revolution in plant bioimaging. Nature Reviews Molecular Cell Biology 3, 520-530

Burkhard P, Stetefeld J and Strelkov SV (2001) Coiled coild: a highly versatile protein folding motif. Trends in Cell Biology 11, 82-88

Calcutt, J. (2009) ABP195, a novel plant actin-binding protein. *PhD thesis, University of Durham, Durham, UK*

Chen X-Y and Kim J-Y (2005) Transport of macromolecules through plasmodesmata and the phloem. *Physiologia Plantarum* 126(4), 560-571

Clough SJ. & Bent AF. (1998) Floral dip: a simplified method of Agrobacterium-mediated transformation of Arabidopsis thalians. Plant Journal 16, 735-743

Concenco G and Galon L (2011). Plasmodesmata: Symplastic Transport of Herbicides Within the Plant, Herbicides, Theory and Applications 21, 455-470

Cooper JA and Schafer DA (2000) Control of actin assembly and disassembly at filament ends. Current Opinions in Cell Biology 12, 97-103

De la Cruz EM, Mandinova A, Steinmetz MO, Stoffler D, Aebi U and Pollard TD (2000) Polymerization and structure of nucleotide-free actin filaments. Journal of Molecular Biology 295, 517-526

Deeks MJ*, Calcutt J*, Ingle EKS*, Hawkins TJ*, Chapman S, Dixon M, Cartwright F, Smertenko AP, Oparka K, and Hussey PJ (2011) A novel superfamily of actin-binding proteins link actin to membranes in higher plants. *Current Biology (Submitted for review)* *These authors share co-first authorship.

Deeks MJ and Hussey PJ (2005) Arp2/3 and SCAR: plants move to the fore. *Nature Reviews Molecular Cell Biology* 6, 954-964

Deeks MJ, Cvrcková F, Machhesky LM, Mekitová V, Ketelaar T, Zárky V, Davis B and Hussey, PJ (2005) Arabidopsis group Ie formins localize to specific cell membrane domains, interact with actin-binding proteins and cause defects in cell expansion upon aberrant expression. *New Phytologist* 168(3), 529-540

Deeks MJ, Hussey PJ and Davies B (2002) Formins: intermediaries in signal-transduction cascades that affect cytoskeletal reorganization. *Trends in Plant Science* 7, 492-498

De Ruijter NCA and Emons AMC (1999) Actin-binding proteins in plant cells. *Plant Biology* 1, 26-35

Ding B, Turgeon R and Parthasarathy MV (1992) Substructure of freeze-substituted plasmodesmata. *Protoplasma* 169, 28-41

Ding B, Kwon M-O and Warnberg L (1996) Evidence that actin filaments are involved in controlling the permeability of plasmodesmata in tobacco mesophyll. *The Plant Journal* 10, 157–164

Doerna P. Jørgensen J-E, You, R, Steppuhn J and Lamb C. (1996) Control of root growth and development by cyclin expression. *Nature* 380 520-523

Drøbak BK, Franklin-Tong VE and Staiger CJ (2004) The role of the actin cytoskeleton in plant cell signalling. *New Phytologist* 163, 13-30

Edwards K., Johnston C and Thompson C (1991) A simple and rapid method for the preparation of plant genomic DNA for PCR analysis. Nucleic Acids Research 19, 1349

Ehlers K and Kollmann R (2001) Primary and secondary plasmodesmata: structure, origin and functioning. Protoplasma 216, 1-30

Escobar NM, Haupt S, Thow G, Boevink P, Chapman S and Oparka K (2003) High-throughput viral expression of cDNA green fluorescent protein fusions reveals novel subcellular addresses and identifies unique proteins that interact with plasmodesmata. *Plant Cell* 15, 1507-1523

Falconer MM. and Seagull RW. (1985) Immunofluorescent and Calcofluor White Staining of Developing Tracheary Elements in Zinnia elegans L. Suspenstion Cultures. Protoplasma 125, 190-198

Fernandez-Calvino L, Faulkner C, Walshaw J, Saalbach G, Bayer E, Benitez-Alsonso Y and Maule A (2011) Arabidopsis plasmodesmal proteome. PLoS ONE 6(4), e18880

Fisher DB (1999) The estimated pore diameter for plasmodesmal channels in the Abutilon nectar trichome should be about 4 nm rather than 3 nm. Planta 136, 77-89

Friml J., Benková E., Blilou I., Wisniewska J., Hamann T., Ljung K., Woody S., Sandberg G., Scheres B., Jürgens G., and Palme K. (2002) AtPIN4 mediates sink-driven auxin gradients and root patterning in Arabidopsis. *Cell* 108, 661-673

Fu Y, Li H and Yang Z (2002) The ROP2 GTPase controls the formation of cortical fine F-actin and the early phase of directional cell expansion during Arabidopsis organogenesis. *Plant Cell* 14, 777-794

Geisler M, Kolukisaoglu HU, Bouchard R, Billion K, Berger J, Saal B, Frangne N, Koncz-Kálmán Z, Koncz C, Dudler R, Blakeslee JJ, Murphy AS, Martinoia E, Schulz B. (2003) TWISTED DWARF1, a unique plasma membrane-anchored immunophilin-like protein, interacts with Arabidopsis multidrug resistance-like transporters AtPGP1 and AtPGP19. *Molecular Biology of the Cell* 14(10), 4238-4239

Gomord V, Denmat LA, Fitchette-Laine AC, Satitat-Jeunemaitre B, Hawes C and Faye L (1997) The C-terminal HDEL sequence is sufficient for retention of secretory proteins in the endoplasmic reticulum (ER) but promotes vacuolar targeting of proteins that escape the ER. *Plant Journal* 11(2), 313-325

Holdaway-ClarkeTL, Walker NA, Hepler PK and Overall RL (2000) Physiological elavations in cytoplasmic free calcium by cold or ion injection result in transient closure of higher plant plasmodesmata. *Planta* 210(2), 329-335

Horton P et al (2006) Protein subcellular localization with WoLP PSORT. *Proceedings of the 4th Annual Asia Pacific Bioinformatics Conference APBC06,* 39-48

Hruz T, Laule O, Szabo G, Wessendorp F, Bleuler S, Oertle L, Widmayer P, Gruissem W and P Zimmermann (2008) Genevestigator V3: a reference expression database for the meta-analysis of transcriptomes. *Advances in Bioinformatics* 2008, 420747

Hu S, Brady SR, Kovar DR, Staiger CJ, Clark GB, Roux SJ and Muday GK (2000) Identification of plant actin-binding proteins by F-actin affinity chromatography. *The Plant Journal* 24(1) 127-137

Huala E, Dickerman A, Garcia-Hernandex M, Weems D, Reiser L, LaFond F, Hanley D, Kiphart D, Zhuang J, Huang W, Mueller L, Bhattacharyya D, Bhaya D, Sobral B, Beavis B, Somerville C and Rhee SY (2001) The Arabidopsis Information Resource (TAIR): a comprehensive database and web-based information retrieval, analysis and visualisation system for a model plant. *Nucleic Acids Research* 29, 102-105

Hussey PJ (ed) (2004) The plant cytoskeleton in cell differentiation and development. *Blackwell Scientific Publishers, Oxford.*

Hussey PJ, Ketelaar T and Deeks MJ (2006) Control of the actin cytoskeleton in plant cell growth. *Annual Review of Plant Biology* 57, 109-125

Hussey PJ, Allwood EG and Smertenko AP (2002) Actin-binding proteins in the Arabidopsis genome database: properties of functionally distinct plant actin-depolymerizing factors/cofilins. *Philosphical Transactions of the Royal Society of London B.* 357, 791-798

Kandasamy MK and Meagher RB (1999) Actin-organelle interaction: association with chloroplast in Arabidopsis leaf mesophyll cells. *Cell Motility and the Cytoskeleton.* 44, 110-118

Kandasamy M, McKinney EC and Meagher RB (2002) Functional nonequivalency of actin isovariants in Arabidopsis. *Molecular Biology of the Cell* 13(1), 251-261

Karnovsky,MJ. (1965) A formaldehyde-glutaraldehyde fixative of high osmolality for use in electron microscopy. J. Cell Biol. 27: 137A-138A.

Kawakami S, Watanabe Y and Beachy RN (2004) Tobacco mosaic virus infection spreads cell to cell as intact replication complexes. *PNAS* 101(16), 6291-6296

Ketelaar T and Emons AMC (2001) The cytoskeleton in plant cell growth: lessons from root hairs. New Phytologist. 152, 409-418

Kobayashi I, Kobayashi Y and Hardham AR (1994) Dynamic reorganisation of microtubules and microfilaments in flax cells during the resistance response to flax rust infection. Planta 195(2) 237-247

Koncz C. & Schell J. (1986) The promoter of TI-DNA gene 5 controls the tissue-specific expression of chimeric genes carried by a novel type of Agrobacterium binary vector. *Molecular and General Genetics* 204, 383-396

Kong S-G and Wada M (2011) New insights into dynamic actin-based chloroplast photorelocation movement. *Molecular Plant* Epub ahead of print

Lee J-Y, Wang X, Cui W, Sager R, Modla S, Czymmek K, Zybaliov B, van Wijk K, Zhang C, Lu H and Lakshmanan V (2011) A plasmodesmata-localized protein mediates crosstalk between cell-to-cell communication and innate immunity in Arabidopsis. *Plant Cell* Epub ahead of print

Lehmann P, Bohnsack MT and Schleiff E (2010) The functional domains of the chloroplast unusual positioning protein 1. *Plant Science* 180(4), 650-654

Lucas WJ, Ding B and van der Schoot C (1993) Tansley Review, 56. Plasmodesmata and the supracellular nature of plants. *New Phytologist* 125, 435-476

Lucas WJ, Bouche-Pillon S, Jackson DP, Nguyen L, Baker L, Ding B and Hake S (1995) Selective trafficking of KNOTTED1 homeodomain protein and its mRNA through plasmodesmata. *Science* 270, 1980-1983

Lucas WJ, Ham BK and Kim JY (2009) Plasmodesmata – bridging the gap between neighbouring plant cells. *Trends in Cell Biology* 19(10), 495-503

Luschnig C, Gaxiola RA, Grisafi P and Fink GR (1998) EIR1, a root-specific protein involved in auxin transport, is required for gravitropism in Arabidopsis thaliana. *Genes and development* 12, 2175-2187

McElver J, Tzafrir I, Aux G, Rogers R, Ashby C, Smith K, Thomas C, Schetter A, Zhou Q and Cushman MA (2001) Insertional mutagenesis of genes required for seed development in Arabidopsis thaliana. *Genetics* 159, 1751-1763

Meagher RB and Fechheimer M (2003) The Arabidopsis cytoskeletal genome. *In Somerville CR and Meyerowitz EM (eds), The Arabidopsis Book, American Society of Plant Biologists, Rockville MD*

Melby TE, Ciampaglio CH, Briscoe G and Erickson HP (1998) The symmetrical structure of structural maintenance of chromosomes (SMC) and MukB proteins: long, antiparallel coiled coils, folded at a flexible hinge. *Journal of Cell Biology* 142(6), 1595-1604

Mezitt LA and Lucas WJ (1996) Plasmodesmal cell-to-cell transport of proteins and nucleic acids. *Plant Molecular Biology* 32, 251-273

Miller D, de Ruijter NCA, Bisseling T and Emons AMC (1999) The role of actin in root hair morphogenesis: studies with lipochito-oligosaccharide as a growth stimulator and cytochalasin as an actin perturbing drug. *Plant Journal.* 17, 141-154

Mongrand S, Stanislas T, Bayer EMF, Lherminier J and Simon-Plas F (2010) Membrane rafts in plant cells. *Trends in Plant Science* 15(12), 1360-1385

Müller S, Smertenko A, Wagner W, Heinrich M and Hussey PJ (2004) The plant microtubule-associated protein AtMAP65-3/PLE is essential for cytokinetic phragmoplast function. *Current Biology* 14(5), 412-417

Nick P (1999) Signals, motors and morphogenesis – the cytoskeleton in plant development. *Plant Biology.* 1, 169-179

Nordgård O, Dahle O, Anderson TO and Gabrielsen OS (2001) JAB1/CSN5 interacts with the GAL4 DNA binding domain: a note of caution about yeast two-hybrid interactions. *Biochimie* 83, 969-971

Oikawa K, Kasahara M, Kiyosue T, Kagawa T, Suetsugu M, Takahashi F, Kanegae T, Niwa Y, Kadota A and Wada M (2003) CHLOROPLAST UNUSUAL POSITIONING1 Is Essential for Proper Chloroplast Positioning. *Plant Cell* 15, 2805-2815

Oparka KJ, Roberts AG, Boevink P, Santa Cruz S, Roberts IM, Pradel KS, Imlau A, Kotlizky G, Sauer N and Epel B (1999) Simple, but not branched, plasmodesmata allow the non-specific trafficking of proteins in developing tobacco leaves. *Cell* 97, 743-754

Overall RL and Blackman LM (1996) A model of the macromolecular structure of plasmodesmata. *Trends in Plant Science* 1, 307-311

Paez-Valencia J, Patron-Soberano A, Rodriguez-Leviz A, Sanchez-Lares J, Sanchez-Gomez C, Valencia-Mayoral P, Diaz-Rosas G and Gaxiola R (2011) Plasma membrane localization of the type I H^+-PPase AVP1 in sieve element-companion cell complexes from Arabidopsis thaliana. *Plant Science* 181(1), 23-30

Pollard TD, Cooper JA (1986) Actin and actin-binding proteins. A critical evaluation of mechanisms and functions. *Annual Review of Biochemistry* 55, 987-1035

Pollard TD, Blanchoin L and Mullins RD (2000) Molecular mechanisms controlling actin filament dynamics in nonmuscle cells. *Annual Review of Biophysics Biomol Struct* 29, 545-576

Pollard TD and Borisy GG (2003) Cellular motility driven by assembly and dissembly of actin filaments. *Cell.* 112, 453-465

Qin Z, Kreplak L and Buehler MJ (2009) Hierarchical structure controls nanomechanical properties of vimentin intermediate filaments. *PLoS ONE* 4(10), e7294

Radford JE and White RG (1998) Localization of a myosin-like protein to plasmodesmata. *Plant Journal.* 14, 743-750

Raven, JA (1993) The evolution of vascular plants in relation to quantitative functioning of dead water-conducting cells and stomata. *Biological reviews* 68(3), 337-363

Reddy ASN and Day IS (2001) Analysis of the myosins encoded in the recently completed Arabidopsis thaliana genome sequence. *Genome Biology* 2, 0024.1-0024.17

Riechmann JL, Heard J, Martin G, Reuber L, Jiang C, Keddie J, Adam L, Pineda O, Ratcliffe OJ, Samaha RR, Creelman R, Pilgrim M, Broun P, Zhang JZ, Ghandehari D, Sherman BK and Yu G. (2000) Arabidopsis transcription factors: genome-wide comparative analysis among eukaryotes. *Science* 290(5499), 2105-2110

Roberts AG and Oparka KJ (2003) Plasmodesmata and the control of symplastic transport. *Plant, Cell and Environment* 26, 103-124

Rose A and Meier I (2004) Scaffolds, levers, rods and springs: diverse cellular functions of long coiled-coil proteins. *Cellular and Molecular Life Sciences* 61, 1996-2009

Rose A, Manikantan S, Schraegle SJ, Maloy MA, Stahlberg EA and Meier I (2004) Genome-wide identification of *Arabidopsis* coiled-coil proteins and establishment of the ARABI-COIL database. *Plant Physiology* 134, 927-939

Rutschow HL, Baskin TI and Kramer EM (2011) Regulation of solute flux through plasmodesmata in the root meristem. *Plant Physiology* 155, 1817-1826

Schliwa M and Woehlke G (2003) Molecular motors. *Nature* 422, 759-765

Schmid M, Davison TS, Henz, SR, Pape UJ, Demar M, Vingron M, Scholkopf B, Weigel D and Lhomann JU. (2005) A gene expression map of Arabidopsis thaliana development. *Nat Genet* 37(5), 501-506

Schmidt A and Hall MN (1998) Signalling to the actin cytoskeleton. *Annual Review of Cell and Developmental Biology* 14, 305-338

Skirpan AL, McCubbin AG, Ishimizu T, Wang X, Hu Y, Dowd PE, Ma H and Kao T-H (2001) Isolation and characterisation of kinase interacting protein 1, a pollen protein that interacts with the kinase domain of PRK1, a receptor-like kinase of Petunia. *Plant Physiology* 126, 1480-92.

Smertenko AP, Deeks MJ and Hussey PJ (2010) Strategies of actin reorganisation in plant cells. *Journal of Cell Science* 123, 3019-3028

Staves MP, Wayne R and Leopold C (1997) Cytochalasin D does not inhibit gravitropism in roots. *American Journal of Botany* 84 (11), 1530-1535

Steinmetz MO, Stoffler D and Hoenger A (1997) Actin: from cell biology to atomic detail. *Journal of Structural Biology* 119, 295-320

Su L, Liu Z, Chen C, Zhang Y, Wang X, Zhu L, Miao L, Wang X and Yuan M. (2010) Cucumber Mosaic Virus movement protein severs actin filaments to increase the plasmodesmal size exclusion limit in Tobacco. *The Plant Cell.* 22(4), 1373-1387

Toshima J, Toshima JY, Amano T, Yang N, Naruminya S and Mizuno K (2001) Cofilin phosphorylation by Protein Kinase Testicular Protein Kinase I and its role in integrin-mediated actin reorganisation and focal adhesion formation. *Molecular Biology of the Cell* 12, 1131-1145

Ueda H, Yokota E, Kutsuna N, Shimada T, Tamura K, Shimmen T, Hasezawa S, Dolja W and Hara-Nishimura I (2010) Myosin-dependent endoplasmic reticulum motility and F-actin organisation in plant cells. *Proceedings of the National Academy of Science USA* 107, 6894-6899

Walshaw J and Woolfson DN (2003) Extended knobs-into-holes packing in classical and complex coiled-coil assemblies. *Journal of Structural Biology* 144(3), 349-361

Wang Y, Gao R and Lynn DG (2002) Ratcheting up vir gene expression in Agrobacterium tumefaciens: coild coils in histidine kinase signal transduction. *Chembiochem* 3(4), 311-317

Wasteneys GO and Galway ME (2003) Remodelling of the cytoskeleton for growth and form: an overview with some new views. *Annual Reviews in Plant Biology* 54, 691-722

White RG, Badelt K, Overall RL and Vesk M (1994) Actin associated with plasmodesmata. *Protoplasma* 180, 169-184

Winter D, Vinegar B, Nahal H, Ammar R, Wilson GV and Provart NJ (2007) An ‘Electronic Fluorescent Pictograph’ browser for exploring and analyzing large-scale biological data sets. *PLoS ONE* 8, 718

Yu M, Yuan M and Ren H (2006) Visualization of actin cytoskeletal dynamics during the cell cycle in tobacco (Nicotiana tabacum L. cv Bright Yellow) cells. *Biol. Cell* 98, 295-306